Assessment of small intestinal viability - A bioimpedance approach

Runar J. Strand-Amundsen

Department of Clinical and Biomedical Engineering,

Oslo Hospital Services,

Oslo University Hospital

Department of Physics,

University of Oslo

2018

Series of dissertations submitted to the
Faculty of Mathematics and Natural Sciences, University of Oslo
No. 2087

ISSN 1501-7710

Cover: Hanne Baadsgaard Utigard.
Print production: Reprosentralen, University of Oslo.

List of papers

Paper I:

R. J. Strand-Amundsen, C. Tronstad, H. Kalvøy, Y. Gundersen, C. D. Krohn, A. O. Aasen, L. Holhjem, H. M. Reims, Ø. G. Martinsen, J. O. Høgetveit, T. E. Ruud and T. I. Tønnessen.

In-vivo characterization of ischemic small intestine using bioimpedance measurements

Physiological measurement. 37 (2) (2016) https://doi.org/10.1088/0967-3334/37/2/257

Paper II:

R. J. Strand-Amundsen, H. M. Reims, C. Tronstad, H. Kalvøy, Ø. G. Martinsen, J. O. Høgetveit, T. E. Ruud and T. I. Tønnessen

Ischemic small intestine – In-vivo versus ex-vivo bioimpedance measurements

Physiological measurement. 38 (5) (2017) http://dx.doi.org/10.1088/1361-6579/aa67b7

Paper III:

R. J. Strand-Amundsen, C. Tronstad, H. Kalvøy, T. E. Ruud, J. O. Høgetveit, Ø. G. Martinsen and T. I. Tønnessen

Small intestinal ischemia and reperfusion – Bioimpedance measurements

Physiological measurement. 39 (2) (2018) https://doi.org/10.1088/1361-6579/aaa576

Paper IV:

R. J. Strand-Amundsen, H. M. Reims, F. P. Reinholt, T. E. Ruud, R. Yang, J. O. Høgetveit and T. I. Tønnessen

Ischemia/Reperfusion Injury in Porcine Intestine – Viability Assessment

World J Gastroenterol. 24 (18): 2009-2023 (2018) http://dx.doi.org/10.3748/wjg.v24.i18.2009

Paper V:

R. J. Strand-Amundsen, C. Tronstad, H. Reims, F. Reinholt, J. O. Høgetveit T. I. Tønnessen

Machine learning for intraoperative prediction of viability in ischemic small intestine

Physiological measurement. 39 (10) (2018) https://doi.org/10.1088/1361-6579/aae0ea

Acknowledgements

After my wife got pregnant with our first child, we decided that it would be wise for me to pursue a different career than the one I had in the military with the implicit prospect of traveling abroad for six months at regular intervals. The words of J.R.R Tolkien; “It's a dangerous business, Frodo, going out your door. You step onto the road, and if you don't keep your feet, there's no knowing where you might be swept off to” resonates with my feelings at that time about leaving the secure and known world of the military to pursue a new and somewhat intangible path.

Looking back, I am very grateful for my wife motivating me to make that leap of faith. While writing the finishing words of this thesis, my thoughts wander to the many people that I have met on the journey. People that have made this work possible, that have inspired, assisted and guided me in the exploration of the many pathways that have unfolded during the process. I did not meet monsters on this journey, but I do feel that I have walked among giants.

Jan Olav Høgetveit has been an inspirational, insightful and resourceful mentor. He is the one that started me on the path of pursuing a thesis in the first place and the one who introduced me to the group at the Institute for Surgical Research that led to the topic of the thesis. His example in leadership is an inspiration.

Tor Inge Tønnessen has been a constant source of guidance and inspiration. Ever positive and always focused on solutions, he is a driving force. Having had the privilege of working with him for some years has left me in awe over his capacity and range of skills.

Christian Tronstad is one of those people who possesses a unique combination of personality and skills, where I find myself lucky to know him and to call him a friend. His assistance and contributions have been invaluable.

Håvard Kalvøy has taken me in under the wings of the Department of Clinical and Biomedical engineering and has facilitated my work at the Department. He is always ready to help, with a positive and energetic outlook.

Tom Erik Ruud was the one who started me on the path of investigating the electrical properties of the small intestine, and the one who inspired the possible clinical application of the research. He has been a source of guidance and inspiration along the way.

Ørjan Martinsen has been a source of inspiration, knowledge and guidance for the application of electrical bioimpedance in the field of medicine and is a primus motor for the bioimpedance group.

I want to thank ***Ansgar O. Aasen*** who accepted me into the group at the Department of Surgical Research and set the stage for the startup of this research.

I want to thank ***Henrik Reims*** and ***Finn Reinholt*** at the Department of Pathology for their contributions and support. I am forever indebted to the assistance that they volunteered.

I want to thank my colleagues, Ole Elvebakk, Fred Johan Pettersen and Tormod Martinsen at the Department of Clinical and Biomedical engineering, for the help, friendship and the supportive approach that they have shown.

I want to thank Runkuan Yang who stood with us day and night during the pig experiments, constantly ensuring that we were well fed with dumplings and updated on microRNA research.

I want to thank my colleagues at Sensocure; Rune Veddegjerde, Lars Holhjem, Berit Brosvik, Stein Ivar Hansen, Anette Loennechen, Trond Herje, Arnstein Arnesen, Henrik Holland and Heidi Ludvigsen, for their support, friendship and assistance. Rune has endured many of the late-night animal experiments and has been of invaluable assistance.

I want to thank the Vivi Bull Stubberud and the staff at the Institute for Surgical Research at Oslo University Hospital for the help, assistance and resources that they provided, that supported the initiation of this work. I am indebted to Linda Engvik and the skilled staff at the Intervention Center at Oslo University Hospital, for the resources, people and assistance that they provided, that made it possible to conduct the long duration experiments.

Sherasz Yacub at the Department of HPB Surgery at Oslo University Hospital took the time to discuss and guide me with respect to the clinical aspects of viability assessment and is the one who is facilitating the upcoming work where we want to investigate the electrical properties of the human jejunum.

I want to thank Ellen Hellesylt and her staff at the Department of Pathology at Oslo University Hospital who made the difficult job of preparing of the histological samples for light microscopy. I also want to thank Sverre-Henning Brorson at The Core Facility for Electron Microscopy, Oslo University Hospital, for his work with preparation of samples for transmission electron microscopy.

I want to thank my friends and former colleagues in the Norwegian Armed Forces that have inspired and motivated this work.

Last, and most importantly, I want to express my gratitude for my family. My parents and siblings have always been a source for inspiration and motivation. My kind and loving wife Eline has patiently supported me in the work with this thesis. Carrying the effects of having at times a semi-present husband with a mind occupied with multithreading. I am indebted to my children; Amalie, Brage, Asbjørn and Sissel, who have patiently endured the effects of the workload, while offering quite amusing perspectives with respect to the thesis along the way. According to the children at the kindergarten Sissel attends, I am employed as a pig herder.

Contents

1 Introduction

This thesis is focused on assessment of the viability of the small-bowel, after ischemic insult[1], by means of bioimpedance measurements. It describes how electrical parameters measured on the small intestine change during ischemia and reperfusion and discusses pros and cons of in-vitro versus in-vivo models of ischemia. The thesis also describes the creation of a reference model for intestinal viability in a pig model, and finally, it describes how machine learning can be a relevant tool for analysis of longitudinal bioimpedance data, and how machine learning can be used to classify intestinal viability and histological grading based on bioimpedance measurements combined with the results from the reference model.

As a part of the methodology, the thesis discusses intraluminal microdialysis for detection and monitoring of ischemia and reperfusion, and the use of histology to provide a reference for the viability limit. The thesis combines knowledge and research from the fields of physics and medicine, in order to investigate a solution to a medical problem.

1.1 Assessment of intestinal viability

1.1.1 An introduction to the challenges of intestinal viability assessment

The small intestine is a part of the bowel, on average 6-7 meters long in an adult human (Hounnou *et al.*, 2002), and approximately 30 m^2 in surface area. While the bowel is continuously involved in several vital functions in the human body, it is probably often taken for granted. This could change drastically if one experiences bowel ischemia. Ischemia means a restriction of blood flow, resulting in a lack of O_2 and nutrients in the affected tissue, and insufficient disposal of waste products.

Bowel ischemia is classified into three main types; acute mesenteric ischemia (AMI), chronic mesenteric ischemia and ischemic colitis (Yasuhara, 2005). AMI accounts for about 1 in 1000 acute hospital admissions (Bala *et al.*, 2017). It has been reported that the incidence of AMI increases exponentially with age, but it is not unusual to find patients in the 20's (Tilsed *et al.*, 2016). As the life expectancy of much of the world's population is increasing (Mathers *et al.*, 2015), so are the incidents of AMI (Tilsed *et al.*, 2016). The pathology that contribute to the formation of AMI include emboli[2] (40%-50% of cases), arterial thrombus[3] (25%-30% of cases), non-occlusive ischemia (20% of cases), and venous thrombus (10% of cases) (Tilsed *et al.*, 2016).

Acute bowel ischemia can occur in a variety of clinical settings, including abdominal aortic aneurysm surgery, small bowel transplantation, cardiopulmonary bypass, stoma, or in everyday life if patients should experience arterial or venous mesenteric occlusion[4], mechanical bowel obstruction combined with simultaneous strangulation of the mesenteric blood vessels (strangulation ileus), strangulated hernias, trauma, or shock (Collard and Gelman, 2001). Not everyone is aware that experiencing circulatory shock in a traumatic accident will lead to the body prioritizing the blood flow to vital organs, with the possibility of leaving the bowel in a low-flow or ischemic state for a period of time. While the bowel can

[1] Restriction of blood supply
[2] A wandering blood clot that gets stuck.
[3] A gradually forming clot in a vessel.
[4] Emboli or thrombus

withstand a certain period with low- or no-flow, prolonged ischemia will result in necrosis, and if the necrotic bowel is not removed, peritonitis and sepsis.

The release of harmful substances following reperfusion of ischemic bowel has been linked to multiple organ failure (Collange *et al.*, 2015, Pierro and Eaton, 2004, Klingensmith and Coopersmith, 2016). The mortality rate of patients with bowel ischemia remains high (30-93%), due to the difficulty in diagnosing the disease before irreversible injury occurs in the intestines, and due to the risk of later morbidities[5] (Tilsed *et al.*, 2016, Bala *et al.*, 2017, Brandt and Boley, 2000).

At hospitals around the globe, patients enter daily with diffuse symptoms related to the gut, and in cases where bowel ischemia is diagnosed, they are subsequently admitted for surgery. The main challenge in detecting bowel ischemia is the diffuse symptoms, and reducing the diagnosis period is essential (Haglund, 2001). Angiography is the gold standard for detection of mesenteric ischemia (Hoballah and Lumsden, 2012, van den Heijkant *et al.*, 2013), and biphasic multidetector CT has shown high sensitivity and specificity for detection of AMI (Menke, 2010, Aschoff *et al.*, 2009).

Once diagnosed, the surgical procedure will either be endovascular treatment, laparoscopy[6], or more commonly explorative laparotomy[7] (Beaulieu *et al.*, 2014) where the surgeon makes an incision through the abdominal wall to gain access to the abdominal cavity. The intestines are visually inspected, the ischemic tissue located, and restoration of perfusion initiated if there is still ongoing ischemia. Following the restoration of perfusion, the surgeon assesses bowel viability by palpation, visual inspection of return of color (Figure 1), motility and bleeding of cut ends (Tilsed *et al.*, 2016). This method is not very specific and requires a lot of clinical experience (Urbanavicius *et al.*, 2011, Wyers, 2010, Gorey, 1980), as the appearance of the ischemic or reperfused intestine can be deceptive (Urbanavicius *et al.*, 2011, Bulkley *et al.*, 1981, Mitsudo and Brandt, 1992).

Figure 1. Visual inspection of porcine small intestine

[5] 'Morbidities' meaning complications or side effects following medical treatment.
[6] Miniature surgical incision into the abdominal cavity to gain access to inspect the bowel with laparoscopic tools
[7] Large surgical incision into the abdominal cavity to gain "hands on" access to the bowel

The gold standard for the determination of bowel viability is a second-look laparotomy (within 48h) to reinspect areas of questionable viability (Yanar *et al.*, 2007). From the first laparotomy alone only 50% of non-viable cases have been reported to be correctly identified (Redaelli *et al.*, 1998a). When including the effect of second-look laparotomy, accuracy has been reported to increase to 87- 89% (Bulkley *et al.*, 1981, Redaelli *et al.*, 1998a). In the study made by Bulkley *et al.*, unnecessary bowel resection was reported in 46% of the cases[8].

While it can be challenging, evaluation of intestinal viability is essential in surgical decision-making for patients with acute intestinal ischemia (Bala *et al.*, 2017, Horgan and Gorey, 1992, Tilsed *et al.*, 2016). The surgeon selects resection margins with the aim of removing irreversibly injured bowel, preserving viable bowel, and selecting suitable locations for anastomosis[9]. Failure to remove irreversibly injured bowel can lead to peritonitis, sepsis and death for the patient (Herbert and Steele, 2007), while excessive removal of intestines can lead to short-bowel syndrome (Seetharam and Rodrigues, 2011). Up to 57% of patients need further bowel resection later, and this number includes patients undergoing second-look surgery (40% of the patients) (Clair and Beach, 2016).

In 1992, Horgan and Gorey described the requirements of an ideal viability test (Horgan and Gorey, 1992):

1. The technique must have ready availability, preferably in every operating theatre dealing with abdominal emergencies.
2. The necessary equipment must not be cumbersome or require specialized personnel.
3. The method must be accurate, with a minimum of false-negative results and, more importantly, few false positives. A false-negative result leaves in situ nonviable bowel, which may lead to early perforation and late structuring. This situation may be recovered with further surgical intervention, however. On the other hand, a false positive assessment of bowel viability results in resection of potentially recoverable intestine, which is lost forever and may represent a vital difference for morbidity-mortality and long-term nutrition.
4. The technique must be objective and be reproducible.
5. The method must be cost effective.

These requirements have been used to assess the feasibility of experimental approaches to bowel viability (Urbanavicius *et al.*, 2011, Erikoglu *et al.*, 2005). Additional requirements which we suggest could be added to this list are: a) that the technique should be able to give a clear result in a relatively short period of time and b) that the technique ideally should not be dependent on complex and time-consuming calibration.

1.1.2 Experimental approaches to viability assessment

Over the years, different researchers have investigated a number of experimental approaches with the aim of providing the surgeon with methods to increase the accuracy of intraoperative intestinal viability assessment, but few methods have proven applicable so far

[8] The low positive prediction value was due to skewed classes

[9] The joining together of (viable) parts of the intestine

(Urbanavicius *et al.*, 2011). Many of the methods touch upon both detection of ischemia and assessment of viability. Table 1 shows an overview over the experimental approaches related to the assessment of intestinal viability.

Table 1. *An overview over experimental approaches to assessment of intestinal viability*

Focusing on detection of blood flow:	**Focusing on other parameters:**
Intravital microscopy (Yasumura *et al.*, 2003)	Bowel wall contractility measurements (Dutkiewicz *et al.*, 1997)
Doppler ultrasound (Bulkley *et al.*, 1981)	Microdialysis (Deeba *et al.*, 2008) (flow, permeability and metabolic changes)
Pulse oximetry (Erikoglu *et al.*, 2005)	Electrical bioimpedance (Carey *et al.*, 1964) (electrical properties tied to structural changes)
Hydrogen gas clearance (Mishima *et al.*, 1979)	
Radioisotope studies (Prinzen and Bassingthwaighte, 2000)	
Fluorescence studies (Holmes *et al.*, 1993, Boni *et al.*, 2016, Johnson *et al.*, 2016)	
Infrared imaging (Moss *et al.*, 1978)	
Laser doppler flowmetry (LDF) (Humeau *et al.*, 2007)	
Visible light spectrophotometry (VLS) (Karliczek *et al.*, 2010)	
Near-infrared spectrophotometry (Kohlenberg *et al.*, 2005)	
Diffuse reflectance spectroscopy (Karakas *et al.*, 2014)	
pH measurement (Millan *et al.*, 2006))	

Of the methods listed in Table 1, visible light spectrophotometry (VLS) and laser doppler flowmetry (LDF) have been most frequently tested on humans (Urbanavicius *et al.*, 2011). The sensor principle of VLS is transmission of visible light around 475-625 nm wavelengths, penetrating about 2 mm into the tissue. The rate of absorption is used to measure the concentrations of hemoglobin and to estimate oxygen saturation (StO_2). VLS allows for point measurements of small tissue samples (Benaron *et al.*, 2005) and is a promising tool for measurement of intestinal wall oxygen saturation. VLS can be used without direct tissue contact (Karliczek *et al.*, 2010). The limitations of VLS are:

1. A specific level of StO_2 with respect to tissue ischemia or viability limit has not yet been defined (Urbanavicius *et al.*, 2011).
2. The presence of intestinal contents affects the accuracy of the measurements and the reproducibility of the results (Urbanavicius *et al.*, 2011).
3. A 90^o angle between probe and tissue is required for optimal measurements (Myers *et al.*, 2009).

With LDF, the principle (velocimetry) is to measure the frequency change of light when reflected by moving objects such as hemoglobin. The output signal is then proportional to the number of blood cells per minute moving in the tissue volume under measurement

(Redaelli *et al.*, 1998b). LDF has been investigated for prediction of anastomotic insufficiency, with promising results (Vignali *et al.*, 2000) (Seike *et al.*, 2007). The limitations of LDF are:

1. In the tissue area under investigation, the velocity measurement represents the average velocity in all adjacent vessels and does not consider the heterogeneity of blood flow.
2. LDF measurement is sensitive to motion artefacts.
3. Large standard deviations of the flow parameters have been reported during measurements (Singh *et al.*, 2009, Singh *et al.*, 2008) requiring continuous measurement with a secure fixation of the probe (Seike *et al.*, 2007).
4. LDF is sensitive to blood pressure changes (Seike *et al.*, 2007).
5. LDF requires tissue contact and may disturb local blood flow (Karliczek *et al.*, 2010).
6. The cut-off levels indicating ischemia vary between studies and models (Humeau *et al.*, 2007, Kashiwagi, 1993).

Singh *et al.* compared VLS and LDF with surface and intraluminal catheter probes for assessment of serosal and mucosal oxygenation and blood flow, and found that VLS can accurately diagnose mucosal ischemia from the mucosal side, while LDF could be useful in detecting ischemia from the serosal side (Singh *et al.*, 2009). There appears to be no consensus on which experimental method (Table 1) is most feasible with respect to the ideal viability assessment requirements, (Horgan and Gorey, 1992, Urbanavicius *et al.*, 2011) and many of the experimental approaches seem better suited to detect the presence of ischemia, than for the assessment of intestinal viability. So far, no method has surpassed palpation and visual inspection performed by an experienced clinician, followed by a second-look laparotomy, as the gold standard (Tilsed *et al.*, 2016, Bala *et al.*, 2017).

1.2 General introduction to electrical bioimpedance

One of the experimental approaches suggested for viability assessment is the use of electrical bioimpedance[10] measurements (Urbanavicius *et al.*, 2011). Bioimpedance means measuring the passive electrical properties of a tissue. For a thorough introduction to bioimpedance, the book *Bioimpedance and Bioelectricity Basics* (Grimnes and Martinsen, 2015) is recommended.

1.2.1 Bioimpedance notation

Table 2. *Bioimpedance notation*

U	Electric field [V]
I	Current [A]
R	Resistance, real part of impedance [Ω]
$\boldsymbol{X}$	Reactance, imaginary part of impedance [Ω]
X_L	Inductive part of reactance [Ω]
X_C	Capacitive part of reactance [Ω]
$\boldsymbol{Z}$	Impedance [Ω]
$\lvert Z \rvert$	Impedance modulus [Ω]
$\boldsymbol{Y}$	Admittance [S]
Z'	Measured real part of impedance, *Re*
Z''	Measured imaginary part of impedance, *Im*

[10] When using the word 'bioimpedance' in this thesis, it is always referring to 'electrical bioimpedance'

$\boldsymbol{j}$	Notation for an imaginary value. $j^2 = -1$
ω	The angular frequency ($2\pi f$)
C_0	The capacitance with no dielectric between the electrodes [F]
ε_0	Vacuum permittivity: 8.854E-12 [F/m]
ε_r	Relative permittivity [F/m]
$\boldsymbol{\varepsilon(\omega)}$	Complex permittivity as a function of frequency [F/m]
$\varepsilon'(\omega)$	Dielectric constant. Lossless permittivity. (ε') [F/m]
$\varepsilon''(\omega)$	Loss factor. Dielectric loss. (ε'') [F/m]
$tan\ \delta$	Loss tangent/dissipation factor
$tan\delta m$	Maximum $tan\ \delta$ amplitude over a frequency range
φ	Phase angle [deg]
δ	Loss angle [deg]
π	Pi, ratio of a circle's circumference to its diameter
τ	Time constant, Tau
R_s	Low frequency resistance
$R\infty$	High frequency resistance

1.2.2 Impedance basics

The forces that create the phenomenon that we call electricity are based on repulsion between similar charges and attraction between opposite charges. An electrical charge, symbolized q, is a property of matter as to the ratio between electrons (negative) and protons (positive), leaving three possible states; neutral, positive or negative.

The interaction between attractive or repulsive forces can create a force leading to a movement of charge, which is known as electric current (I=dq/dt). Some materials have free charge carriers (conductors), while other materials have only fixed charge carriers (dielectrics). In the electrical circuit (dry) the typical charge carrier is the free moving electron, while in biological tissues and liquids the charge carrier is the ion[11]. The ion is an atom or molecule with an uneven number of electrons and protons. The ability of a charge to move within/along a conductor depends on factors like the material properties and the temperature of the conducting material, the geometry of the conductor and the properties of the charge carrier.

The relationship between an applied alternating electric field and the resulting alternating current is described as admittance ($\boldsymbol{Y}$), with the reciprocal being impedance ($\boldsymbol{Z}$), meaning a quantification of the opposition to current flow. In many instances the relationship between applied voltage (U) and resulting current (I) is linear, as described in Ωs law.

$$\boldsymbol{U} = \boldsymbol{Z} \bullet I \tag{1}$$

[11] Such as Na^+, Cl^-, K^+ etc.

Z consists of two components, resistance (R) and reactance (X). With direct current (DC) there is only resistive losses and no phase shift between the voltage and current ($X = 0$). With alternating current (AC), part of the energy can be stored as charge buildup (polarization) along and/or in dielectrics (opposing change in voltage) or as magnetic fields in inductors (opposing change in current), in addition to the resistive losses. X can be negative; capacitance ($-X_C$) and positive; inductance (X_L).

$$|Z| = \sqrt{(R^2 + (X_L - X_C)^2)} \qquad [\Omega] \tag{2}$$

The introduction of X_C and X_L creates the need for another dimension, called the complex or imaginary plane (Figure 2, left). R is a representation of in-phase energy loss, but when energy is stored as X_C or X_L, the energy storage is not instant but is a relaxation process (Grimnes and Martinsen, 2015), requiring time, causing a time delay between the voltage and current, resulting in a phase-shift proportional to the capacitive or inductive properties of the conductor (Figure 2, right). In a complex plane this phase shift can be described as an angle between the imaginary (Im) and the real part (Re) of the complex impedance (Figure 2, left).

$$\text{Phase angle } \varphi = atan\left(\frac{Im}{Re}\right) \text{ [rad]} \tag{3}$$

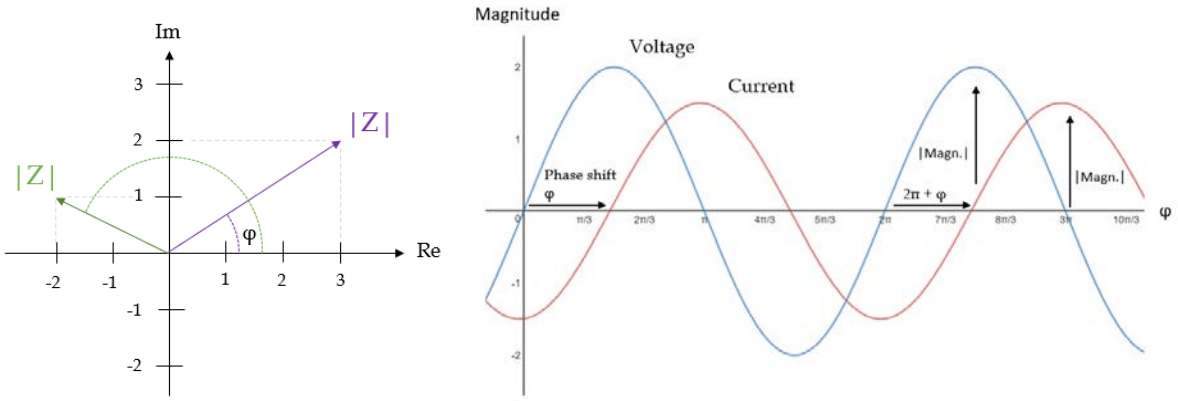

Figure 2. Left: The real and imaginary components of two impedances (Z and Z) plotted in the complex plane, with phase angles φ. **Right:** Example of phase shift and magnitude difference between an applied voltage and the resulting current.

1.2.3 *tan δ*

While many are familiar with the phase angle φ, not all are familiar with the loss angle δ and the corresponding *tan δ*, used to describe loss in non-ideal capacitors. The phase angle φ is the out-of-phase component divided by the in-phase component, while the loss angle δ is the in-phase component divided by the out-of-phase component (Grimnes and Martinsen, 2015). For an ideal capacitor, the current leads the voltage by 90°, while for an ideal resistor the current and voltage are in-phase. In tissue there are no ideal resistors or capacitors, and δ is the difference in angle from the ideal capacitor (Figure 3).

$$\delta = 90^o - \varphi \qquad \text{(Grimnes and Martinsen, 2015)} \tag{4}$$

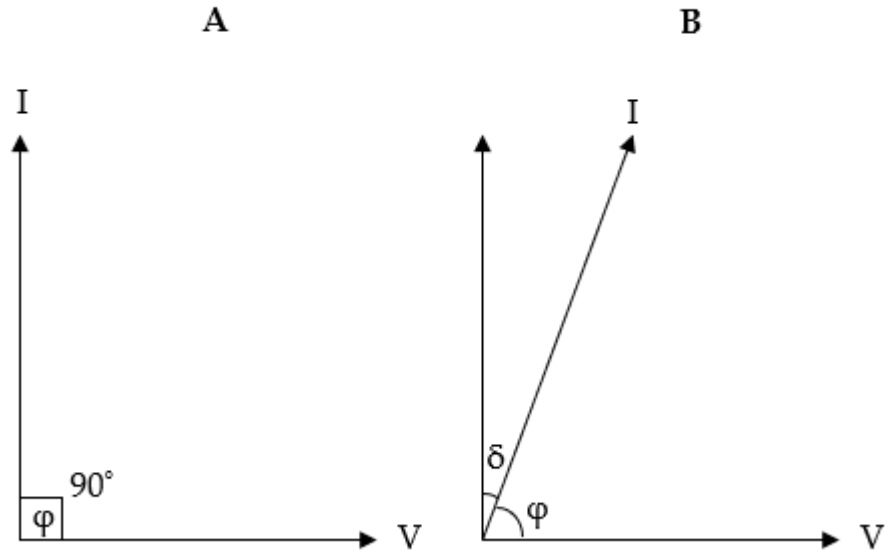

Figure 3. A: The phase relationship between charging current (I) and applied voltage (V) in an ideal capacitor. **B:** The phase relationship between charging current (I) and applied voltage (V) in a lossy dielectric material.

tan δ, also known as loss tangent, dielectric loss or dissipation factor, is a measure of the loss rate of oscillating electric energy. The energy lost is dissipated as heat. *tan δ* is often used when describing the properties of dielectrics and is calculated as a ratio between the complex components of permittivity. *tan δ* is the ratio between the imaginary and real part of the permittivity.

$$\boldsymbol{\varepsilon(\omega)} = \varepsilon'(\omega) - j\varepsilon''(\omega) \qquad [\mathrm{F/m}] \qquad (5)$$

$$\varepsilon'(\omega) = \frac{-Z''}{C_0(Z'^2 + Z''^2)\omega} \qquad [\mathrm{F/m}] \qquad (6)$$

$$\varepsilon''(\omega) = \frac{Z'}{C_0(Z'^2 + Z''^2)\omega} \qquad [\mathrm{F/m}] \qquad (7)$$

As we see from equations (6) and (7), *tan δ* is the ratio between the real and imaginary part of ***Z***.

$$tan\ \delta = cot\ \varphi = \frac{\cos\varphi}{\sqrt{1-cos^2\varphi}} = 2\pi f R^* C^* = \frac{\varepsilon''}{\varepsilon'} = \frac{R*}{X*} \qquad [\mathrm{Dimensionless}]^{12} \qquad (8)$$

As it is a ratio parameter, *tan δ* may differ at similar values of ***Z***. While ***Z*** is strongly dependent on the distance between two electrodes, *tan δ* will vary less with changes in electrode distance, because it represents the relationship between the real and imaginary components of ***Z*** (Heo and Jung, 2011).

[12] *R**, *C**, *X** are the equivalent series components.

1.3 Tissue and tissue states versus electrical properties

1.3.1 The passive electrical properties of tissue

The passive electrical properties of tissue are given primarily by a combination of the following factors (Grimnes and Martinsen, 2015):

a) Ionic concentration
b) Volume fraction of fluid
c) Distribution of fluid in the tissue structures
d) The ion-permeability of cell membranes and membrane structures
e) Polarization mechanisms

Biological tissue is a very heterogenous domain with complex structures containing mazes of liquid spaces and tunnels, separated by diverse membranes, often resulting in a combination of serial and parallel paths where the electric current can travel depending on the frequency of the applied signal. Biological tissue is neither an ideal conductor nor an ideal dielectric but carry properties of both. Thus, the impedance of tissue is always frequency dependent.

The structural origins resulting in the electrical/dielectrical properties of the tissue is a combination of microscopic structures (Figure 4) like cell membranes, intracellular space with organelles, ion-channels and extracellular space, and the macrostructures of different organs, the vascular system, connective tissue, membranes (like the serous or mucous), tissue layers, tissue interfaces and the skin. The different tissue types have different cell structures, varying in density, size, and connective layout. Some tissue structures, like myocytes[13], have anisotropic properties, due to their shape and length.

In biological tissue the reactive properties are mainly capacitive ($X_L \approx 0$) (Grimnes and Martinsen, 2015). The dielectric structures behind the capacitive reactance are the low conductive cell membranes (10^{-6} S/m) (Grimnes and Martinsen, 2015) and the membrane structures surrounding most types of tissue. The cell membranes consist of thin lipid layers that contain several types of ion-selective semi-permeable[14] channels related to cell function and intercell communication. The cell membrane permeability is dynamic (Bischof *et al.*, 1995), depending both on the internal state in the cell and external variables.

When applying DC to biological tissue, current implies mass transport[15], and the conducting paths are primarily movement of ions in the extracellular liquids between the cellular structures, ion movement in the vessels of the vascular system and in the cell-to-cell ion-channels. When applying AC, the cell membranes and other membrane structures act as capacitors with charge building up along the dielectric structures, and the AC moves with the frequency of the alternating polarization. Thus, at low frequencies the paths in the extracellular space dominate, while at higher frequencies current paths are opened across membrane structures (Figure 4). The effect is typically a reduction in measured impedance with higher frequency.

[13] Muscle cells
[14] As some ions are allowed to pass, while others are not.
[15] Movement of ions

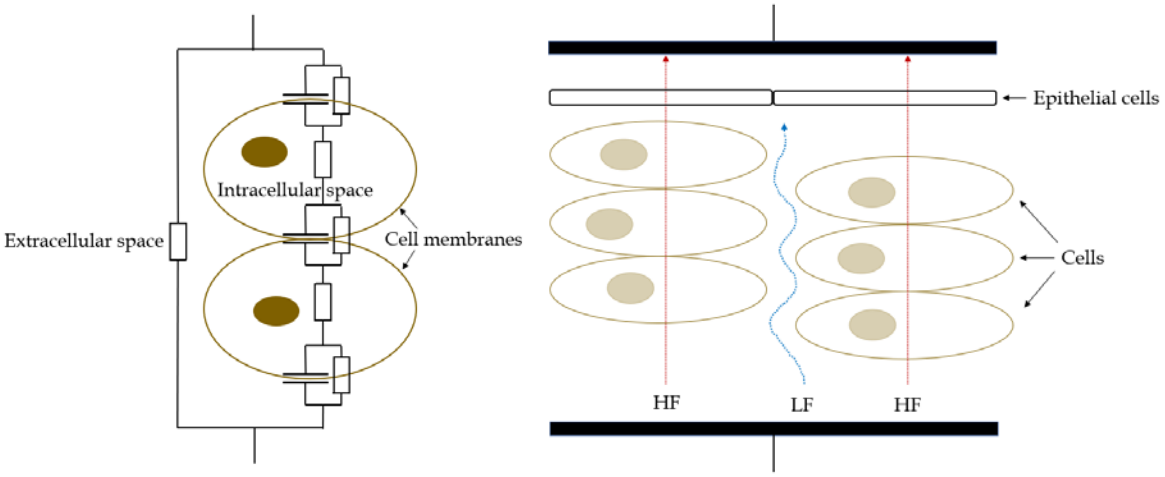

Figure 4. Left: An electrical model on the cellular level, with the current paths across the extracellular space (resistor), and the current paths across the cell-membranes (capacitor|| resistor) and intracellular space (resistor) (with permission, Antoni Ivorra) (Ivorra, 2005). **Right:** An example of the frequency dependence of current paths across tissue. HF = High frequency current, LF = low frequency current.

As polarization requires a certain amount of time for the dipole moments to align with the applied electric field, permittivity in tissue will decrease with increasing frequency. The following six mechanisms are a summary of the theories with respect to exogenic polarization in biological matter (Kumar, 2011, Grimnes and Martinsen, 2015, Polk and Postow, 1996):

a) Dipolar orientation
b) Macrostructural polarization
c) Ordering of water structure
d) Counter-ion polarization
e) Interfacial polarization
f) Delocalization of electrons

The polarization mechanisms give rise to the dielectric dispersion areas (Schwan, 1957, Dean *et al.*, 2008) found in biological tissue (Figure 5):

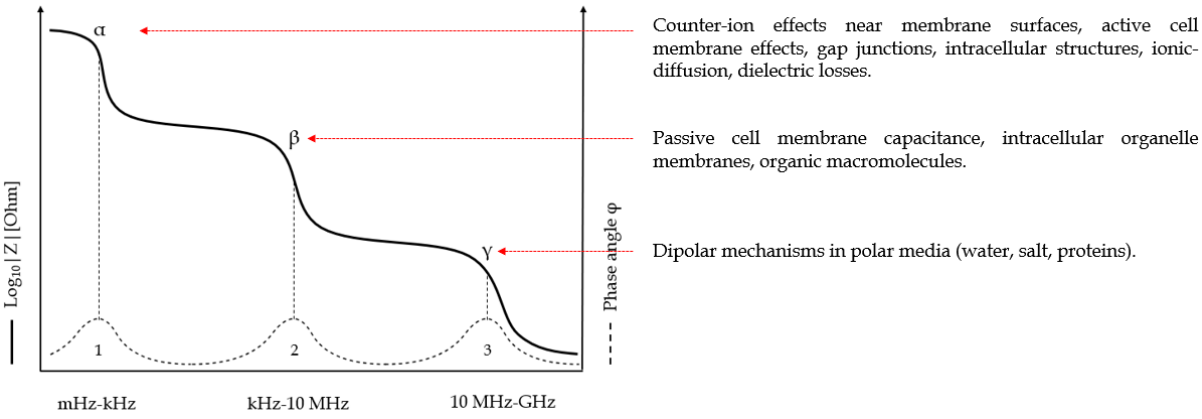

Figure 5. An idealized representation of impedance modulus |Z| and phase angle φ as a function of dispersion regions *α, β and γ* in biological tissue.

1.3.2 Ischemia/reperfusion and the effect on passive electrical properties of tissue

With ischemia, the delivery of oxygen, nutrients, and the removal of waste products, fails to meet the demands of the tissue and the metabolism switches to anaerobic. The limited supply of adenosine triphosphate combined with the accumulation of metabolic products, calcium increase, and reduced pH, give rise to cellular ionic imbalance. This leads to intracellular edema, mitochondrial alterations, calcium overload and changes to the cell membrane (Gutierrez, 1991). Over time ischemia will lead to cell death if perfusion is not restored.

Electric bioimpedance has been utilized to investigate changes in electrical parameters during ischemia in various tissues (Gersing, 1998, Gheorghiu and Gersing, 2002, Schafer *et al.*, 1998, Martinsen *et al.*, 2000, Salazar *et al.*, 2004, Casas *et al.*, 1999, Kun and Peura, 1994, Asami, 2007, Schafer *et al.*, 1999, Ivorra, 2005). Ischemia leads to physical alterations on several levels in the tissue, resulting in changes over time in the electrical properties. Several mechanisms have been generally accepted by researchers as connections between changes in electrical parameters and ischemia-related physical changes in the tissue:

1. The closing of gap junctions leading to an increase in low frequency (LF) resistance (Schwan, 1957, Foster and Schwan, 1989, Asami, 2007), and to changes in or disappearance of the α dispersion (Schafer *et al.*, 1998, Gersing, 1998).
2. The narrowing of extracellular pathways due to the gradual swelling of cells when the pump function fails, leads to an increase in LF resistance (Gersing, 1998, Grimnes and Martinsen, 2015).
3. Formation of extracellular edema leading to reduced impedance over the frequency spectrum (Radhakrishnan *et al.*, 2007, Moore-Olufemi *et al.*, 2005).
4. A reduction in temperature in the tissue due to reduced circulation, resulting in an increase in impedance (Grimnes and Martinsen, 2015).
5. The presence of the β dispersion (see figure 5) has been linked to the integrity of the cell membrane. As the cell membranes lose integrity, the β dispersion will gradually disappear (Pauly and Schwan, 1964, Peyman and Gabriel, 2005).
6. Reduced membrane resistance caused by the opening of ion channels and increasing membrane permeability as it gradually fails due to prolonged ischemic exposure, leads to a decrease in LF resistance. (Schafer *et al.*, 1998, Grimnes and Martinsen, 2015).
7. Cell necrosis leads to a decrease in overall impedance (Martinsen *et al.*, 2000).

A simplified approach is to view the real part of the measured impedance as reflecting the relative contribution of fluid, and the imaginary part of the impedance to reflect the relative contribution of cell membranes and membrane structures. Thus, a low phase angle φ (or a high *tan δ)* can be associated with decreased cell integrity or cell-death (Gupta *et al.*, 2009), and the disappearance of the Beta dispersion (β) as the cell membranes collapse (Grimnes and Martinsen, 2015). Using a Cole model (Cole, 1940) with parameters for intracellular R and extracellular R, as well as membrane capacitance, the rupture of cell membranes equals removing a series capacitor, creating a more parallel system resulting in increasing capacitance (Dodde *et al.*, 2012). These mechanisms are easier to interpret in a large semi-

homogenous tissue structure like the kidney or spleen, than in a more complicated, multilayered and far-from-homogeneous tissue like the small intestine.

1.4 Previous work with bioimpedance and the small intestine

In order to approach the questions of estimation of injury to intestinal tissue and assessment of viability, researchers have studied the electrical properties of the small intestine, using in-vivo and ex-vivo models on various animals. The earliest report we have found about electrical measurements on the in-vivo small intestine was made in 1964 (Carey *et al.*, 1964). The impedance of ischemic canine small intestine was measured over a 15 min ischemia interval, using a 3-electrode setup on the surface of the intestine, reporting that ischemia led to gradually increasing impedance (Carey *et al.*, 1964).

Takeyoshi *et al.* measured in situ using the Ussing chamber technique on canine colon and small bowel (Takeyoshi *et al.*, 1996), reporting decreasing impedance across the small intestinal wall during ischemia. Gonzales *et al.* measured *in-vivo* on 16 rabbits, using a four-electrode probe inside the lumen on the mucosal side of the small intestine (Gonzalez *et al.*, 2003), reporting that initially there was an increase in impedance in the ischemic tissue compared to the control, and that after longer duration of ischemia there was decreased impedance compared to the control.

Matsuo *et al.* investigated the viability of strangulated rat small intestine (ileum) in-vivo, using a coaxial 2-electrode probe on the serosa (Matsuo *et al.*, 2004) introducing the use of the *tan δ* parameter. Radhakrishnan *et al.* measured in-vivo with two small wire electrodes on the surface of rat intestine and found that intestinal edema led to decreasing impedance (Radhakrishnan *et al.*, 2007). Beltran *et al.* have done a lot of work related to experiments and instrumentation using a four-electrode probe inside the intestinal lumen and have reported the ability to detect mucosal injury (Beltran *et al.*, 2007, Beltran *et al.*, 2013b, Beltran and Sacristan, 2015).

Bloch *et al.* however evaluated this method and reported that they were not able to detect early changes in the electrical parameters of the alimentary tract during progressive hemorrhage or re-transfusion (Bloch *et al.*, 2017). The results of Bloch *et al.* show that the previously reported results with detection of mucosal ischemia with the use of intraluminal electrode catheters might be overrated. We have not found any bioimpedance method providing a solution for assessment of intestinal viability.

1.5 The small intestine

The small intestine (Figure 6) has three distinct regions, the duodenum, jejunum and ileum and is an organ performing several vital functions in the body, including:

1. Bile from the liver and enzymes from the pancreas are mixed with the food content in the small intestine, through peristalsis.
2. The digestion of proteins, lipids and carbohydrates.
3. The absorption of nutrients, minerals and water.
4. An important part of the immune system, holding a large part of the gut bacterial flora.

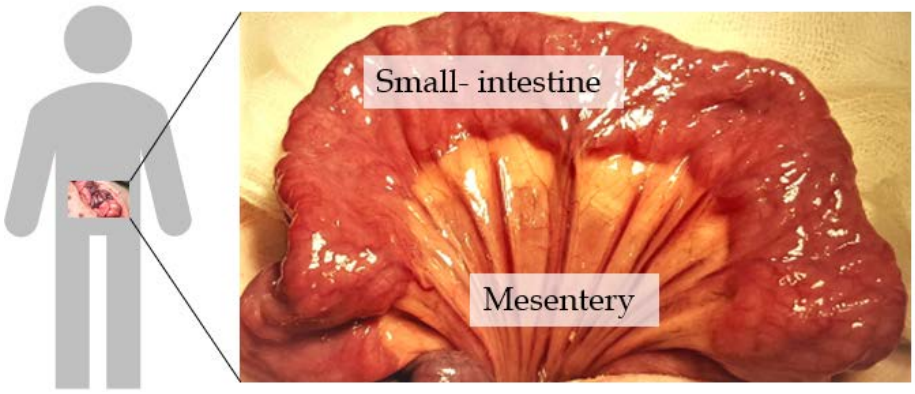

Figure 6. The small intestine with mesentery (vascular supply). The intestine shown in the picture is from a pig.

The blood flow to the intestines is supplied by three arteries. The gastroduodenal artery supplies the stomach and the duodenum. The superior mesenteric artery supplies most of the small intestine and the proximal large intestine. The inferior mesenteric artery supplies the rest of the large intestine. There are several anastomoses between the arteries, to prevent interruption in blood flow to the intestines, and the arteries and veins branch into smaller vessels that enter and exit the intestine through the mesentery. The complex vascular supply is of benefit in certain cases of ischemia, as the blood can move via collaterals, but this also complicates the task of assessing the scope of intestinal injury following ischemia. The circular wall of the small intestine consists of a flexible multilayer structure (Figure 7).

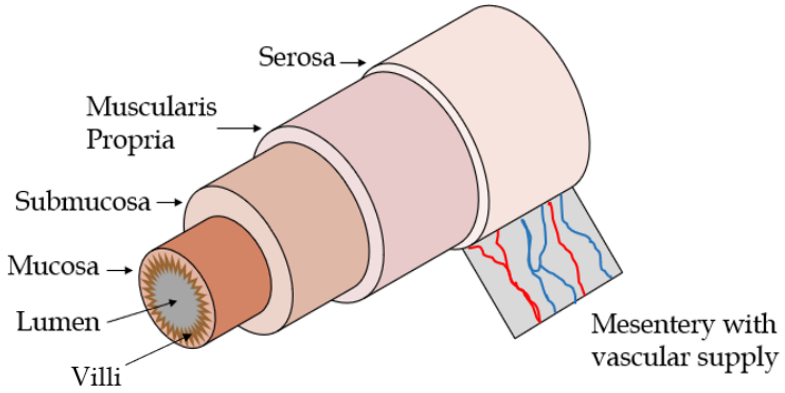

Figure 7. A simplified overview of the layer structure of the small intestine

1.5.1 The pathology of ischemic injury in the small intestine

Histologically, early epithelial detachment at the villus tip can be observed after the onset of ischemia, followed by extension of the sub-epithelial space and epithelial lifting along the villus side, gradual denudation of villi, and loss of villi (Takeyoshi *et al.*, 1996). In these first stages, the ischemic damage occurs at the mucosal side, and the intestine is still viable. These are followed by infarction of the crypt layer and transmucosal infarction (Takeyoshi *et al.*, 1996). Mucosal necrosis will usually heal without surgery. Mural necrosis may to a certain extent heal without surgery, while transmural necrosis ends with perforation, leading to

peritonitis and sepsis (Chou *et al.*, 2006). Formation of scar tissue following the healing of ischemia/reperfusion injury can cause strictures to develop later (Swerdlow *et al.*, 1981, Mitsudo and Brandt, 1992).

1.5.2 Ischemia as a primer for reperfusion injury

There are several mechanisms occurring in ischemic tissue that make it susceptible to ischemia reperfusion injury (IRI) when reperfusion is later introduced. Ischemia promotes the expression of proinflammatory gene products and bioactive agents within the endothelium, while repressing other gene products that have protective effects (Parks and Granger, 1986, Carden and Granger, 2000). Adenine nucleotide catabolism gives rise to intracellular accumulation of hypoxanthine (after more than 60 minutes of ischemia) (Linfert *et al.*, 2009), which is converted into reactive oxygen species (ROS) after reperfusion (Kaminski *et al.*, 2002, Parks and Granger, 1986). Resident polymorphonuclear leukocytes[16] (PMN) migrate from the intravascular space to the interstitium during hypoxia. This migration might disrupt the endothelial barrier causing extravascular fluid leakage and edema formation (Eltzschig and Collard, 2004).

1.5.3 Reperfusion injury

While there is a series of underlying etiologies[17] that can result in intestinal ischemia, an early part of the clinical treatment in all cases is the restoration of perfusion (Kalogeris *et al.*, 2012). While reperfusion is essential to prevent further tissue damage, it can in itself cause both local and systemic responses that have the potential to induce injury far beyond the direct damage caused by the ischemia (Eltzschig and Collard, 2004, Yandza *et al.*, 2012, Parks and Granger, 1986).

At the onset of reperfusion, the post-ischemic tissue experiences initial reactive hyperemia (Dabareiner *et al.*, 2001). An important cause for IRI is the accumulation of ROS in the reperfused tissue, together with the reintroduction of molecular oxygen. At an early stage after reperfusion, ROS are generated from hypoxanthine accumulated during ischemia and the freeing of intracellular iron. At a later stage, more ROS is generated by PMN, accumulating in the reperfused tissue as a part of the immune response (Yandza *et al.*, 2012).

ROS can cause increased microvascular permeability, edema, thrombosis and cell death. Other important causes for IRI are calcium overload, opening of the mitochondrial permeability transition pore, endothelial dysfunction, and pronounced inflammatory responses (Yellon and Hausenloy, 2007). The leakage of components from dying cells will amplify the inflammatory response (Grootjans *et al.*, 2010).

With small intestinal IRI the initial inflammation can be sterile, but as the microvascular and structural permeability changes, the translocation of molecules and the passage of microbes across the intestinal wall creates non-sterile inflammation. PMNs also release pro-inflammatory cytokines that activate humoral protein cascades such as the coagulation and complement systems (Kong *et al.*, 1998). These activations can cause reduced microcirculation and thrombosis. The combination of the many mechanisms occurring

[16] White blood cells
[17] Cause of disease

during reperfusion, can create self-perpetuating systemic inflammation (Kong *et al.*, 1998). Thus, reperfusion is a complex phenomenon, with the potential of drastically increasing the level of injury in intestinal tissue.

2 Aim and objectives

The overall aim of this work is to develop new methods based on electrical bioimpedance that can improve the accuracy and precision of intraoperative assessment of intestinal viability. The potential benefits are a reduction in the frequency of short bowel syndrome caused by excessive removal of suspicious bowel, a reduction in anastomotic leakage caused by selection of unviable or irreversibly injured locations for resection margins and a possible reduction in the occurrence of sepsis due to non-viable bowel being left in the patient. In addition, an early assessment with high accuracy can reduce the surgical stress experienced by a patient, if there is no need for second- or third-look operations. The motivation for this work is based on the potential to reduce the high mortality and morbidity rates associated with acute mesenteric ischemia (AMI).

To achieve the overall aim, we defined the following objectives:

1. To examine the feasibility of measuring the passive electrical properties of the porcine small intestine.
2. To assess how the passive electrical properties of the porcine small intestine are influenced by ischemia.
3. To examine the possibility of using an ex-vivo model instead of an in-vivo model for AMI.
4. To assess how the electrical properties of the porcine small intestine are affected by reperfusion.
5. To investigate the viability limit in a porcine model of intestinal ischemia, to provide a reference.
6. To investigate methods to analyze the bioimpedance data in order to classify viability and histological grade, following ischemia-reperfusion injury in porcine small intestine.

3 Methodological considerations

3.1 The pig as a model for intestinal ischemia (papers I-V)

We selected the pig model for viability assessment of the small intestine, as it has important anatomical and physiological similarities to humans (Douglas, 1972), the pathophysiology of ischemia/reperfusion in the porcine model is similar to humans, and because this model has been suggested as a reference standard in intestinal transplantation research (Yandza *et al.*, 2012). The main differences between the human and pig small intestine are related to the length, and some small differences in the structure of the vascular system in the mesentery and in the intestinal villi (Ziegler et al., 2016).

3.1.1 Ethical approval

The animal protocols were designed to minimize pain or discomfort to the animals and reduce the overall number of animals used. The experiments were approved by the Norwegian Food Safety Authority (FOTS ID 5143, 8304, 12695) and conducted in accordance

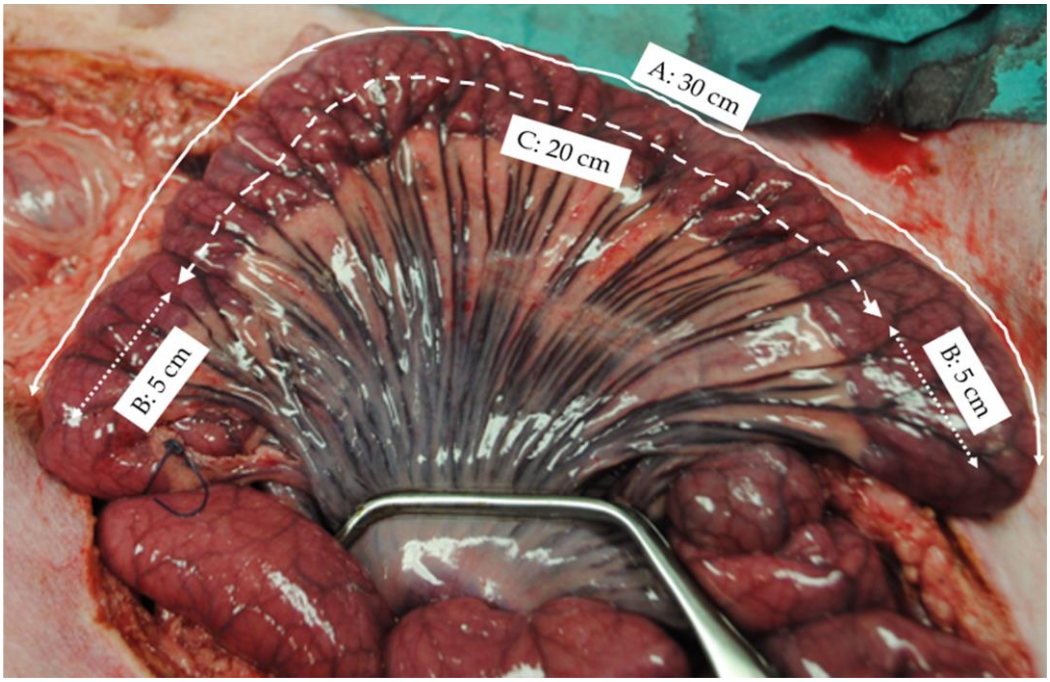

Figure 8. Segmental mesenteric occlusion of a segment (A: 30 cm, whole line) of porcine jejunum, creating two edge zones of marginal tissue hypoxia (B: 5 cm, dotted line) and a central zone of warm ischemia (C: 20 cm, dashed line).

with Norwegian animal welfare guidelines (FOR-2015-06-18-761) and EU directive (2010/63/EU).

3.1.2 Segmental mesenteric occlusion model (papers I-V)

The segmental mesenteric occlusion (SMO) model (Gonzalez et al., 2015, Noer and Derr, 1949) was selected as it provides a well-defined area of ischemic injury affecting the whole intestinal wall in the occluded segment (Yandza *et al.*, 2012), as opposed to the commonly used intestinal ischemia model of occlusion of the superior mesenteric artery (Gonzalez *et al.*,

2015, Megison *et al.*, 1990). The SMO model simulates ischemic injury as caused by strangulation-obstruction. Ischemia was induced by atraumatic clamping (Figure 8) of the arteries and veins of the jejunal mesentery on the selected segments[18] (Chan *et al.*, 1998, Gonzalez *et al.*, 2015). Reperfusion (papers III-V) was initiated by releasing the clamps and verified by observing the return of color in the individual arteries and veins and in the previously ischemic segment. The details of the surgical procedures, anesthesia and monitoring are described in papers I-IV (Strand-Amundsen et al., 2016, Strand-Amundsen et al., 2018a, Strand-Amundsen et al., 2017, Strand-Amundsen et al., 2018b).

3.1.3 Study population (papers I-V)

Table 3 shows an overview of the study population in the 3 experiments included in this thesis.

Table 3. An overview of the study population

	Experiment I	**Experiment II**	**Experiment III**
Study	I	II	III-V
Type of experiment	In-vivo	In-vitro	In-vivo
Number of pigs	7	6	15
Sex [f/m]	4 f	5 f	11 f
Weight [kg]	26.5 - 30.0	49.9 - 58.6	44.3-58.6
Control segments*	1	1	2
Ischemia only segments*	1	3	0
Ischemia/reperfusion segments*	0	0	5-6
Histology	LM**	LM**	LM**/TEM***

* in each pig

**Light microscopy

***Transmission electron microscopy

As can be observed in Table 3, with increasing experiment number, we increased the number of parallel ischemic segments used in each pig. In addition to the study population of experiments I-III, 5 pigs were used in a pilot experiment to assess different electrode setups and materials (unpublished results).

3.1.4 Using several parallel ischemia/reperfusion models in the same pig (papers III-V)

A 50 kg pig has approximately 15 meters of small intestine (McCance, 1974), allowing for the creation of several parallel SMO models (Chan *et al.*, 1998, Cook *et al.*, 2008, Moeser *et al.*, 2007, Yandza *et al.*, 2012), reducing the total number of animals needed for the experiment. However, there are some disadvantages with parallel ischemia/reperfusion models in the same pig.

a) The cytokine levels are reduced for each repeated reperfusion in the same pig, due to increasing tolerance levels (Cavaillon *et al.*, 2003, Ruud *et al.*, 2007).
b) Following the late reperfusion intervals, we observed systemic effects with periods of increasing heart rate, decreasing blood pressure, fever, and increasing permeability of the intestines. These effects are probably related to the release of increasing quantities of harmful substances following the late reperfusion intervals (Willerson, 1997, Carden and Granger, 2000).

[18] In study I and II there was only one ischemic segment in each pig. In study III there were parallel segments in the same pig.

To assess how these effects influenced the state of the surrounding perfused jejunum, we inspected the control tissue after 12 hours of experiment duration and found only light changes using light microscopy and transmission electron microscopy (Strand-Amundsen et al., 2018a). Microdialysis and histological grading systems did not indicate any changes in the control specimens. So, although some minor changes could be observed in the control intestine, we find it unlikely that this had any confounding effects on the outcome of the experiments.

3.2 Bioimpedance

3.2.1 Instrumentation (papers I-III, V)

For all experiments, a Solartron® 1260 Impedance/gain-phase analyzer (Solartron Analytical, United Kingdom) was used with a 1294A interface. Solartron 1260 uses a single-sine digital lock-in[19] after sampling the signals with 16 bits ADC, and uses 3 frequency dependent methods for lock-in. For frequencies above 65.5 kHz Solartron uses an analogue phase locked loop for both output and reference signal. For 300 Hz – 65.5 kHz a digital heterodyning process is used. Below 300 Hz the measurements were done directly by the ADC (Grimnes and Martinsen, 2015). We used the Solartron to apply a controlled voltage, while measuring the resulting current and calculating the admittance/equivalent impedance. The Solartron was controlled, data logged, and measurements acquired by the Zplot® software (Copyright © 1990-2015 Scribner Associates, USA). A 50 mV AC RMS signal was applied across the electrodes while sweeping the frequencies from 1 Hz to 1 MHz in 61 steps.

3.2.2 Factors influencing the bioimpedance measurements

There are several factors in addition to the passive electrical properties of tissue that influence bioimpedance measurements. These should be removed or compensated for before analysis of data is performed, either during measurements in real-time or during post-processing.

3.2.2.1 Tissue temperature

The ionic mobility in the tissue is affected by temperature, resulting in an approximate 2% increase in conductivity per increased degree Celsius (Schwan HP and Foster KR, 1980). We monitored the surface temperature of the small intestine using an IR-thermometer (bosotherm medical, Bosch + Sohn, Germany).

3.2.2.2 Intrinsic properties of electrodes and the experimental setup

The electrodes have intrinsic electrical properties that are in series with the measured electrical properties (two electrode setup). In addition, the instruments and wiring will affect the measurements, especially with respect to stray reactance (Grimnes and Martinsen, 2015). To compensate for this, the electrodes and experimental setup were characterized, and the measured data compensated for the stray properties of the setup.

3.2.2.3 Electrode polarization impedance.

The electrodes are the interface between the biological tissue and the electronic measurement system. When applying a voltage across metal electrodes placed in contact with tissue, there is a charge carrier transition between the metal surface with free moving electrons, and the

[19] Phase-sensitive rectifier

tissue with ionic charge carriers. The innate properties of the metal and an applied voltage across the electrodes, attracts ions of opposite charge. These ions form a charge layer (polarization) near the surface of the electrode, which again attracts more ions resulting in a double layer and a diffusion layer (Ishai *et al.*, 2013). The effect of the polarization is an unwanted frequency-dependent impedance in series with the electrodes. The contribution from electrode polarization can be reduced by increasing the electrode surface, using non-polarizable electrodes, or electrodes with rough surface structures (Kalvoy *et al.*, 2011, Schwan, 1968). Using 9 mm diameter (Area = 63.6 mm^2) non-polarizable Ag/AgCl electrodes resulted in very low electrode polarization impedance, that started to dominate gradually below 100 Hz.

3.2.2.4 Geometric effects

The measured electrical properties (conductance/resistance) are a function of the volume independent specific electrical properties (conductivity/resistivity) of the tissue combined with a parameter known as the cell constant K [cm^{-1}], accounting for the geometric aspect.

$$K = \frac{Resistance}{Resistivity} \tag{9}$$

For a parallel plate electrode setup, the geometric properties d = distance between electrodes, and A = electrode area, can be used with the specific resistivity to calculate the resistance and capacitance:

$$Resistance = \frac{Resistivity \bullet d}{A} \tag{10}$$

$$Capacitance = \frac{\varepsilon_0 \varepsilon_r A}{d} \tag{11}$$

The cell constant is relevant for measurement of homogenous substances like liquids. In a multilayered tissue like the small intestine, the specific electrical properties vary, and other approaches (3.2.8) are more relevant to account for geometric effects.

3.2.2.5 Compression and displacement in soft tissues

When measuring on soft tissue like the small intestine, exerting pressure on the intestinal walls not only affect the contact area, but can strongly influence the measured electrical properties (Dodde *et al.*, 2012, Dodde *et al.*, 2015, Moqadam *et al.*, 2015). Pressure can also lead to mechanical displacement of the layered structures. When there is serosal or submucosal edema, the intestinal wall is even more sensitive to pressure as a high pressure will result in the excess liquid being squeezed out from the measurement area between the electrodes, affecting the measurement. Studies on the electrical effect of tissue compression (4-electrode test setup) has reported that for compression of tissue up to 50% of its original volume, there is an increase in resistance, while for compression over 50% there is a decrease in resistance (eq.10), and also an increase in capacitance (eq.11) (Dodde *et al.*, 2012).

The size of the electrodes used influences the pressure sensitivity of the electrode setup, with small electrodes resulting in larger variability due to pressure (Keshtkar and Keshtkar, 2008). As the intestinal tissue is layered and heterogenous, it is difficult to compensate for the effects of compression, and our approach was to use large electrodes and

minimal pressure sufficient to ensure good electrical contact[20] without causing significant compression. To verify the effects, pilot bioimpedance measurements were done with various grades of compression, and on single, double and triple layers of intestine. We aimed to avoid mechanical pressure higher than the capillary pressure of around 20 mmHg, as that would cause local ischemia between the electrodes during the measurement period.

3.2.3 Electrode setup

3.2.3.1 Previous work

The most commonly used electrode setup to measure the electrical properties of the small intestine has been to use an intraluminal 4-electrode ring setup (Bloch *et al.*, 2017, Beltran *et al.*, 2005, Beltran *et al.*, 2013a, Beltran *et al.*, 2007, Beltran *et al.*, 2013b, Beltran and Sacristan, 2015, Gonzalez *et al.*, 2007, Gonzalez *et al.*, 2003), sending a current between the outer electrode rings, while measuring the voltage across the inner electrode rings, with the assumption that some of the current passes through the mucosal layer affecting the measured complex impedance (Figure 9).

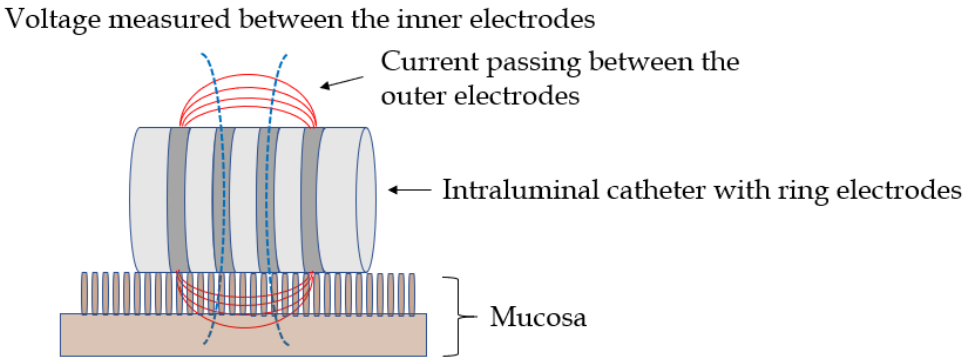

Figure 9. The most commonly found electrode setup for measurement of the electrical properties (of the mucosal part) of the small intestine.

As the current with the intraluminal 4-ring electrode setup will only pass through a small part of the mucosa, we estimate that this method is not usable with respect to assessment of intestinal viability.

3.2.3.2 Selecting the electrode setup for measurement on the small intestine

A general problem in bioimpedance is the selection of measurement volume (Grimnes and Martinsen, 2015). When utilizing bioimpedance, the researcher typically has some questions in mind with respect to the electrical properties of some part of a tissue. Choosing a relevant electrode setup is essential for the later results. A typical setup is to use a 2-electrode setup[21], where a known sinusoidal voltage is applied across the electrodes, and the resulting current is measured. A limitation for using the 2-electrode setup is the unwanted contribution arising from electrode polarization impedance. A 3-electrode setup is inherently monopolar and can be used to influence the depth of the measurement. A monopolar electrode setup allows for the electrical properties near one electrode to dominate the measurement, as opposed to a bipolar setup. A 4-electrode setup measures transfer impedance and allows for

[20] Exclude air between the intestinal surface and the electrodes
[21] Each electrode acting both as stimulating and pickup electrode

measurement without the contribution of electrode polarization impedance. While a 4-electrode setup can be relevant in many settings, it is also more vulnerable to errors than with bipolar electrode setups (Grimnes and Martinsen, 2007).

With the aim of being able to assess intestinal viability, it is important that the electrode setup is sensitive to the structural changes of the small intestine that occur as a function of ischemia or reperfusion. The pathophysiological changes that occur in the small intestine as a result of ischemia are starting at the villi tips of the mucosa, with a gradual development of injury through the deeper layers of the intestine (Mitsudo and Brandt, 1992, Haglund *et al.*, 1987) (Figure 10). At the same time, it is important not to use an electrode setup that will puncture the small intestine, as this can lead to increased risk of morbidity.

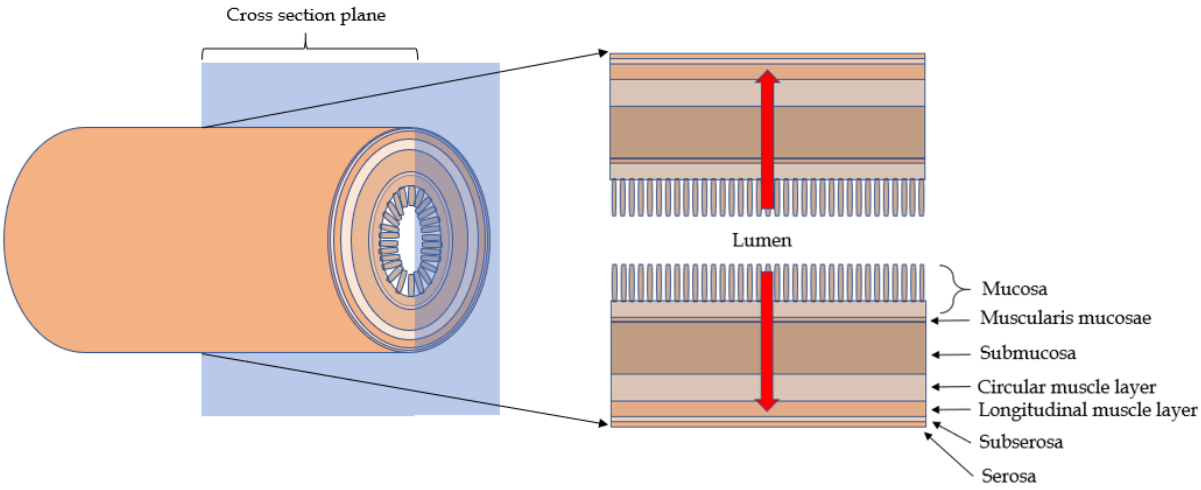

Figure 10. A cross section plane of the small intestine with layers. The red arrows show the general direction of the time dependent development of ischemic injury through the layers of the small intestine.

For selection of an electrode setup, a series of different setups were evaluated during a series of pilot tests on 5 pigs (unpublished work). We investigated a monopolar setup using needle electrodes, as well as 2-, 3- and 4-electrode setups with various electrode materials (Ag/AgCl, stainless steel, Au), electrode sizes (1mm – 10mm) and electrode layouts (Figure 11). We tested measurement along the side of the intestine, versus trans-intestinal measurements.

During the pilot tests, ischemia was induced in the small intestine of 5 pigs, and the setup with two electrodes on opposite sides, perpendicular to the surface of the small intestine (see Figure 11), was found to best capture the electrical properties of the whole intestinal layer structure and was most sensitive to the changes that occur during ischemia (unpublished work). As a voltage was applied across the electrodes and a small current passed through the intestinal tissue between the electrodes, the measurements are trans-intestinal.

The results from the needle measurements varied a lot with needle location and peristalsis made it difficult to place the needle at the exact same spot each time. The reason for not selecting an electrode setup with electrodes along the intestinal surface was that the modelled sensitivity area (Finite Element Method modelling - COMSOL Multiphysics) with this setup remained near the surface due to the well conducting serosa, and the higher resistivity of the sub-serous layer.

The reason for not selecting a 4-electrode setup is that it is more vulnerable to errors than bipolar setups (Grimnes and Martinsen, 2007), and due to challenges with optimal electrode placement on the intestinal surface with respect to equipotential lines. As the surface of the small intestine is quite well conducting, the current easily shunts across the surface of the pickup-electrodes, resulting in the potential of the PU[22] electrodes being brought to a level which is closer to that of the CC[23] electrodes. This leads to an overestimation of the transfer impedance and can also lead to measuring a positive phase angle (Grimnes and Martinsen, 2007).

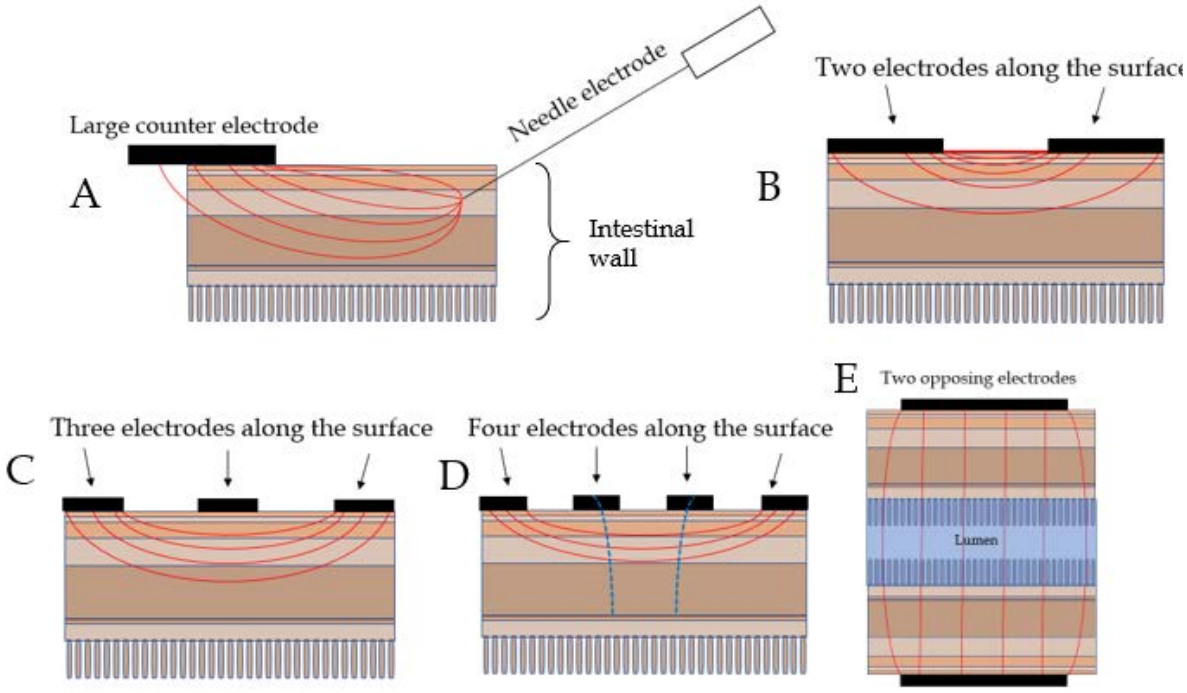

Figure 11. Principle sketches of various electrode setups tested on the small intestine (A-E). Red lines are current paths.

3.2.4 FEM Modelling (paper I)

COMSOL Multiphysics 4.3 (Comsol Group, Sweden) was used to estimate the current density distribution and thereby the sensitivity area of the many electrode setups used in the 5 pig pilot tests. Figure 12 shows an arrow plot of the proportional current density in a 2D model of a cross-section of the small intestine, where an alternating voltage is being applied between two opposing electrodes at low (100 Hz) and high (1 MHz) frequencies. The parameters used for modelling the various layers of the small intestine are based on the tissue data from the Italian national research council/Institute for applied physics/IFAC-CNR (Andreuccetti *et al.*, 2000), which uses the data from Gabriel & Gabriel (Gabriel and Gabriel, 1996).

[22] Pick Up
[23] Current Carrying

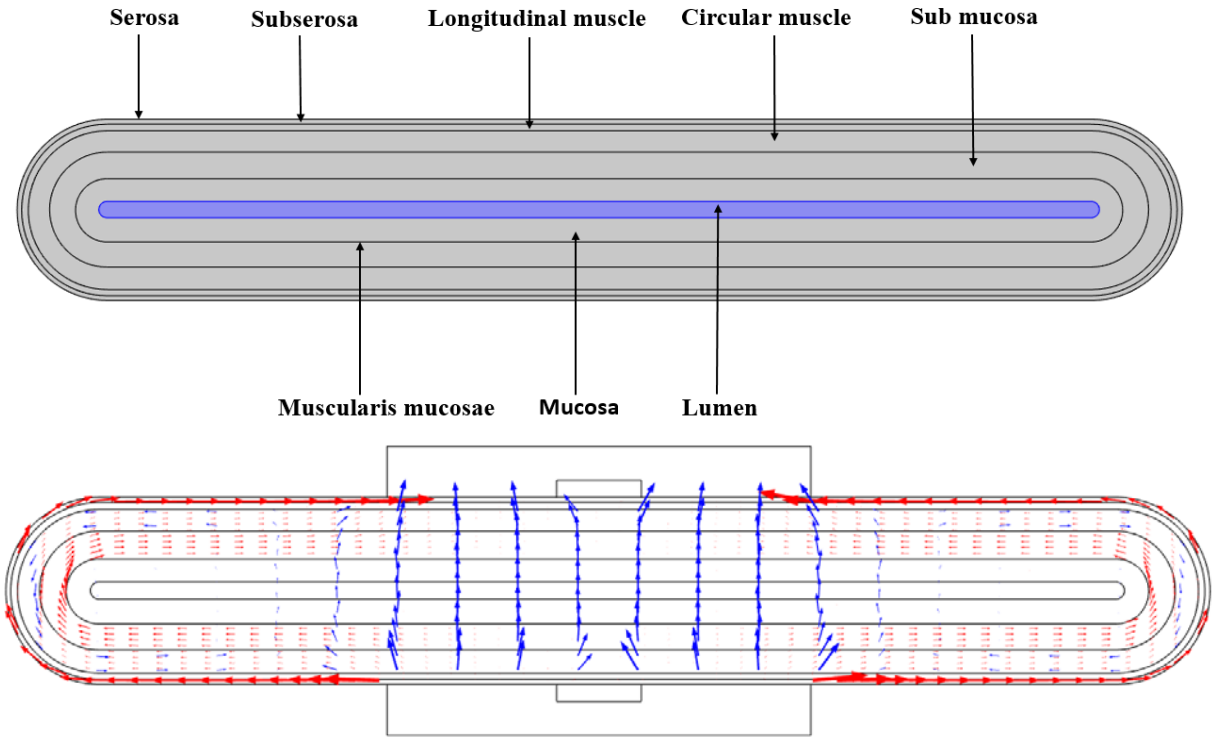

Figure 12. (From paper I, figures 4 and 5). **Top:** Layer structure of the COMSOL Multiphysics 2D model of the small intestine. **Bottom:** COMSOL Multiphysics 2D model with a cross sectional view of the layers of the small intestine with a pair of electrodes placed against the serosa. The red arrows show the proportional current density distribution when applying voltage across the electrodes at 100 Hz and the blue arrows show the proportional current density distribution at 1 MHz (Strand-Amundsen et al., 2016).

With the 2-electrode setup, the dominating part of the sensitivity area is estimated to be in the tissue close to and between the electrodes (frequency dependent). At low frequencies a large part of the current moves in the outer layers of the intestine, while at higher frequencies, the current moves through the deeper layers of the intestine.

3.2.5 Electrode size and material (paper I)

The decision to use 9 mm diameter electrodes was made after observing that the microvascular structure and tissue structure of the small intestine varies a lot on small scale, but there are repetitive patterns on the 2-3 mm scale (Figure 13). By having an electrode that covers several repetitions of the tissue patterns, we get an averaging effect with respect to small-scale variations in tissue structure between the electrodes. Both the Au and the Ag/AgCl electrodes performed well and the Ag/AgCl electrodes were chosen based on the availability, and due to the lower contribution of polarization impedance. With the steel electrodes the polarization impedance dominated gradually below 20 kHz, even when using 10 mm diameter electrodes, reducing the usable frequency range in a 2-electrode setup.

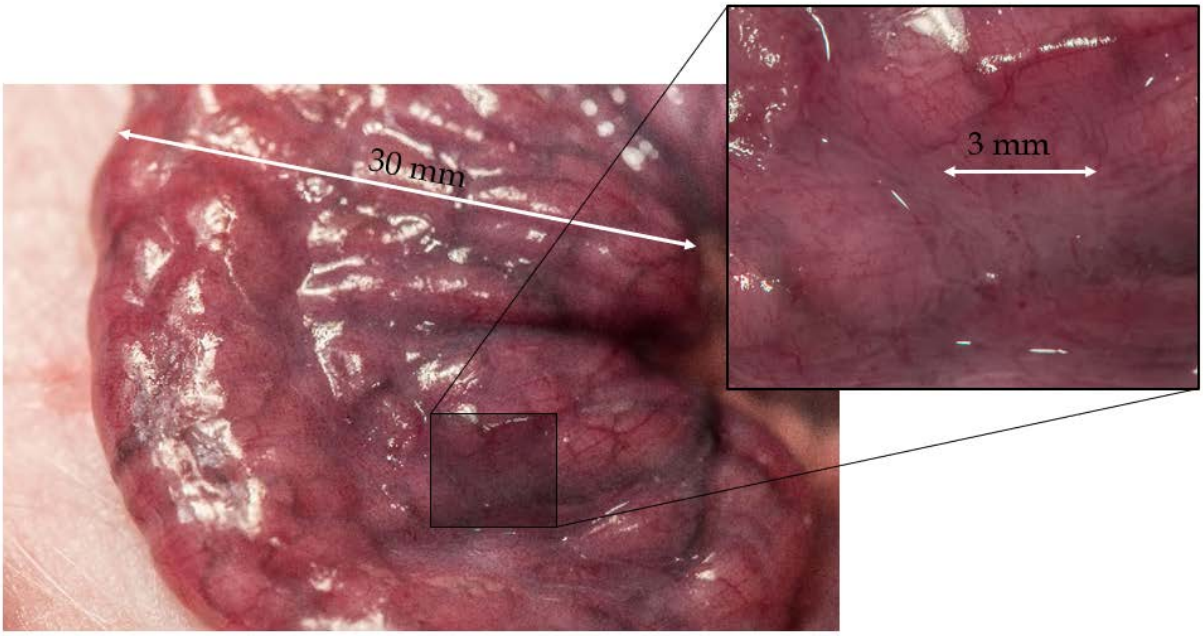

Figure 13. Image showing repetitive patterns of vascular structures visible through the semi-transparent serosa on pig jejunum.

Ag/AgCl electrodes have a constant potential with respect to a similar reference electrode and low impedance to DC and low-frequency signals. It has been shown that using Ag/AgCl electrodes will exert toxic effects on smooth muscle in-vitro (Lukanov and Atmadjov, 1979, Jackson and Duling, 1983) and induce pathological changes when implanted in-vivo (Cote and Gill, 1987). The toxic effect is due to Ag+ interfering with transmembrane Ca 2+ flux (Petering, 1976, Cote and Gill, 1987). It has been shown that when injecting small amounts of Ag+ into an animal, the Ag+ will bind to plasma proteins, resulting in no toxic effect (Klein, 1978). Thus, Ag+ toxicity remains a problem mainly in small scale in-vitro settings, where the available free protein concentration is small. To counter this effect, we stored the Ag/AgCl electrodes in plasma protein during the experiments between the measurements, the exposure time between tissue and electrode was reduced to a minimum, and we used only alternating voltages with no DC component.

3.2.6 Selected electrode setup (papers I-III, V)

After investigating a series of electrode metals, setups and layouts, a 2-electrode setup (Figure 14) with 9 mm diameter Quickels® (Quickels System AB, Sweden) Ag/AgCl electrocardiography disc electrodes (intrinsic R = 0.18 Ω, X = 0 Ω), was chosen for the experiments (Strand-Amundsen *et al.*, 2016, Strand-Amundsen *et al.*, 2017, Strand-Amundsen *et al.*, 2018b). With the 2-electrode setup, the dominating sensitivity area (modelled by COMSOL Multiphysics) is within 1 cm of the sides of the electrodes (at 100 Hz, and closer at high frequencies).

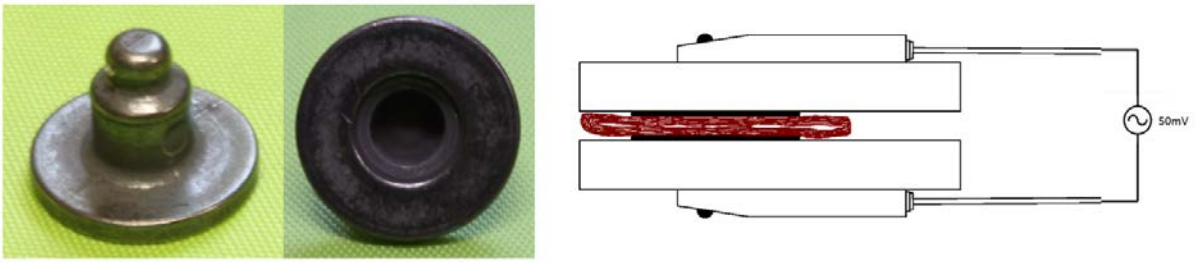

Figure 14. Left: (From paper I, figure 3). The Quickels® (Quickels System AB, Sweden) Ag/AgCl electrocardiography electrodes. **Right:** The positioning of the electrodes (black), mounted on plexiglass (white), showing the positioning of the electrodes with respect to a cross-section of the small intestine (red-brown) (Strand-Amundsen et al., 2016).

3.2.7 Electrical properties of the small intestine and equivalent models

The electrical properties of the small intestine in the range between 1MHz and 10 GHz can be found online (Andreuccetti *et al.*, 1997) based on the measurements made by Gabriel and Gabriel (Gabriel, 1996, Gabriel *et al.*, 1996). Using 4 Cole-Cole (Cole and Cole, 1941) expressions they provide modeled electrical permittivity parameters for the small intestine over a range from 10 Hz to 10 GHz. The Cole expression is a relaxation model for the typical dispersion regions found in biological tissue (Schwan, 1957, Cole, 1940), and describes a depressed semicircle in a Nyquist plot (x = real, y = imaginary). The impedance ($\boldsymbol{Z}$) of the Cole expression is described as:

$$\boldsymbol{Z} = R_\infty + \frac{R_S - R_\infty}{1 + (j\omega\tau)^\alpha} \tag{12}$$

R_s = low frequency resistance, R_∞ = high frequency resistance, ω = 2πf, τ = time constant, α = dimensionless exponent.

The electrical properties of biological tissues are commonly modeled using a constant phase element (CPE) (Jossinet *et al.*, 1993, Grimnes and Martinsen, 2015).

$$\boldsymbol{Z}_{\text{CPE}} = A(j\omega)^a \tag{13}$$

A is pseudo capacitance, [Ω] if α = 0 and [F] if α = 1. α = describes how much the element behaves like a capacitor or a resistor. α = 0 => ideal resistor, α = 1 => ideal capacitor.

Rigaud *et al.* reported the impedance and phase measured on 9 samples of in-vitro small intestine excised from sheep (1 kHz to 10 MHz), and proposed a two-dispersion model for intestinal tissue (Rigaud *et al.*, 1995):

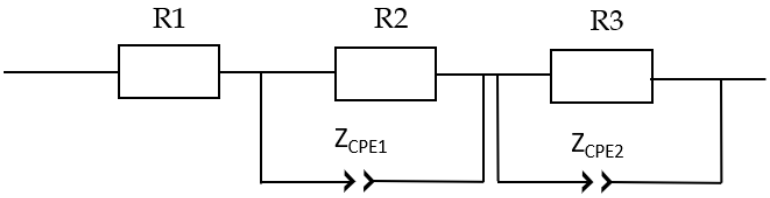

Figure 15. Suggested model for the electrical properties of in-vitro small intestine (Rigaud *et al.*, 1995). R = resistors, and Z_{CPE} = Impedance of a constant phase element.

Where

$$\boldsymbol{Z} = R_1 + \frac{R2}{1+\left(\frac{R2}{A_{CPE1}}\right)(j\omega)^{\alpha_{CPE1}}} + \frac{R3}{1+\left(\frac{R3}{A_{CPE2}}\right)(j\omega)^{\alpha_{CPE2}}} \tag{13}$$

and

$$\boldsymbol{Z}_{CPE1} = \frac{A_{CPE1}}{(j\omega)^{(\alpha)CPE1}} \;,\; \boldsymbol{Z}_{CPE2} = \frac{A_{CPE2}}{(j\omega)^{(\alpha)CPE2}} \tag{14}$$

We found this model to be adequate for the frequency range we used (1 *Hz*-1 *MHz*). We had an additional dispersion at lower frequencies due to electrode polarization. Figure 16 shows a comparison between the mean values of impedance and phase measured by Rigaud *et al.* on in-vitro sheep intestine (100 Hz was the lower limit) and the typical impedance and phase measured we measured on in-vivo pig small intestine.

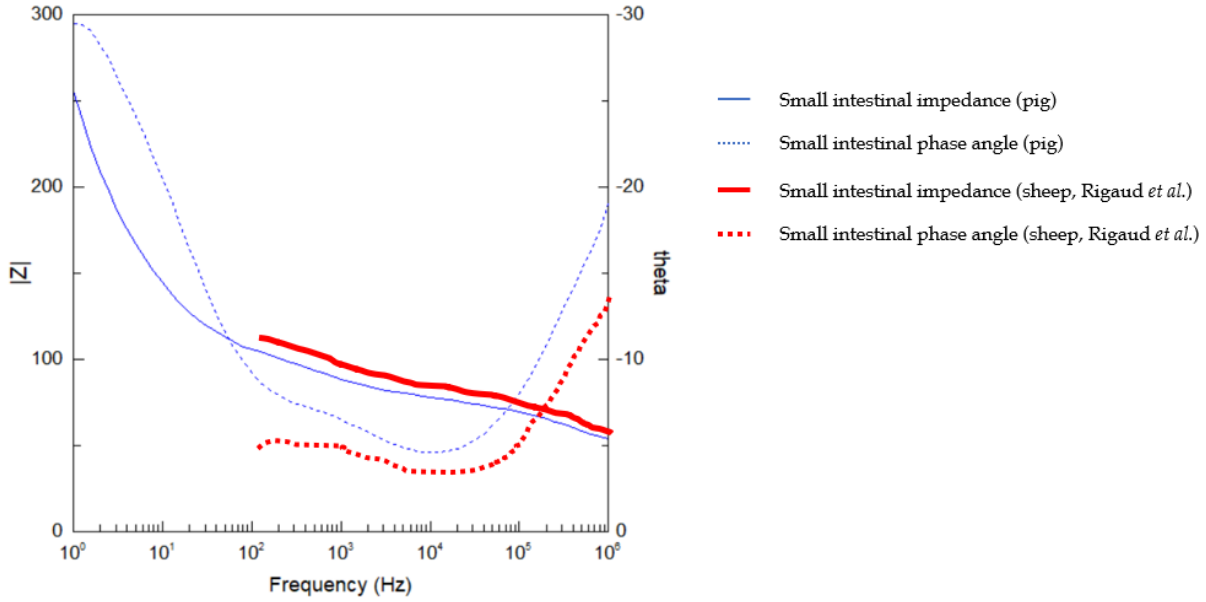

Figure 16. Impedance and phase of small intestine. A comparison between our results on pig intestine and the results reported by Rigaud *et al.* on sheep intestine (Rigaud *et al.*, 1995). © Institute of Physics and Engineering in Medicine. Reproduced by permission of IOP Publishing. All rights reserved.

3.2.8 Selection of ischemia/reperfusion sensitive electrical parameters (paper I, III)

The intestinal wall consists of multiple layers of dissimilar tissue types, and these have dissimilar dielectric properties (Gabriel *et al.*, 1996). At the membrane interface between two

dissimilar tissue layers we can expect a build-up of charge giving rise to interfacial polarizations (Pethig, 1987). In addition, peristalsis in the small intestine makes the assumption of a specific thickness of the intestinal wall invalid. Just by touching the wall of perfused intestine, a response contraction is triggered. Amplifying this effect is the hyperperistalsis with spastic movement for a period of time at the onset of ischemia.

It has been suggested that the loss angle, *tan δ* (or alternatively the phase angle) is a good parameter for the evaluation of the electric properties of tissue, as it is not dependent on the distance between the electrodes (two-electrode setup) (Heo and Jung, 2011). This includes an assumption about the tissue being isotropic, which is clearly not the case with the small intestine. To increase the degree of homogeneity by averaging over a relatively large tissue area, we used large electrodes (9 mm diameter) and trans-intestinal measurements. We found that the ratio parameters like the phase angle (tan φ) or the loss angle (*tan δ*) varied less between subjects than the parameters *Re*, *Im*, and ***Z***, while being sensitive to changes caused by ischemia and reperfusion (Figure 17 and Figure 22).

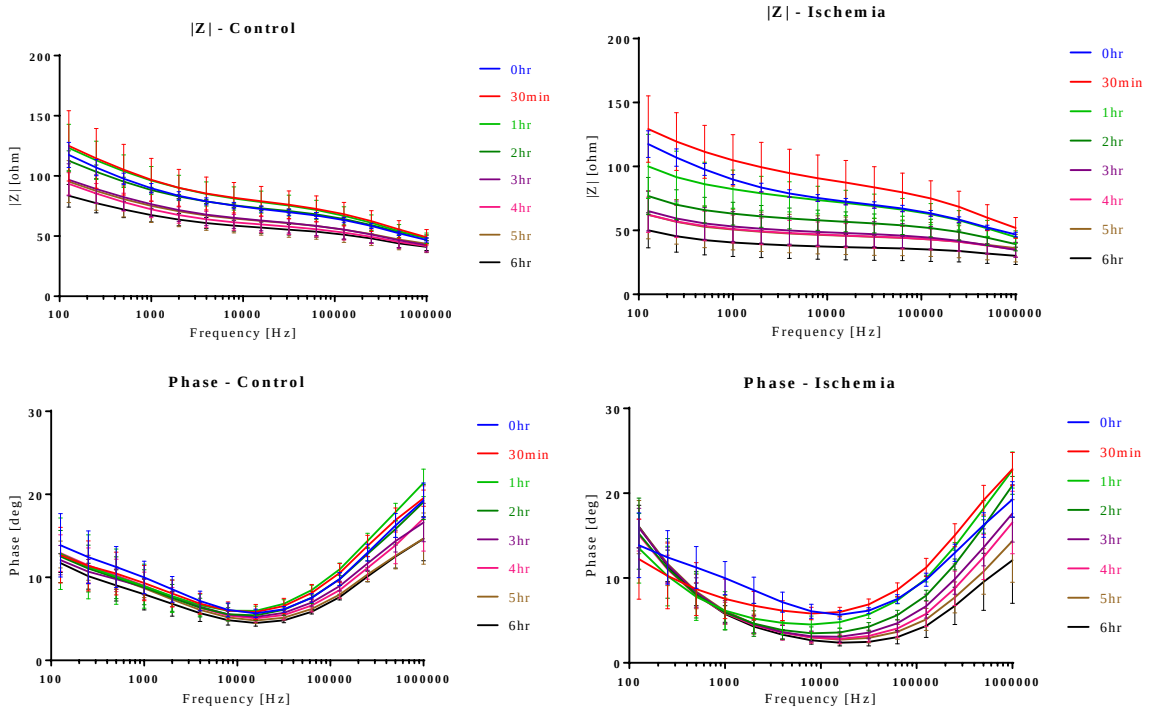

Figure 17. (From paper I, figures 6-9). Electrical parameters of ischemic versus control small intestine. **Top:** Impedance (|Z|) [Ω]. **Bottom:** Phase (φ) [deg] - **Left:** Control. **Right:** Ischemia. Each line shows the mean with 95% confidence interval of 7 measurements (one from each pig) in the same time window (+/- 8 min of the selected hour) (Strand-Amundsen et al., 2016).

When choosing between *tan φ* or *tan δ*, we found that *tan δ* was more linearly sensitive to the changes during ischemia and reperfusion, as the denominator *X* decreases relatively more during ischemia than the numerator *R* (Figure 22).

3.3 Microdialysis (paper IV)

When investigating the use of bioimpedance to measure the electrical properties of the small intestine at various tissue states and durations, we wanted to simultaneously use other methods to monitor the state of the small intestine, to act as reference for tissue injury and a verification of tissue state. We used intraluminal microdialysis to assess how changes in metabolic substrate levels changed with ischemia and reperfusion, and to assess if microdialysis could be used to assess intestinal tissue viability.

Ischemia-reperfusion related changes in local substrate concentration can be measured using microdialysis (Tenhunen et al., 1999, Pischke et al., 2012, Solligard et al., 2005). The principle is to place a tubular microdialysis membrane[24] with a diameter < 1 millimeter in the tissue of interest, pump a slow steady flow of isotonic[25] colloid[26] fluid through the inside of the membrane and on to a sampling vial. The tubular membrane will act like a small capillary blood vessel, and the low mass hydrophilic substances in the area surrounding the probe will diffuse through the porous membrane due to differences in concentration gradient (Sommer, 2005). The selectivity of the method is based on the pore size of the membrane, preventing larger molecules like proteins to enter the dialysate. The microdialysis sample thus gives a representation of the local average substrate concentration in the tissue near the probe, during the sample time-interval (Figure 18).

For the small intestine, intraluminal microdialysis has been shown to be more reliable than intramural microdialysis (Emmertsen et al., 2005, Sommer and Larsen, 2004). With intramural microdialysis there are issues with fixating a microdialysis membrane within a spastic and thin multi-layered intestinal wall, local injury to the tissue and irritation caused by the membrane (Anderson et al., 1994), and in addition, the lactate production in the various layers of the small intestine may differ due to redistribution of perfusion within the layers (Vallet *et al.*, 1994, Cassuto *et al.*, 1979).

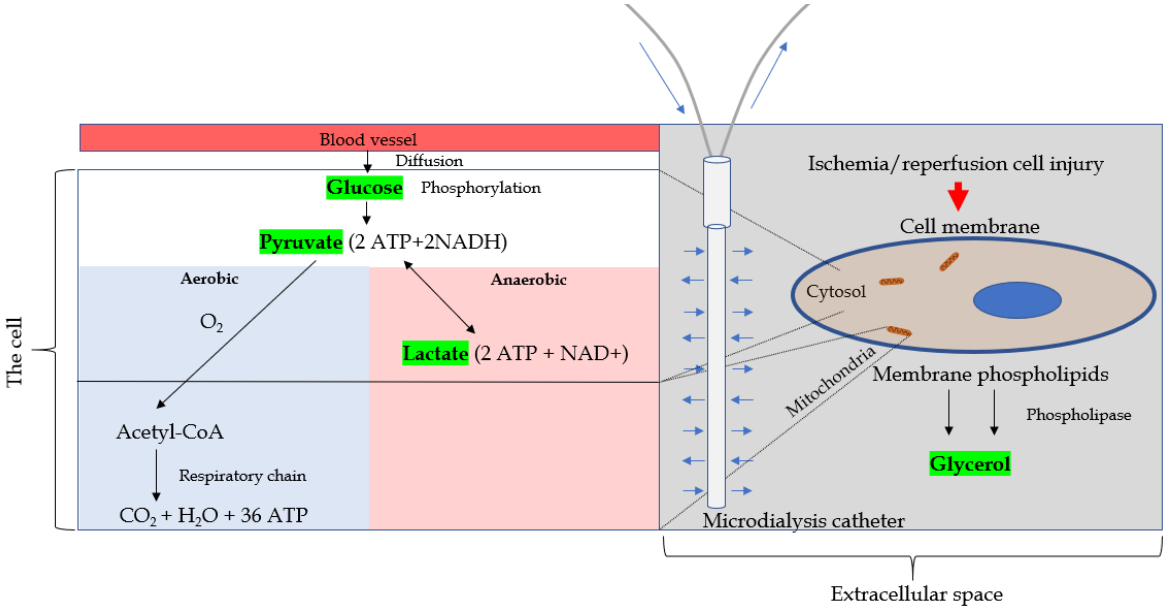

Figure 18. The microdialysis catheter in an extracellular environment with sources of glucose (diffusing from the blood vessels), pyruvate (glycolysis or metabolized lactate), lactate (dehydrogenase) and glycerol (disintegrating cell membranes).

[24] Hollow fiber membrane with pore size determining cut-off.
[25] Fluid that will not upset the osmotic balance with respect to the tissue/cells.
[26] Large molecules of one substance, dispersed in a second substance.

The substrates of interest using intraluminal microdialysis in the small intestine are primarily lactate and glycerol. Lactate is an end-product of anaerobic metabolism that with increasing permeability of the mucosal barrier passes into the lumen (Solligard *et al.*, 2008), and glycerol is released from disintegrating cell membranes (Edsander-Nord *et al.*, 2002).

Glucose and pyruvate can normally not pass into the lumen (Waelgaard et al., 2012), and ischemia/reperfusion experiments have shown that intraluminal microdialysis measurements of these substrates can be unreliable (Hogberg *et al.*, 2012, Sommer and Larsen, 2004).

3.4 Visual inspection (paper IV)

While return of color and peristalsis does not correlate uniformly with intestinal viability (Horgan and Gorey, 1992, Glotzer *et al.*, 1962), these are still the most common criteria in the clinical assessment of intestinal viability (Tilsed *et al.*, 2016).

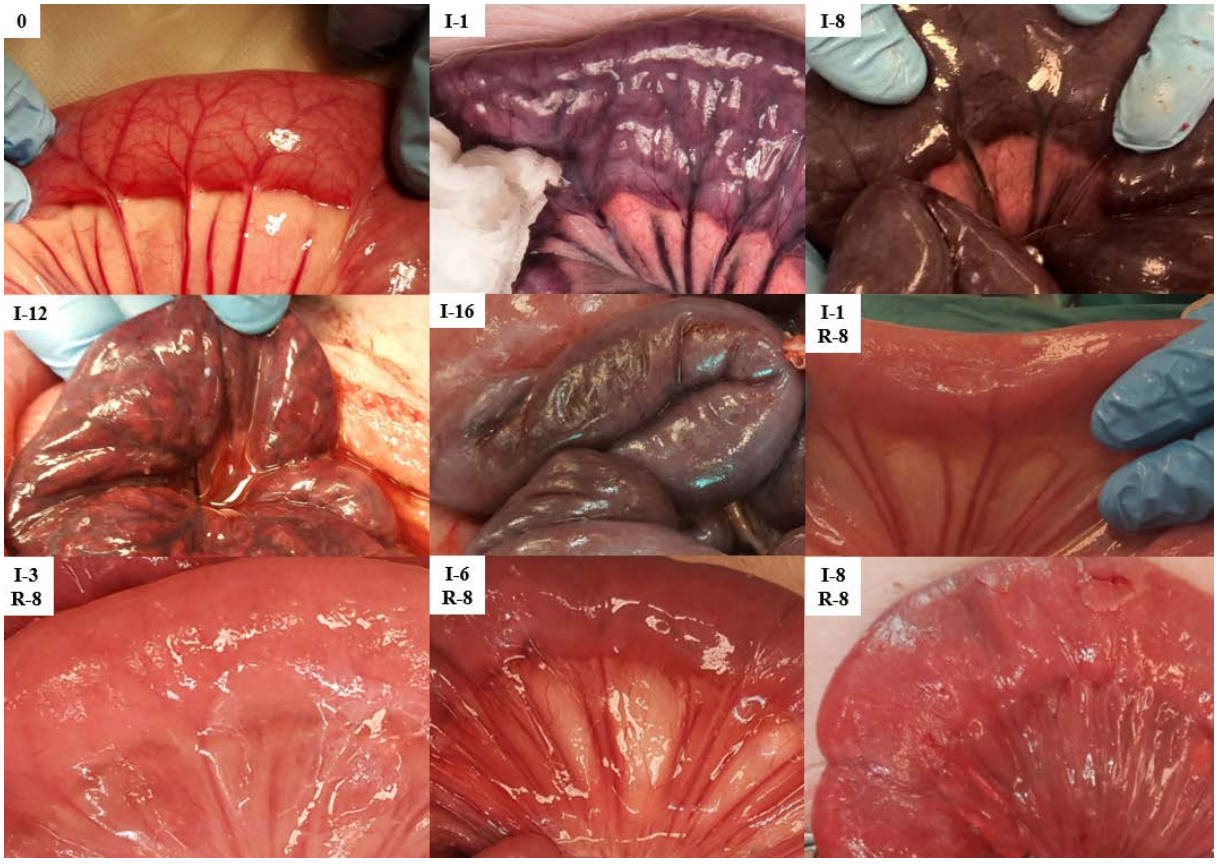

Figure 19. (From paper IV, figure 1). Jejunum at selected intervals of ischemia and reperfusion. **0:** Perfused jejunum at the start of the experiment. **I-1:** 1 hour of ischemia. **I-8:** 8 hours of ischemia. **I-12:** 12 hours of ischemia. **I-16:** 16 hours of ischemia**. I-1 R-8:** 1 hour of ischemia and 8 hours of reperfusion. **I-3 R-8:** 3 hours of ischemia and 8 hours of reperfusion. **I-6 R-8:** 6 hours of ischemia and 8 hours of reperfusion. **I-8 R-8:** 8 hours ischemia and 8 hours of reperfusion (Strand-Amundsen et al., 2018a).

We wanted to compare these criteria with the use of bioimpedance to assess intestinal viability.

The presence of peristalsis in the bowel segments was monitored by visual observation and palpation, and registered hourly for the duration of the experiments. We photographed the intestinal segments hourly to monitor alterations in color (Figure 19).

3.5 Histology (papers I-V)

In order to investigate and provide a reference for the structural and cellular changes in the small intestine as a function of tissue state (perfused, ischemic, reperfused), and to observe how these changes associate with changes in electrical parameters, we collected biopsies for histology. See Table 3 for an overview of the experiments and type of histological analysis.

Visualization of parameters or structures of interest is done through staining, and inspection and analysis are done using light microscopy (LM), scanning electron microscopy or transmission electron microscopy (TEM). With LM the changes in cell morphology and tissue structures are observed, while TEM is used for the study of changes on a cellular and subcellular level (Figure 20).

3.5.1 Light microscopy – methodology (papers I-V)

We collected intestinal full-thickness biopsies from pigs (experiment I-III) for LM at selected time intervals from control jejunum, ischemic jejunum and reperfused jejunum. The sections were reviewed with LM by two pathologists (HMR & FPR) and pathological changes in each layer of the intestine were assessed.

3.5.2 Transmission electron microscopy methodology (papers IV-V)

In experiment III, biopsies were collected at selected time intervals, and a series of ultrathin sections were created from each sample. The sections were examined by TEM by one pathologist (FPR). The focus was on cellular and subcellular changes as a basis of estimating tissue viability in the muscularis propria.

3.5.3 Cell viability - histology

If a cell receives sufficient injury during IRI, necrotic, necroptotic, apoptotic or autophagic pathways will be triggered (Kalogeris *et al.*, 2012). In the pathway of necrosis, irreversible cellular damage occurs when the depletion of energy results in the inability to maintain cellular integrity. Possible mechanisms include cellular acidosis, loss of adenine nucleotides from the cell, generation of oxygen free radical species, increases in concentration of metabolic products and degradation of membrane phospholipids (Gutierrez, 1991).

With necrosis, typical cell changes observable by LM and/or TEM are the swelling of the cytoplasm and organelles, pyknosis of the nucleus, organelle dissolution, disruptions of the plasma membrane, leakage of cellular content into the extracellular space and adjacent inflammation (Negroni *et al.*, 2015). With apoptosis, typical cell changes are cell shrinkage and fragmentation into nucleosome-size fragments with intact plasma membrane containing structurally intact organelles, and no adjacent inflammation (Elmore, 2007).

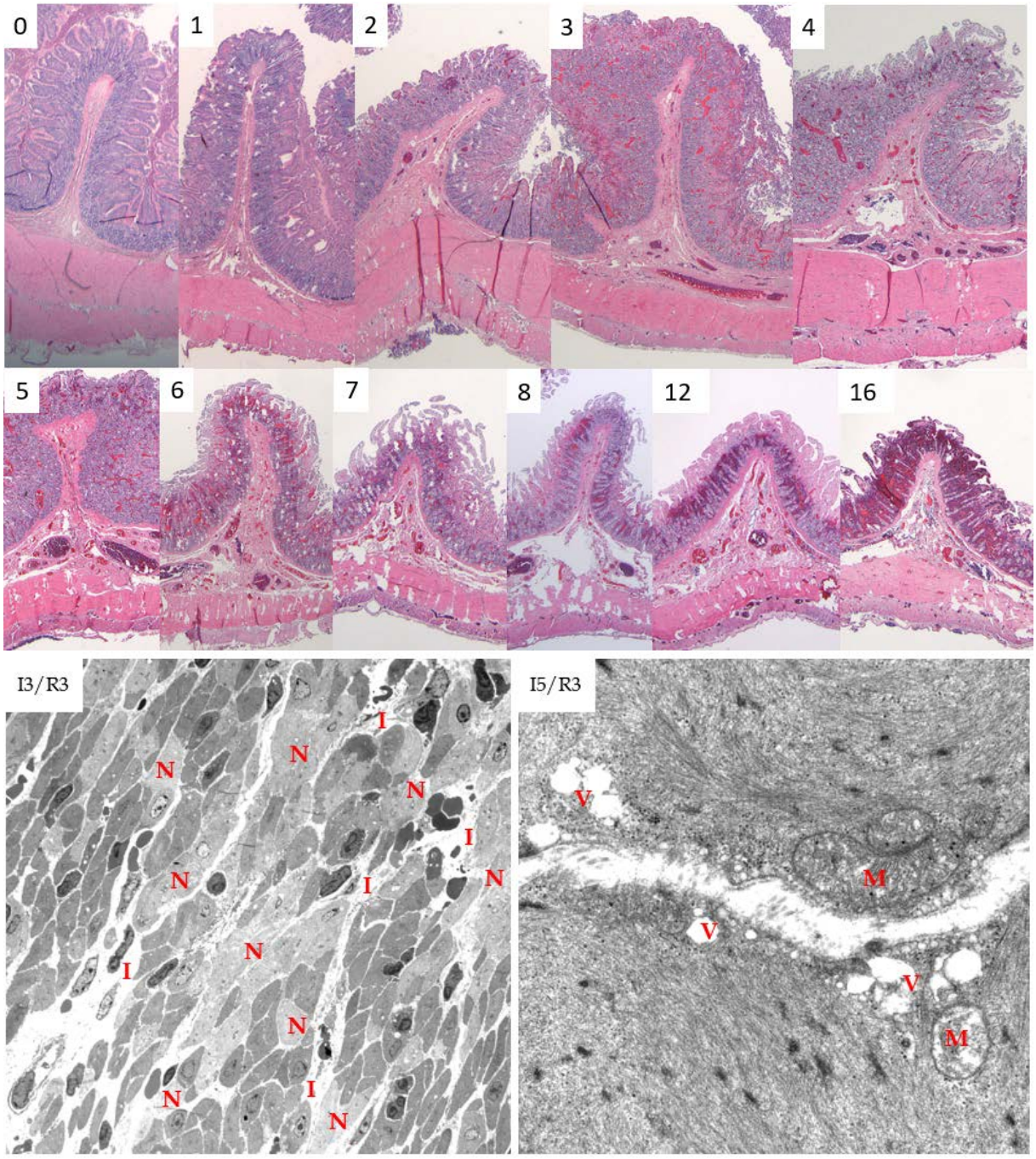

Figure 20. Top: Light microscopy of jejunum biopsies sampled at selected time intervals of ischemia. Images are indexed with a number showing ischemic duration in hours. **Bottom:** Transmission electron microscopy of jejunum (muscularis propria) sampled at selected time intervals of ischemia and reperfusion. Images are indexed with I = ischemia hours and R = reperfusion hours. **I-3/R-3:** Focal multi cell necrosis (N), interstitial inflammation (I), vacuolization of sarcoplasm (small white dots in cells). **I-5 R-3**: Vacuolization of sarcoplasm (V), swollen, partly vacuolated mitochondria (M).

3.5.4 Histological grading systems (papers IV-V)

We aimed to apply histological grading systems as an aid in the assessment of the viability state of the tissue. There is presently no standard classification method for the histological assessment of ischemia/reperfusion damage in the gut (Quaedackers *et al.*, 2000) and several approaches have been proposed, focusing on different aspects of the damage process (Swerdlow *et al.*, 1981). Many previous studies related to intestinal viability have

concentrated on mucosal injury (Chiu *et al.*, 1970, Parks and Granger, 1986, Ahren and Haglund, 1973, Clark and Gewertz, 1991, Weixiong *et al.*, 1994). A commonly used histological classification system for ischemic mucosal lesions is based on the grading system proposed by Chiu *et. al* (Chiu *et al.*, 1970), including modifications proposed by Park *et al.* (Park *et al.*, 1990) to include evaluation of damage in the deeper layers of the intestine. Swerdlow *et al.* developed a classification system with more focus on the pathological changes in the deeper layers of the small intestine (Swerdlow *et al.*, 1981). This classification system has later been modified (Plonka *et al.*, 1989, Hegde *et al.*, 1998). In experiment III we used and compared the two above mentioned histological grading systems. See Figure 21 for a comparison of the two.

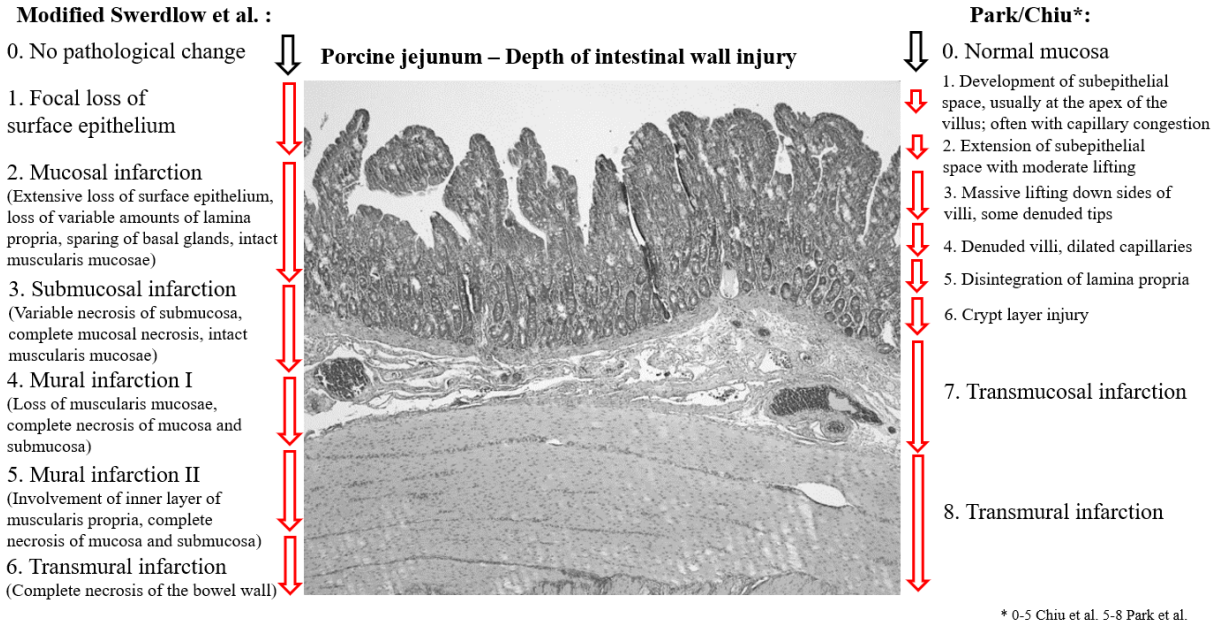

Figure 21. Comparison of modified Swerdlow (Swerdlow *et al.*, 1981, Plonka *et al.*, 1989, Hegde *et al.*, 1998) and Park/Chiu (Park *et al.*, 1990, Chiu *et al.*, 1970) systems for grading of histological damage on the intestine.

3.6 Data analysis and classification performance (papers I-V)

Bioimpedance measurements (chapter 3.2.1) gives a series of real and complex components of impedance as a function of the selected frequency range and number of measurement points. These components can be used to calculate a variety of immittance parameters[27]. We chose the *tan δ* parameter as it was found to be sensitive to changes in the ischemic intestine, while being not very sensitive to electrode distance (Strand-Amundsen et al., 2016).

In order to assess the hypotheses related to the aims in this work (chapter 0), we used linear mixed effects models (LME) to model and investigate the time development of *tan δ* as a function of ischemia or perfusion (Strand-Amundsen et al., 2016). A linear mixed-effects model (LME) has been suggested as a relevant tool for analysis of repeated measurements and longitudinal data (Ma et al., 2012), allowing for both random and fixed effects. Repeated measurements ANOVA was used to investigate at which time points the differences between electrical parameters occur between the ischemic and perfused intestine (Strand-Amundsen et al., 2017, Strand-Amundsen et al., 2018b). Repeated measurements ANOVA is less flexible

[27] Resistance, reactance, conductance, susceptance, phase angle, loss angle etc.

with the structure of random effects compared to LME, requires an equal number of timed effects, and cannot handle missing data or time-dependent covariates. RM ANOVA was also used with the microdialysis data to perform comparisons of the intraluminal lactate and glycerol levels between the control and ischemia/reperfusion segments of jejunum (Strand-Amundsen et al., 2018a).

Using LME and RM ANOVA we found that there was a statistically significant association between *tan δ* and time in the ischemic intestine, that was significantly different from *tan δ* in the control intestine (Strand-Amundsen et al., 2016). When investigating the effects of reperfusion, we found that the time development of *tan δ* and *tanδm* during ischemia/reperfusion was difficult to separate as there were non-linear patterns (Figure 23). Thus, we decided to investigate the use of machine learning, specifically neural networks, to evaluate classification performance of bioimpedance data related to viability and histological tissue state.

3.6.1 Machine learning and bioimpedance (paper V)

Repeated bioimpedance measurements give a series of longitudinal datasets consisting of several base-parameters[28], each as a function of frequency. With the possibility of transforming these base-parameters into a series of immittance parameters at different frequencies and adding the complexity of non-linear patterns in the time development of the bioimpedance data during events like ischemia/reperfusion, machine learning appears as a relevant approach.

Machine learning is a powerful tool that can be used to investigate associations, learn patterns and develop classification models from large sets of complex data. A simple way to introduce machine learning is to picture someone with near perfect patience and with a vast ability to structure, remember and assess data, going through the data methodically, creating layers of algorithms to compare and assess the data, evaluating every possible combination of the data between the layers, in order to learn associations that are hard to find by conventional statistical methods. The algorithms in machine learning are designed to learn directly from the data without requiring a predetermined equation to model the data. With supervised machine learning, the aim is to finds patterns using both input data and output data. And the patterns that are learned are used to develop predictive models.

Methods for classification[29] learning have been increasingly available over the last few years, along with increases in accessible computing power. Many of the popular classification learning algorithms are well suited for capturing non-linear relations between many input features and a target, such as artificial neural networks (ANN). Artificial neural networks consist of layers, where each layer consists of a series of nodes. Each node can be connected to all nodes in the next layer.

Feed forward neural networks[30] (FFN) are networks where the data only moves in one direction from the input layer and ending in the output layer, without any loops. Recurrent neural networks on the other hand are networks where there are feedback loops and data can be kept in "memory".

With respect to bioimpedance measurements, recurrent neural networks (RNN) are of interest because of the possibility of learning temporal patterns and non-linear associations

[28] Real and imaginary component of impedance
[29] With classification, as opposed to regression, the output variables are organized into groups.
[30] One of the first and simplest types of ANN's

in multivariate time-series during events such as ischemia and reperfusion. A limitation with RNNs is the problem with learning long term dependencies resulting in vanishing or exploding gradients (Hochreiter and Schmidhuber, 1997, Bengio et al., 1994).

One particular type of RNN introduced by Hochreiter and Schmidhuber in 1997, overcame this problem by using a more nuanced structure of hidden layers and changing the dynamics of back propagation. The new units that were introduced were called long short-term memory (LSTM) units. Adding LSTM units to RNN proved very successful for learning time-series patterns (Hochreiter and Schmidhuber, 1997).

We investigated and compared the classification abilities of two types of ANN:

1. Using end-point bioimpedance measurements with FNN.
2. Using LSTM-RNN with bioimpedance data history over different periods of time.

The targets for classification were 'intestinal tissue viability'[31] and 'histological injury'[32]. We used the results from the previous viability assessment and histological grading on jejunal tissue biopsies (Strand-Amundsen et al., 2018a) as a reference. Prediction of tissue viability was assessed for different data points and segments, based on estimation of clinical application and relevance of the method. Classification using all or clinically relevant intervals of history of repeated measurements with different labels, was compared to classification using single measurement points at selected intervals, employing suitable machine learning approaches for both cases (Strand-Amundsen et al., 2018c).

As with all powerful tools, the possibility and limitation of overfitting is always present. To reduce the probability of overfitting we implemented machine learning with reduced bias from hyperparameter tuning, by applying repeated double cross-validation (Filzmoser *et al.*, 2009) with selection of the hyperparameter set within an inner 5-fold cross-validation (CV) loop, and prediction in an outer 5-fold CV loop.

The final hyperparameter set was determined by finding the most frequent optimal hyperparameter set over all runs and outer fold iterations (Filzmoser et al., 2009). The final prediction performance was determined by extracting the outer loop predictions belonging to the final hyperparameter set and calculating its mean and standard deviation over all runs and outer folds.

[31] Binary

[32] According to histological grading method

4 Results

The results section first gives a brief summary of results from each published paper, followed by a topical overview of results.

4.1 Summary of main results from published works

4.1.1 Paper I (*In-vivo* characterization of ischemic small intestine using bioimpedance measurements)

1. The 2-electrode setup with trans-intestinal measurements is sensitive to ischemia related changes in the small intestine.
2. There are statistically significant changes in the electrical parameters of intestine as a function of tissue state (ischemia/perfusion).
3. The overall trend in electrical parameters measured using a 2-electrode trans-intestinal setup on the jejunum of 7 pigs shows a distinct time development as a function of ischemia, significantly different from those in perfused small intestine, when comparing the results at hourly intervals.
4. There is less variation between the individual pigs when using the ratio parameters like *tan δ*, than when using resistance/reactance/impedance.
5. Histology from samples of in-vivo ischemia and in-vivo perfused intestine show a series of distinct structural changes as a function of ischemia that can be associated with the measured changes in electrical parameters.

4.1.2 Paper II (Ischemic Small Intestine – In-vivo versus Ex-vivo bioimpedance measurements)

1. The time development of electrical properties in ischemic small intestine ex-vivo differs significantly ($p<0.0001$) from the electrical properties in ischemic small intestine in-vivo at several time intervals, when comparing them to the baseline and between in-vivo and in-vitro at select timepoints.
2. The difference may be explained by the formation of edema in the in-vivo model, as suggested by histological findings.
3. With the ex-vivo model we observed a time development of electrical properties matching the typically reported impedance behavior in ischemic tissue, while with the in-vivo model the formation of edema appears to partly mask this behavior.

4.1.3 Paper III (Small Intestinal Ischemia and Reperfusion – Bioimpedance measurements)

1. When comparing the *tan δ* parameter in ischemic and control jejunum, we found that it was significantly different ($p<0.016$) after the onset of ischemia, and for the duration of the experiment (16 hours), showing that trans-intestinal bioimpedance measurements can be used to assess whether small intestine is ischemic or not.
2. Comparing the control tissue 30 cm from the ischemic area with the control tissue 60 cm from the ischemic tissue, we found that the mean *tan δ* amplitude in the frequency range (3900-6300 Hz) was significantly higher ($p< 0.036$) in the control tissue closer to the ischemia/reperfusion area after 10 hours of experiment duration. This indicates that trans-intestinal bioimpedance measurements might have a usefulness for detecting inflammation in intestinal tissue.

3. Following reperfusion, the time development of *tanδm* amplitude and frequency overlapped and periodically increased above the *tanδm* in the ischemic intestine, showing that not only does reperfusion cause changes in the electrical parameters, but that these changes can be larger than the changes caused by ischemia itself.
4. Valuable information for viability assessment could be provided by looking at the time-development of the *tan δ* parameter following reperfusion.

4.1.4 Paper IV (Ischemia/Reperfusion Injury in Porcine Intestine – Viability Assessment)

1. In the porcine model with segmental occlusion of the jejunal mesentery, the intestinal tissue was judged (histology) to be probably irreversibly damaged when exposed to ≥ 4 hours of ischemia and then reperfused.
2. Using microdialysis to monitor intraluminal lactate and glycerol allowed us to closely monitor the onset and duration of ischemia, and the onset of reperfusion, but we were unable to find enough association between tissue viability and metabolic markers to be clinically relevant.
3. The sequence of ischemia/reperfusion injury using the SMO model does not completely follow the outwards direction from the mucosa to the outer muscular layer, as most current histological grading and classification system suggest.
4. Evaluation of intestinal viability based on the return of color and the presence of peristalsis did not match well with histologic assessment of tissue viability.

4.1.5 Paper V (Machine learning for intraoperative prediction of viability in ischemic small intestine)

1. Good prediction of porcine small intestinal tissue viability is possible based on a single bioimpedance measurement. This measurement should be made just before the onset of reperfusion.
2. Employing LSTM-RNN on repeated bioimpedance measurements during reperfusion allows an even better prediction of intestinal viability and also results in improved accuracy in classifying the level of histological grade.
3. LSTM-RNN is a promising tool for classification of multivariate time series of bioimpedance data.

4.2 Bioimpedance - Results

4.2.1 tan δ and ischemia (paper I and III)

tan δ measured on the jejunum (control) showed an initial dispersion around 11 kHz (Figure 22, top). *tan δ* measured on the control remained around that characteristic frequency (f_c) for the duration of the experiments.

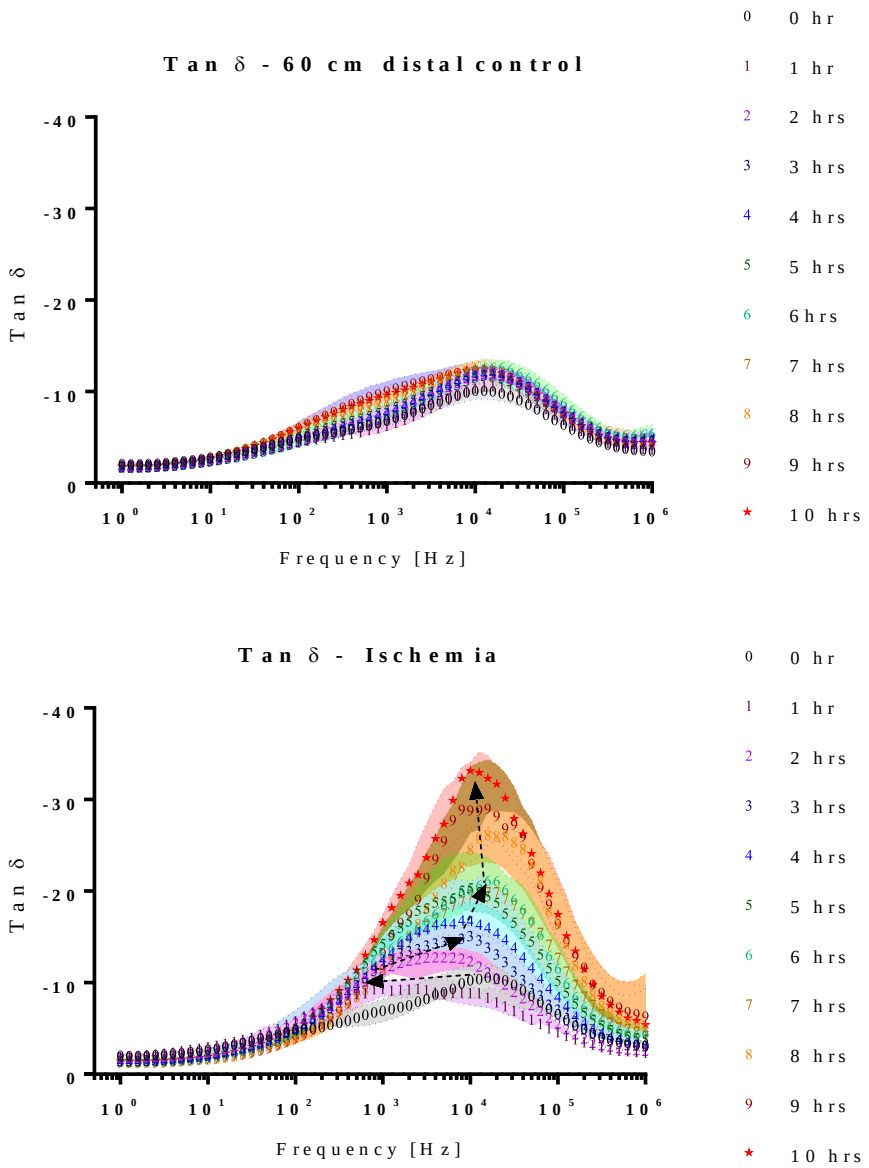

Figure 22. (From paper III, figures 1 and 2). *tan δ* measured hourly over a duration of 10 hours on porcine small intestine. **Top:** Control jejunum **Bottom:** Ischemic jejunum. Plot shows the median (n = 11 pigs). The black dotted arrows show the general time development direction of the maximum *tan δ* amplitude (*tanδm*). The confidence bands show the 95% CI of the median (Strand-Amundsen et al., 2018b).

In the ischemic[33] jejunum the absolute value of *tan δ* showed a low frequency increase and a high frequency decrease, during the first hour of ischemia (Figure 22, bottom). For the duration of the experiment the f_c and the absolute value of *tan δ* gradually increased.

4.2.2 In-vivo versus in-vitro (paper II)

In order to investigate the possibility of using an ex-vivo model instead of an in-vivo model, with the implicit benefit of reducing the resources needed to conduct an experiment, we resected 3 (15 cm) jejunum samples from 6 pigs, giving a total of 18 samples. The resected samples were kept in an air-tight container with 2 mL of saline (Ringer-acetate, B. Braun), placed in a temperature-controlled bath at 38°C[34] for 10 hours, and bioimpedance measurements were performed every 30 minutes.

We found significant differences in the measured electrical parameters, when doing baseline- and time-interval- comparisons between the ex-vivo and in-vivo results (Strand-Amundsen et al., 2017). The trend was that after the start of ischemia in-vitro a time development with higher impedance was measured than in the in-vivo intestinal tissue.

Li *et al.* (mouse muscle), Halter *et al.* (breast tumor), and Haemmerich *et al.* (porcine liver), all reported the same trend, when comparing results from in-vivo with ex-vivo bioimpedance measurements, where ex-vivo they measured higher resistivity and higher reactance than in ischemic in-vivo tissue (Li *et al.*, 2014, Halter *et al.*, 2009, Haemmerich *et al.*, 2002). The main associated histopathological difference between the in-vivo and ex-vivo samples that we observed was the gradual formation of edema in the in-vivo tissue. This indicates a cause for the difference in electrical parameters, as the formation of edema in tissue is reported to result in a reduction in measured impedance (Radhakrishnan *et al.*, 2007). Towards the end of the experiment (10-hour duration) the development of electrical parameters was converging (Strand-Amundsen et al., 2017). This might be because a large part of the cells in both models are necrotic by the end of a 10-hour experiment

4.2.3 Electrical properties and reperfusion (paper III)

When investigating the effects of reperfusion on the electrical properties of the small intestine, we observed that in the reperfused intervals there was an abrupt increase in *tanδm* for some hours after reperfusion (Figure 23). The tendency was that a longer period of ischemia followed by reperfusion resulted in a larger initial increase in *tanδm* amplitude.

[33] Mesenteric full occlusion warm ischemia.

[34] Normal bowel temperature in healthy pigs

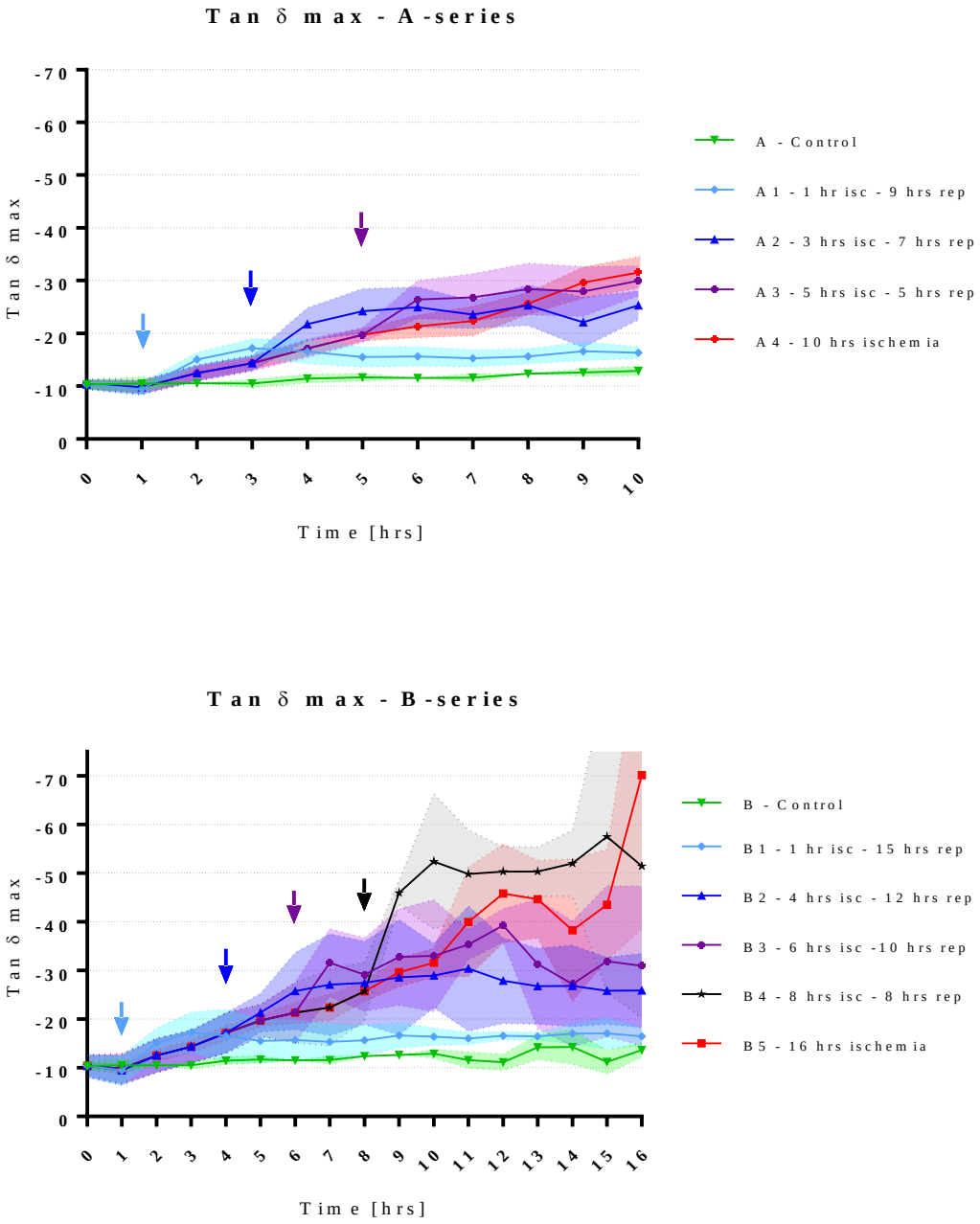

Figure 23. (From paper III, figure 4). Mean *tanδm* values plotted versus time. Solid lines are intended only as guides. **Top:** A-series in experiment III (n=11 pigs). **Bottom:** B-series in experiment III (n=4 pigs). Coloured arrows show time points for start of reperfusion. The confidence band show the 95% CI of the mean. For better readability, we scaled the Y-axis without showing the top parts of the CI band from the last two hours of the 8-hour ischemic/8-hour reperfusion, as well as the last hour of the 16-hour ischemic tissue (Strand-Amundsen et al., 2018b).

4.2.4 Summary of associations between pathological changes and electrical properties (papers I, III, IV)

a) The irritation caused by handling of the small intestine was estimated to cause a small decrease in the impedance of the control tissue (Strand-Amundsen *et al.*, 2016).

b) A comparison between two groups of control tissue (30 cm distal vs 60 cm distal) to the ischemia/reperfused segments was associated with significant changes in *tan δ* in the 3900-6300 Hz range (Strand-Amundsen *et al.*, 2018b), indicating that changes in electrical parameters caused by inflammation can be measured using bioimpedance.

c) The very early change in low frequency phase after 15-30 minutes of bioimpedance was associated with the closing of gap junctions (Strand-Amundsen *et al.*, 2016).

d) With transmission electron microscopy we observed the early swelling of muscle cells (Figure 24) during ischemia (Strand-Amundsen *et al.*, 2018a). As the function of the ionic pumps is reduced by ischemia, there is a shift in the ratio between extracellular and intracellular liquid in the muscle cells, where some of the extracellular liquid is being drawn into the cells by osmosis. The early swelling results in an increase in low frequency resistance (Gersing, 1998, Schaefer *et al.*, 1998). This is probably the dominating phenomenon explaining why the *tanδm* is shifted to a significantly lower frequency after 1 hour of ischemia (combined with the very early effect from the closing of gap junctions (c)).

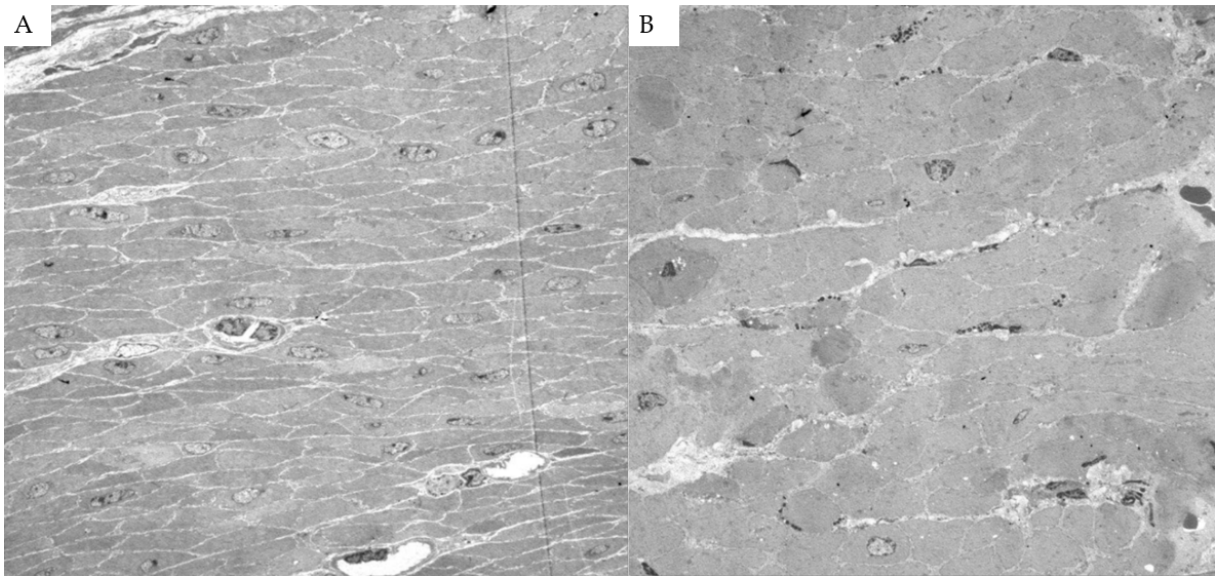

Figure 24. (From paper IV, figure 5). Transmission electron microscopy of jejunum (muscularis propria). **A - Perfused:** Showing intact muscle. **B – Ischemic for 1 hour:** Showing mild intercellular edema, with increased variation in the electron density in the muscle cells. Some minimal fat vacuoles are visible (Strand-Amundsen et al., 2018a).

e) In-vivo, the early formation of intracellular edema was followed by the gradual formation of extracellular edema. This change associated with a gradual decrease in impedance in the ischemic tissue (Strand-Amundsen et al., 2016).
f) As the duration of ischemia increases, the surface epithelium of the mucosa is lost, and deeper layers of the intestinal wall are gradually injured, increasing the ion permeability in the tissue. The associated effect on electrical properties was a decreasing impedance (Strand-Amundsen *et al.*, 2016), where the reactance is decreasing more relative to resistance, observable as an increased amplitude of *tanδm*.
g) The large increase in extracellular edema following reperfusion, and the series of IRI related effects (1.5.3), was associated with a large decrease in impedance (Strand-Amundsen et al., 2018b). This was associated with the increase in *tanδm* for some hours following reperfusion, above the *tanδm* amplitude of the ischemic tissue, with a higher increase for reperfusion at later stages (Figure 23) (Strand-Amundsen *et al.*, 2018b).
h) As opposed to in-vivo, in the in-vitro intestinal tissue there is no gradual formation of extracellular edema, and thus ischemia causes the impedance to increase more and stay higher for a longer time in-vitro (Strand-Amundsen *et al.*, 2017).

4.3 Microdialysis - Results (paper IV)

Using microdialysis to measure intraluminal lactate and glycerol, we were able to closely monitor the onset and duration of ischemia, and the onset of reperfusion (Figure 25). In the segments that were reperfused after ≥ 6 hours of ischemia, we observed increasing leakage of fluid from the intestines into the abdominal cavity and increasing amounts of fluid accumulating inside the lumen. Granger et al. reported a doubling of vascular permeability during ischemia and a fourfold increase in vascular permeability after reperfusion (Granger, 1988).

This probably dilutes the luminal lactate and glycerol concentrations, reducing the ability to estimate the metabolic state of the tissue when using intraluminal microdialysis during prolonged ischemia/reperfusion experiments (Haglund, 1994). The phenomenon is expressed by a gradual decrease in lactate and glycerol levels in the ischemic intestine past the 6-hour duration.

After the start of reperfusion, there appears to be no clear difference in the time course of metabolic marker concentration between reversibly and irreversibly damaged tissue, indicating that prediction of viability based on intraluminal microdialysis alone is unreliable. The present results confirm that intraluminal microdialysis has high specificity and sensitivity for detecting and monitoring ischemia in the small intestine, but poor specificity for predicting viability.

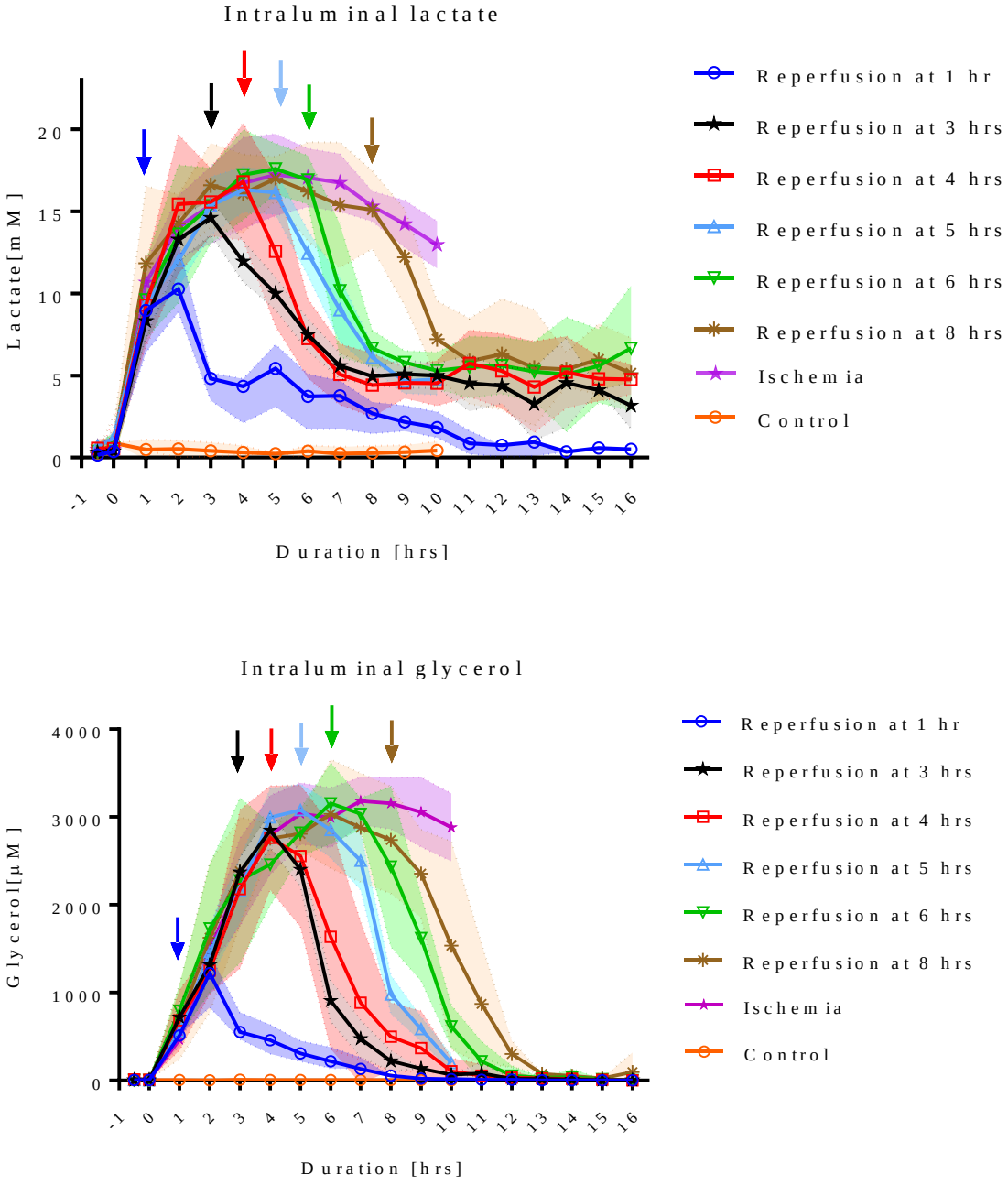

Figure 25. (From paper IV, figure 2). Intraluminal microdialysis in pig jejunum. **Top:** Intraluminal lactate. **Bottom:** Intraluminal glycerol. **Both:** Plots show median with 95% CI bands of the median. Measurements starts with a baseline 30 minutes before the initiation of ischemia at t = 0. Colored arrows show time points for start of reperfusion. Ischemia followed by reperfusion at 1, 3- and 5-hours n = 14. Ischemia followed by reperfusjon at 4, 6- and 8-hours n = 4. Control n = 5 (Strand-Amundsen et al., 2018a).

4.4 Visual inspection – Results (paper IV)

The only change in color from 2-9 hours of full occlusion ischemia was a small variation in the nuance of darkness, showing that intestinal color alone is a poor indicator of viability. The later change in appearance from dark (8 hrs), to patchy colored (11-12 hrs), to overtly

necrotic (15-16 hrs), indicates the time window between the initiation of full occlusion warm ischemia and the presence of pronounced necrotic bowel in the SMO model.

We observed return of color and peristalsis (Table 4) in intestine that histologically contained areas of probably irreversible damage (Figure 26). Following reperfusion, the increase in time before return of color associated with an increase in ischemic exposure, indicating that the time before return of color is affected by the level of tissue injury. However, confounding effects such as internal bleeding and edema in the intestinal wall may have reduced the accuracy of the return of color assessment after the long reperfusion intervals.

Table 4. (From paper IV, table 2). Clinical parameters during ischemia/reperfusion in porcine jejunum (Strand-Amundsen et al., 2018a). Images in Figure 19.

Ischemia [hrs]	Observations on the ischemic jejunum:	Minutes after reperfusion before color has returned [mean ± SD]	Observable peristalsis in # of pigs	Reperfusion [hrs]	Observations on the reperfused jejunum:	# of pigs
0	Normal color					15
1	Purple	0.9 ± 0.1	15 of 15	8	Edema	15
2	Darker purple	2 ± 0.1	2 of 2	8	Edema, slight fibrinous coating	2
3	Darker purple	4 ± 0.3	13 of 13	8	Edema, fluid droplets, slight fibrinous coating	13
4	Darker purple	6 ± 0.7	4 of 4	8	Edema, fluid droplets, fibrinous coating, darker internal hue	4
5	Darker purple	15 ± 1.6	11 of 11	8	Edema, fluid droplets, fibrinous coating, darker internal hue	11
6	Darker purple	26 ± 3.3	3 of 4	8	Edema, fluid droplets, fibrinous coating, deeper red color, darker internal hue	4
8	Black	49 ± 9*	0 of 4	8	Edema, fluid droplets, fibrinous coating, deeper red color, darker internal hue	4
12	Patches of paler color					4
16	Necrotic					4

* There was a lot of internal bleeding in the jejunum, so determination of the time before return of color was difficult.

4.5 Histology results (paper IV)

4.5.1 Light microscopy – Results (paper IV)

LM of cross-sections of jejunum showed gradually increasing signs of injury in the ischemic tissue over time, and more pronounced injury following reperfusion. There was some variation in the pattern and extent of pathological changes between different samples from the same time point, and between different areas within the same samples, but the lesions were reproducible. A simplified overview of the predominant findings at each time point is shown in Figure 26.

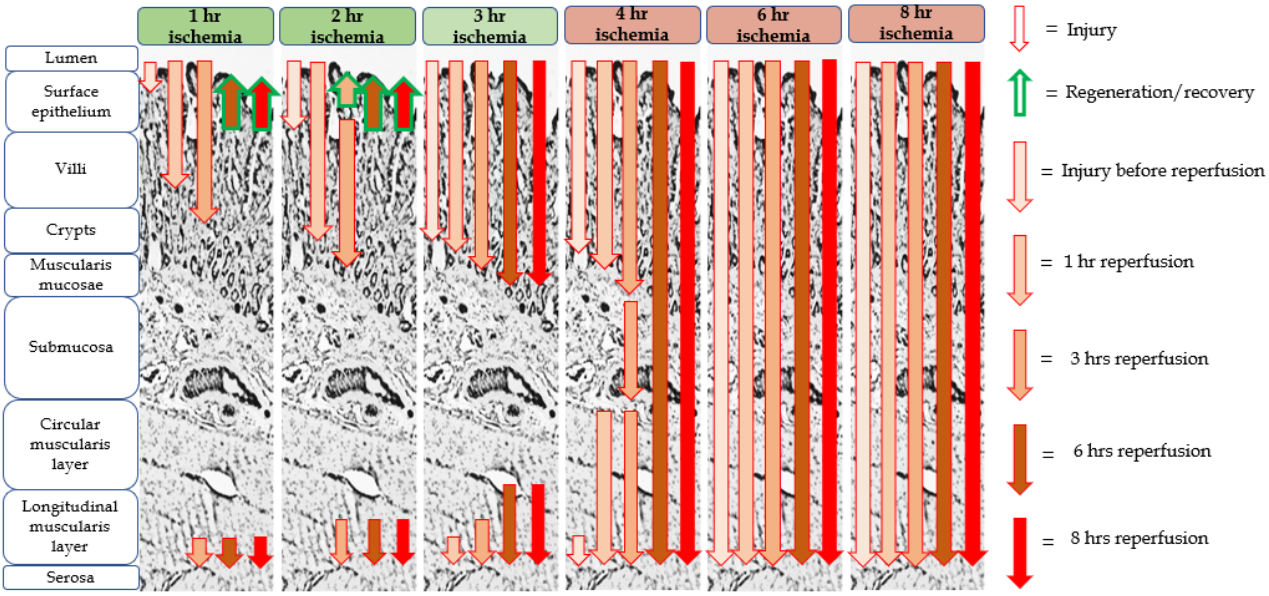

Figure 26. Simplified overview of main findings from light microscopy of 128 biopsies from 5 pigs at selected intervals of ischemia/reperfusion time. The background images represent a cross section of the small intestine, while the left column names the layer structures. The arrows (indexed on the right side of the figure) are used to show general location of injury and/or regeneration at selected durations of ischemia and reperfusion. The cells headers are color indexed: green = probably still viable, red = probable irreversible injury.

The samples of jejunal tissue exposed only to ischemia were considered irreversibly injured by ischemia after 6 hours of exposure, based on the observations of a total loss of crypt epithelium and pronounced smooth muscle cell shrinkage in the muscle layers. Samples that were exposed to both ischemia/reperfusion were considered irreversibly damaged after 4 hours of ischemia followed by more than 2 hours of reperfusion, based on the observations of a total loss of crypt epithelium, extensive shrinkage and loss of myocytes in the outer layer of the muscularis propria (Figure 26 and Figure 27).

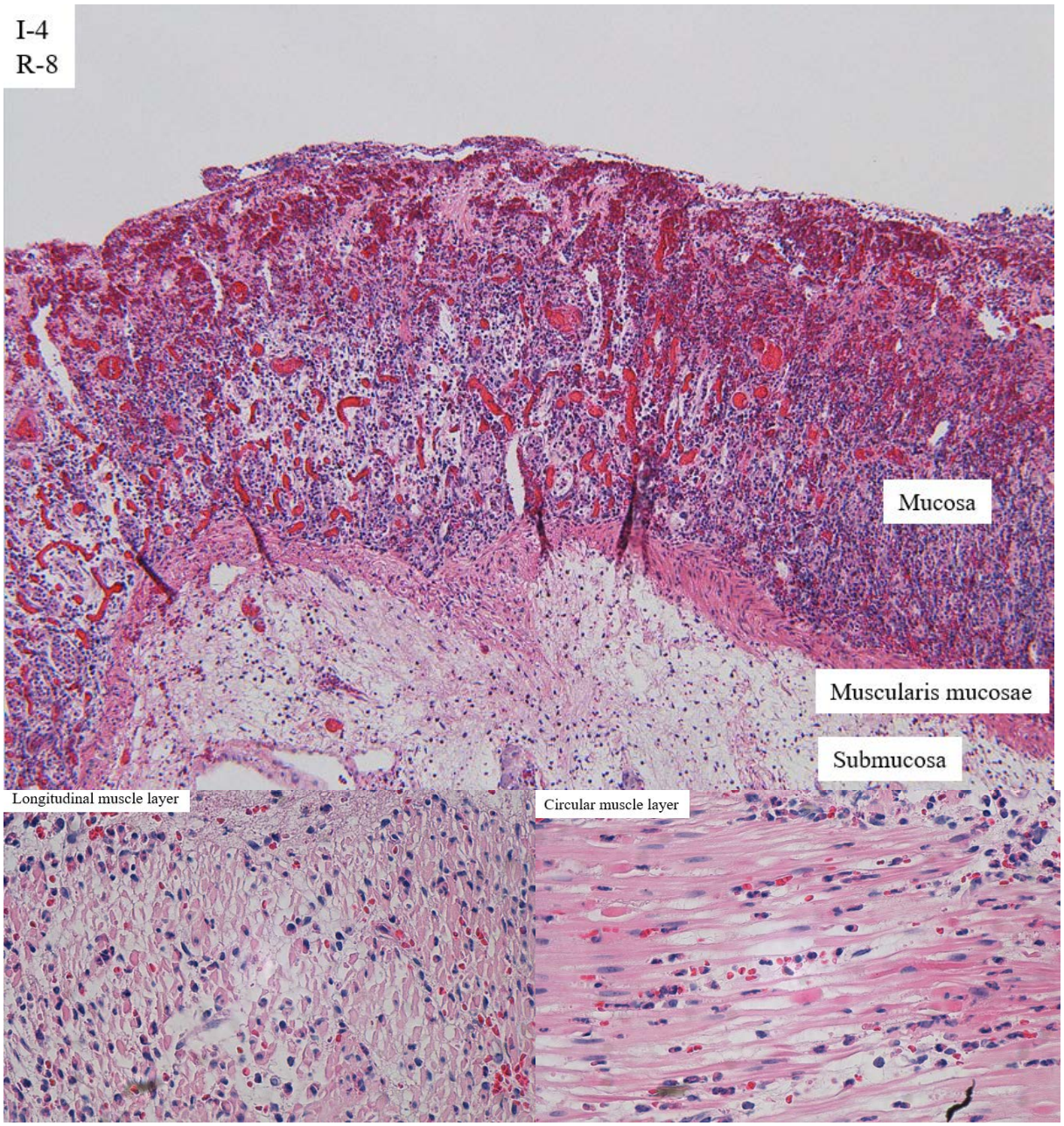

Figure 27. (From paper IV, figure 3). Light microscopy of selected structures of the jejunum after 4 hours of ischemia and 8 hours of reperfusion. **Top:** Mucosa and submucosa (HE, x10), showing necrotic villi, total loss of crypt epithelium, shrinkage of myocytes in the muscularis mucosae, and edema in the submucosa. **Bottom left:** Longitudinal (outer) layer of the muscularis propria, showing edema and extensive shrinkage and loss of myocytes (HE, x60). **Bottom right:** Circular (inner) layer of the muscularis propria, showing edema and extensive myocyte damage (HE, x60) (Strand-Amundsen et al., 2018a).

4.5.2 Histological grading – Results (paper IV)

The predominant findings at each time point are shown in Figure 28. The highest score in both grading systems was reached after 8 hours of ischemia, while more than 3 hours of ischemia gave a full score in both grading systems within two hours following reperfusion (Figure 28).

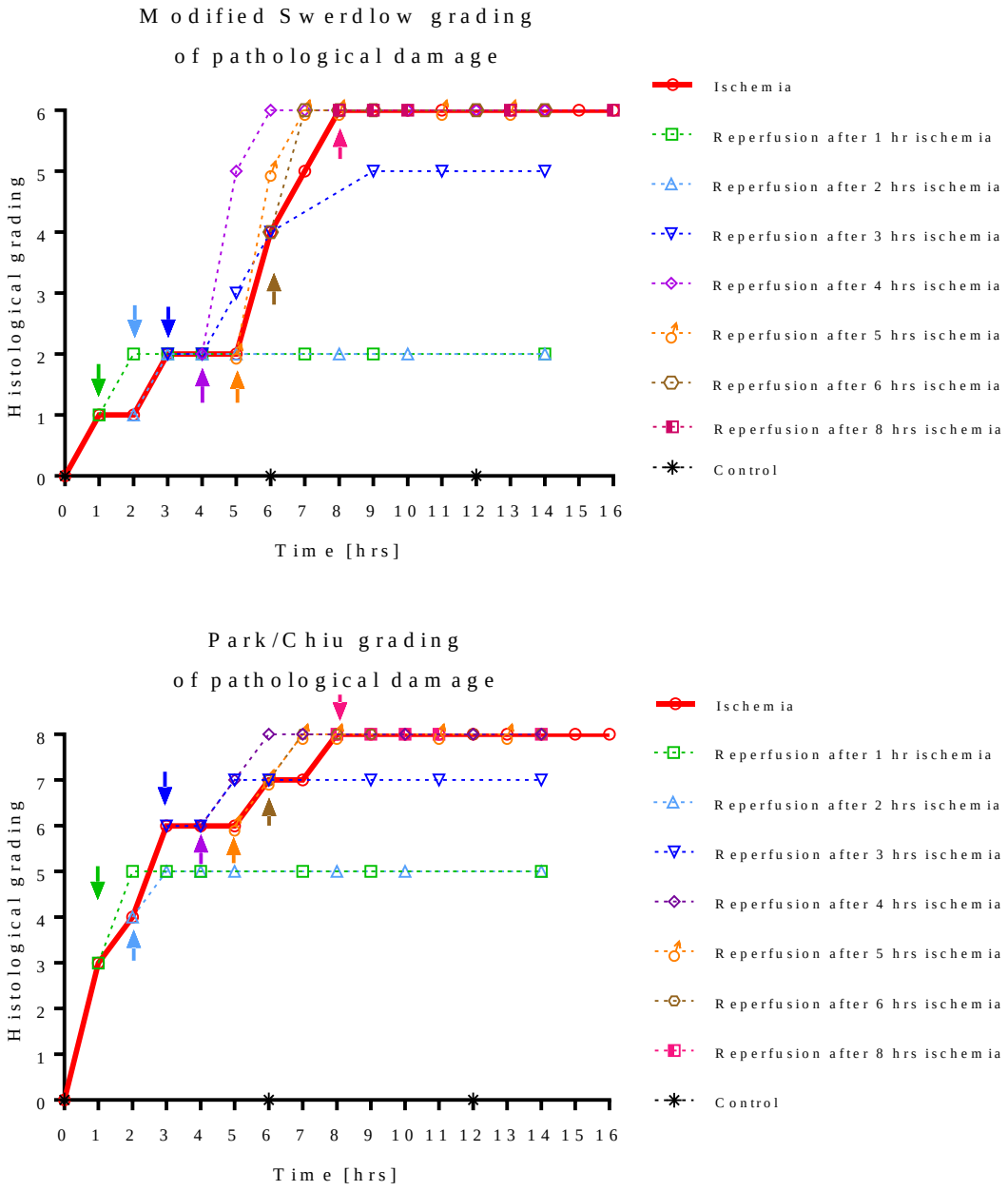

Figure 28. (From paper IV, figure 4). Histological grading of pathological damage (5 pigs, n=128 biopsies total) at selected ischemia/reperfusion intervals (Strand-Amundsen et al., 2018a). Colored arrows show time points for start of reperfusion. Stippled lines show progression of injury following reperfusion. **Top:** Modified Swerdlow (Swerdlow *et al.*, 1981, Plonka *et al.*, 1989, Hegde *et al.*, 1998). **Bottom:** Park/Chiu (Park *et al.*, 1990, Chiu *et al.*, 1970).

4.5.3 Transmission electron microscopy – Results (paper IV)

Using TEM on the muscularis propria and serosa we observed a gradual increase in injury to the cell structures during ischemia (Table 5, left columns), with probable irreversible injury in the muscularis propria after 5 hours of ischemia. Interestingly, even at 7 to 8 hours of ischemia, focal areas of muscle cells still appeared viable, illustrating heterogeneity in the development of ischemic damage to the muscularis propria.

Table 5. (From paper IV, table 4). Summary of main findings from transmission electron microscopy of porcine jejunum at selected intervals of mesenteric occlusive ischemia and reperfusion (Strand-Amundsen et al., 2018a). **C**hanges in the muscularis propria and serosa are described (3 pigs, a total of 58 samples). The table cells with results are color indexed; green = normal/light changes, yellow = visible cell damage, but still probably viable, red = probably irreversible cell damage.

Ischemia [hrs]:	Observations:	Ischemia/ reperfusion [hrs/hrs]:	Observations:
0	Intact musculature. Some variation in the electron density in the muscle cells, focal swollen mitochondria with vacuolized matrixes		
1	Intact musculature. Discrete intercellular edema. Lymphocytes in the interstitial space. Increased variation in the electron density in the muscle cells. Some cells have increased electron density (darker). Some of the mitochondria are more prominent. Some minimal fat vacuoles are visible.	1/3	Inflammation, cell death, sparse fine-vacuolization of the sarcoplasm, slightly swollen mitochondria
2	More prominent variation in electron density between muscle cells. Increased number of vacuoles, some of them are fat vacuoles. Focal edema, thickening of the mitochondrial cristae. Some lysosomes with membrane fragments.	2/3	Inflammation, cell death, more comprehensive fine-vacuolization of the sarcoplasm, slightly swollen mitochondria.
3	Same results as at 2 hours, but a few more interstitial immune response cells are visible. Monocytes, macrophages, and a few granulocytes. Vacuoles in the sarcoplasm. Slightly swollen mitochondria.	3/3	Inflammation, cell death, more comprehensive fine-vacuolization of the sarcoplasm, slightly swollen mitochondria, focal single cell necrosis, swollen cell nuclei
4	Same changes as at 3 hours, but the changes are more prominent as the cells with higher electron density are more condensed, and there are more vacuoles around the mitochondria.	4/3	Pronounced cell shrinking/cell death, swollen cell nuclei, loss of cohesion, interstitial edema
5	Focal edema, variations in electron density, thickening of the mitochondrial cristae, vacuoles in the sarcoplasm, swollen mitochondria, interstitial lymphocytes/monocytes/granulocytes, loss of plasma-membrane and coherence, focal single cell necrosis	5/3	Increased cell shrinking/cell death, swollen cell nuclei, loss of cohesion, interstitial edema
6	Necrosis, focal large vacuoles in some mitochondria	6/3	Increased cell shrinking/cell death, swollen cell nuclei, loss of cohesion, interstitial edema
7	Necrosis with macrophages. Non-necrotic cells appear like the cells at time intervals 3-6 hours.		
8	Like the results at 7 hours		

There was reperfusion-induced inflammation and cell death of varying degrees in all the tissue that had been subjected to ischemia. After 4 hours of ischemia and 3 hours of reperfusion (Table 5, right), there was pronounced cell shrinking/death, swollen cell nuclei, loss of cohesion, substantial interstitial edema and the muscle tissue no longer appeared viable.

4.6 Machine learning and bioimpedance – Results (paper V)

The classification performance using FNN and RNN-LSTM with bioimpedance data (Strand-Amundsen et al., 2018c), to predict intestinal tissue viability and histological grading based on the reference data (Strand-Amundsen et al., 2018a) indicates that good binary prediction of tissue viability is possible based on one bioimpedance measurement before reperfusion and an FNN model. When using the whole time-course of repeated bioimpedance measurement during the experiments a significantly higher accuracy was obtained by utilizing LSTM-RNN (Figure 29).

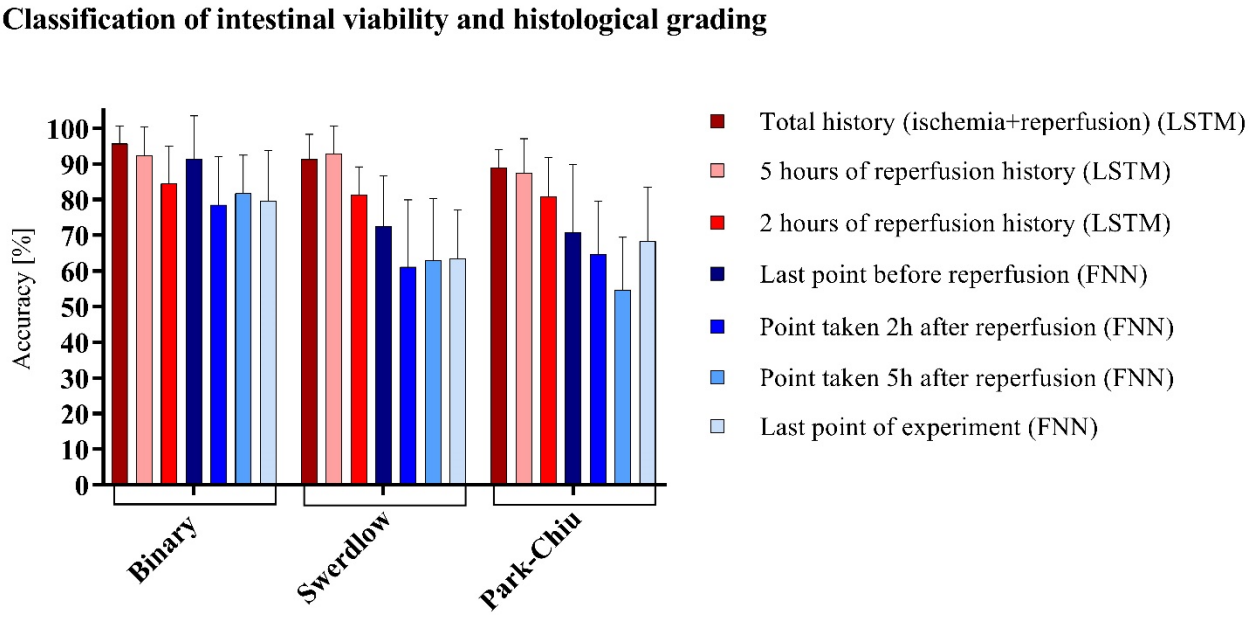

Figure 29. (From paper V, figure 3). Classification of intestinal viability (binary) and histological grading of injury using LSTM-RNN and FNN (Strand-Amundsen et al., 2018c). Mean accuracy with SD are shown as bars with error bar on top. For 'Total history', 'Last point before reperfusion' and 'Last point of experiment' n = 79, for the rest n = 64.

5 Discussion

In chapter 3, "Methodological considerations" some discussion related to details in the methodology was included. In this chapter, the discussion is focused on the aims of the thesis.

5.1 Comparison with relevant work

For a description of previous work with respect to experimental approaches for assessment of the viability of bowel exposed to ischemia/reperfusion, see chapter 1.1.2. For a description of what has been previously done with bioimpedance and the small intestine, see chapter 1.4.

5.1.1 Bioimpedance - Viability assessment of the small intestine

To the best of our knowledge, the present work is the first to use trans-intestinal measurements to assess intestinal viability. Recent studies related to bioimpedance and the small intestine have mainly been focused on intraluminal catheters for assessment of changes in the electrical properties of the mucosa, to detect the presence of ischemia (Gonzalez *et al.*, 2007, Gonzalez *et al.*, 2003, Beltran *et al.*, 2005, Beltran *et al.*, 2013a, Beltran *et al.*, 2007, Beltran *et al.*, 2013b, Beltran and Sacristan, 2015). The 4-electrode ring catheter method has been shown to be unreliable (Bloch *et al.*, 2017).

Comparing the intraoperative use of bioimpedance to the two most commonly used experimental approaches VLS (Karliczek *et al.*, 2010) and LDF (Humeau *et al.*, 2007), we observe that bioimpedance measurements appear as a promising experimental approach for the detection of ischemia and the assessment of intestinal viability. While VLS and LDF assess parameters associated with blood flow, bioimpedance assesses parameters associated with structural changes. The presence or lack of presence of blood flow in itself does not indicate whether a tissue is viable or not. Lack of sufficient blood flow for a certain length of time, however, will ultimately result in irreversible ischemic injury to the affected tissue. While the return of blood flow is used as a parameter related to assessment of intestinal viability (Horgan and Gorey, 1992, Hobson et al., 1979), we observed that there was return of color and thus blood flow to intestinal segments, even after 6-8 hours of ischemia, where histological inspection showed irreversible injury to all layers of the intestine (Figure 26).

While VLS and LDF both can detect the presence of ischemia with high accuracy, the reported accuracies with respect to their use for assessment of tissue viability is lower. Ando *et al.* reported an accuracy of 76% and a sensitivity of 88% for assessment of bowel viability using a non-contact laser tissue blood flowmeter (Ando *et al.*, 2000). The lower accuracy might be related to the observation that return of blood flow can occur in tissue that is irreversible injured (Table 4). A reason to why measurement of bioimpedance has the potential to be more specific with respect to ischemia/reperfusion injury, is that the electrical properties of the small intestine are directly tied to the intestinal layer structure. Ischemia/reperfusion causes significant changes to these structures (Figure 26 and Figure 28) directly affecting the electrical properties.

When using machine learning to classify bioimpedance data (Strand-Amundsen et al., 2018c) versus the reference viability level based on histological inspection (Strand-Amundsen et al., 2018a), the data point just before the initiation of reperfusion yielded the highest accuracy (91.5%) when classifying single measurement points. This is probably due to the non-linear time development of the $tan\ \delta$ parameter following the initiation of reperfusion.

When employing LSTM-RNN on the whole dataset from the experiment including

both ischemia and reperfusion phases, we achieved mean accuracies that were higher (95.7%) than what has previously been reported for the clinical assessment of intestinal viability (Bulkley et al., 1981, Redaelli et al., 1998a). 5 hours of reperfusion history[35] also resulted in a very high mean accuracy (92.4%). The accuracies achieved when using bioimpedance measurements on a pig model, combined with the value of having an objective tool available for the surgeon, indicate that bioimpedance has a potential as a clinically relevant method for assessing intestinal viability.

5.1.2 Microdialysis – Small intestine

While microdialysis is a promising technology with respect to real time assessment of the local metabolic state of tissues, the technological development appears to have been at a standstill for some years. The development of continuous rapid sampling microdialysis instruments, while eagerly awaited, remains for the time being at the experimental stage (Bhatia et al., 2006, Deeba et al., 2008, Rogers et al., 2013).

Our results support the suggested use of intraluminal microdialysis for detecting or monitoring ischemia/reperfusion (Deeba et al., 2008, Solligard et al., 2005, Tenhunen et al., 1999). We were able to detect both the presence of ischemia and the presence of reperfusion (Figure 25) with high accuracy (Strand-Amundsen et al., 2018a).

In comparison to previous experiments using intraluminal microdialysis in ischemia/reperfusion of the small intestine in pigs (Tenhunen *et al.*, 1999, Tenhunen *et al.*, 2001, Sommer and Larsen, 2004, Solligard *et al.*, 2004, Hogberg *et al.*, 2012), we monitored the intestine over a longer time period and investigated a series of ischemia/reperfusion intervals. We did this to gather microdialysis data over the interval of time when irreversible injury to the small intestine occurs, with the hope of finding levels or patterns in the collected parameters that could support using microdialysis for viability assessment. In the few time intervals we found where others have conducted experiments of a similar length, the results were similar (Solligard *et al.*, 2008) (intraluminal lactate, glycerol) to ours. When investigating the use of microdialysis as a method of assessing intestinal viability, we could not find sufficient correlation between tissue viability and metabolic markers to indicate that the method was clinically relevant.

Using state-of-the-art instruments for microdialysis can be perceived as somewhat cumbersome, due to the many steps needed to conduct the measurements and the many potential sources of error. The effect might be that the current technology is favored more in experimental approaches, than for large scale implementation in the clinic. There has been some implementation of microdialysis into clinical practices (Haugaa et al., 2013, Haugaa et al., 2012a, Haugaa et al., 2012b). Still microdialysis appears to be unrivalled in that it provides a real-time window to local tissue metabolism, and we recommend using microdialysis for monitoring of intestinal ischemia and reperfusion.

5.1.3 Histology – Small intestine

Histology has been used quite extensively related to ischemia/reperfusion in the small intestine, and our work adds to this knowledge by a systematic approach to the pathological changes in ischemic and reperfused small intestine. When investigating what others have

[35] 1 measurement every hour, for 5 hours following reperfusion

reported, with respect to a viability limit in the porcine jejunum, little information was found. In most papers discussing viability in the small intestine, observations are reported as histological grading scores or as morphological observations (Quaedackers *et al.*, 2000), but few contain explicit statements about viability. The most common time duration reported for porcine intestine related to viability is that it takes approximately 8 hours of full ischemia to induce transmural necrosis (Amano *et al.*, 1980, Chiu *et al.*, 1970). We observed the same result in the present study (Figure 28).

Irreversible injury in porcine jejunum[36] has been reported to occur after 6.5 hours of ischemia followed by reperfusion (Chan *et al.*, 1998). Chan *et. al* based this estimation on the observation (n=2 pigs) that this was the time of ischemic exposure that the jejunum can take before the mucosa no longer will regenerate. We acknowledge that mucosal necrosis will heal completely in most cases and speculate that the mucosa can regenerate on injured segments of intestine that do not develop into transmural infarction. However, such segments may develop persistent injury with a large degree of fibrosis and stricture formation (Swerdlow *et al.*, 1981). The formation of stricture will lead to the patient later experiencing a new set of problems, including the need for new operations and further removal of intestine. We suggest that mucosal generation might be just one of several parameters on which to base evaluation of intestinal viability.

Our results support what others have reported in that the effects of reperfusion appear to cause additional injury to the small intestine. When accounting for both the effects of ischemia and reperfusion we found that (when using a SMO model) the porcine jejunum appeared probably irreversibly damaged after 4 hours of ischemia followed by more than 2 hours of reperfusion. We generally observed slightly higher levels of injury than Blikslager *et al.* reported in a similar model used on the ileum in pigs (Blikslager *et al.*, 1997), and Chan *et al.* in a similar model on the jejunum in two piglets. As the ileum is more resistant to ischemic damage than the jejunum (Chan *et al.*, 1998) the slightly higher level of injury in the jejunum as compared to Blikslager *et al.* was to be expected.

When comparing the electrical properties of in-vivo versus in-vitro ischemic small intestine, we observed, as previous researchers have reported, that there was a trend towards higher resistivity and reactivity in the in-vitro samples (Li *et al.*, 2014, Halter *et al.*, 2009, Haemmerich *et al.*, 2002). Upon histological inspection of samples from ischemic in-vivo and in-vitro jejunum (Strand-Amundsen et al., 2017), we observed a difference involving the gradual formation of extracellular edema in the ischemic in-vivo small intestine.

In-vivo tissue ischemia promotes the expression of certain pro-inflammatory genes and bioactives, while repressing other "protective" gene products and bioactive agents. This results in a pro-inflammatory state that induces edema and extra-vascular fluid leakage (Kong *et al.*, 1998). The inflammatory response leads to increased vascular permeability and extracellular fluid volume, resulting in edema, especially in the edge zones of marginal tissue hypoxia between the ischemic and perfused intestine (Figure 8). This affects the hydrostatic and oncotic pressure between the ischemic and perfused area, with the possibility of a trickle of intramural collateral flow towards the ischemic area (Haglund, 1994).

In the ex-vivo intestine segment, on the other hand, there is no resupply of liquid in the extracellular space and thus the trans-intestinal resistance is higher for a longer period. These

[36] Irreversible injury defined as lack of mucosal regeneration in samples taken 24 hours after reperfusion

observations give context to the interpretation of data from in-vitro measurements of the electrical properties of the small intestine, as compared to in-vivo and describe why there are differences.

An interesting observation from the present study was that the sequence of ischemia/reperfusion injury using the SMO model did not necessarily follow the outwards direction from the mucosa to the outer muscular layer, as most grading and classification systems suggest (Quaedackers *et al.*, 2000, Haglund *et al.*, 1987). We observed a development of tissue injury in the outer layer of the muscularis propria during ischemia, while the inner muscular layer still appeared viable (Figure 26). We have not found similar reports in literature. We can speculate that this is because either we have focused in more detail (TEM) on changes in all layers of the small intestine during the early stages of ischemia, or this could be something related to the SMO model that we used. The results suggest that there are mechanisms related to the development of ischemia/reperfusion injury in the two layers of muscularis propria that should be investigated further, and we will monitor this in our upcoming experiments.

5.1.4 Deep recurrent neural networks with LSTM units and bioimpedance data

To the best of our knowledge, an LSTM network has not previously been used for classification based on bioimpedance measurements, and there are only a limited number of other studies on this method for the classification of tissue status based on other biomedical sensors. Otte *et al.* applied bidirectional LSTM networks for classification of lung tumor tissue based on optical coherence tomography, outperforming other RNN architectures (Otte *et al.*, 2013).

Given the promising results for this first study applying an LSTM network on bioimpedance measurement, it is likely that the method could be useful in other applications as well, using repeated measurement of bioimpedance spectra. The relationship between the biological processes and electrical changes are rarely completely stationary and linear, reaching either a saturation level or changing in direction as the process evolves (Chester et al., 2014, Spottorno et al., 2008), thus becoming reliant on memory and the history of measurement in order to discriminate between the various stages of the process.

5.2 Validity and advantages

5.2.1 Bioimpedance and viability

We evaluated the use of bioimpedance measurements with the 5 requirements[37] of "the ideal viability test" (Horgan and Gorey, 1992).

1) Bioimpedance measurements can be facilitated using a small medically approved handheld sensor unit with communication to a small display unit. This allows for availability during laparotomy, and with a miniaturized unit also during laparoscopy. Only a small front end is required, allowing for a large degree of freedom with respect to scalability and design.

2) Measurements can be performed by placing a suspect segment of intestine between the electrodes of the handheld sensor unit and measure for a few seconds at selected frequencies, or by repeated measurements at selected intervals over a period of time. The method will depend on the need for accuracy versus the available clinical time-frame. With respect to when bioimpedance data can be collected in a clinical setting, we estimate the

[37] See page 3 for the requirement list

time-frame to be between the identification of the putatively[38] injured bowel segments during laparotomy, to the closing of the incision in the abdominal wall. There is sufficient time available in a typical laparotomy to perform bioimpedance measurements without increasing the duration of the surgery. The measurements require no specialization and the evaluation will be done in the software.

3) Higher accuracies than the current clinical method can be achieved using a single bioimpedance measurement before reperfusion, or by analyzing repeated measurements over a period of time before and/or after reperfusion. In the appendix to paper V, we show an overview of the false positive and false negative rates for the different cases and methods that were compared. The results indicate that it is possible to achieve very low false positive rates, especially when using LSTM-RNN over a series of measurements (paper V, appendix, Table A7, A9).

4) The technique is objective as the estimation is made by a computer algorithm. With respect to reproducibility, this has to be investigated, as the question remains with respect to how translatable these results will be to a model with human intestine.

5) Bioimpedance measurement technology is low-cost, while development of any medical device is expensive due to the regulatory process.

If we include assessment of the two additional suggestions (a, b) that we made in the end of section 1.1, bioimpedance allows for clear results, and, depending on whether one measurement or a series of measurements over time is used, a relatively quick result (as compared to second- or third-look operations). In addition, bioimpedance measurements do not require complex or time-consuming calibration.

Our results indicate that bioimpedance measurements combined with machine learning have the potential to be used as a relevant tool for intraoperative assistance to the surgeon. The evaluation based on assessing the requirements made by Horgan and Gorey regarding the use of bioimpedance measurements, supports this. The potential benefits include a reduction of the need for second- or third-look surgery, which will reduce the surgical stress for the patient. A method with higher accuracy than the present standard has the potential to reduce the frequency of the two most feared post-operative complications, sepsis and short bowel syndrome.

5.2.2 Bioimpedance measurement and neural networks using LSTM units (paper V)

Classification of bioimpedance data from ischemic small intestine injury is complex, as both the ischemic and reperfusion phases show similar characteristics with overlapping electrical parameter values at certain points during the ischemia/reperfusion course (Figure 23). Classification using one measurement point (FNN) relies only on discrimination using the feature space of the current input, with no feedback into the model based on the time-development of *tanδm*.

A standard RNN is able to learn some temporal patterns, but with increasing difficulty as the duration of the dependencies to be captured by the RNN increases (Bengio *et al.*, 1994). The LSTM units overcome this problem by the inherent memory function (input, output and forget gates), allowing recollection of values at arbitrary time intervals and classification of time-series of variable length and lags between important events (Hochreiter and Schmidhuber, 1997). The ability to learn temporal patterns of *tanδm* related to the

[38] Supposed

development of ischemia/reperfusion explains the improved accuracy with the LSTM-RNN model compared to the FNN model.

Training a dataset using LSTM-RNN can be relatively time- and resource-consuming, especially because of the use of repeated-double cross validation, where models with all hyperparameter combinations are trained and validated in the inner loop, which is necessary to avoid overfitting. The time used for the classification training presented in (Strand-Amundsen et al., 2018c) was approximately 90 24-hour periods of calculation on a regular laptop. This can be done over a short time period when utilizing a series of cores on a supercomputer cluster. It is also important to remember that the classification training is a one-time occurrence, and that after the classification training, the output coefficients can be used with real-time bioimpedance measurements to perform calculations taking less than seconds in order to determine the viability of intestinal tissue.

5.3 Limitations

5.3.1 Translation of bioimpedance results from the porcine SMO model

We have only investigated the changes using a SMO model in pigs. While similarities have been reported between pig and human bowel, and the pathology of ischemia in the bowel, still the validity of applying results with pigs onto a human model remains unknown. This remains the focus in an upcoming study.

The SMO model mimics the ischemic injury mechanisms in just one of several different ischemia/reperfusion related pathologies in the small intestine. We have not investigated the changes in electrical properties during non-occlusive ischemia, SMA occlusion, arterial and venous thrombosis/emboli etc. We speculate that these mechanisms might result in differing developments in electrical parameters, especially the mechanisms of non-occlusive ischemia and venous thrombosis. Thus, while we have observed promising results with the SMO model in pigs, a lot of work remains with respect to the other models, before assumptions about general translational use can be made.

We have only investigated the use of bioimpedance measurements in a laparotomy setting and have not investigated the use of bioimpedance measurements in a laparoscopic setting. While a tool can be developed that will allow for laparoscopic trans-intestinal bioimpedance measurements, there are several questions that need to be investigated in order to assess the feasibility of such an approach. These are related to the miniaturization of electrode setups, fixation during measurements and the application of pressure.

5.3.2 Bioimpedance measurements

In the process of placing bioimpedance electrodes against the jejunal wall, small variations in mechanical pressure were a potential source of variation in the bioimpedance measurements. While we tried to control the pressure, the related effects cannot be excluded as a source of variation. Another potential source of variation was the handling and exposure of the intestine to foreign materials during the course of the experiment, which can lead to tissue irritation (Torre *et al.*, 2002).

For the experiments with long duration (16 hours), we observed the gradual formation of visible irritation on perfused segments of intestine close to the ischemic areas. These effects were even larger following reperfusion of the ischemic segments. A limitation to the studies where we used multiple ischemia/reperfusion models in the same pig (Table 3), was the possible confounding effects from the reperfusion of several segments of previously

ischemic intestine in the same pig. This can possibly result in effects on adjacent segments, influencing the measured bioimpedance data.

5.3.3 Microdialysis

The effects related to intraluminal leakage and dilution reduced the quality of the results after 5-6 hours duration of the experiment. More accurate results might have been achieved if we had sealed off the lumen of each segment of the small intestine to reduce the effect of dilution. However, sealing of each luminal segment appears to be not feasible from a clinical perspective, and we aimed to have models that were clinically relevant. If a method could be developed where accurate placement of a microdialysis catheter within the intestinal wall were possible, this might be relevant for a model to avoid the effects of intraluminal leakage. Alternatively, fixation of a microdialysis catheter between the bowel loops can be used, but this approach will rely on changes on the serosal side of the intestine.

5.3.4 Histology

Evaluation of tissue viability based on histological assessment is difficult (Hillman, 2000), as the samples are small and lesions are heterogeneous in composition and distribution (Dabareiner *et al.*, 2001) with areas of viable and necrotic tissue in the same tissue sample (Strand-Amundsen et al., 2018a).

Although we histologically observed injury to the jejunal wall that was considered irreversible, the ability to regenerate is likely to vary with the total volume of damaged tissue, making exact assessments from tissue samples difficult. Total loss of crypt epithelium, for example, might regenerate if the affected area is small, but if the affected area is large the loss can be irreversible[39]. We acknowledge that there is some uncertainty related to the accuracy of the histology-based viability reference that we used, and that follow up studies should be conducted to verify the accuracy of the reference. In the ideal world, we should conduct long term pig experiments where we not only could evaluate whether there was regeneration of mucosa after some days, but where we also could monitor later developing morbidities like stricture or adhesion. But this can be challenging as a) it is difficult to maintain animal welfare when they are to experience bowel related morbidities, and b) it requires a lot of resources.

When comparing the morphological changes with the models for histological grading, we found that the sequence of ischemia/reperfusion injury when using a SMO model did not completely follow the outwards direction from the mucosa to the outer muscular layer, as most grading and classification systems suggest [16, 20]. This observation affects the accuracy of the methods used with this model to grade histological injury (Park/Chiu, modified Swerdlow), as sometimes the classification categories would not be covering the observable morphology.

5.3.5 Machine learning

We could have tuned the classification model further by using a finer grid with more choices for each hyperparameter in the grid search, but a compromise had to be made between the grid size and the execution time of the repeated double cross-validation loops (The presently used loops took a month to run, spread on 3 computers).

When utilizing LSTM-RNN or other types of deep learning, there is a "black box" factor. The algorithms and complex node matrix are such that it is difficult to determine

[39] Much like the loss of skin

exactly which properties and temporal dependencies are captured from the training data. It is difficult to determine whether there is information specific to the experiments in this study that is different or not available in other measuring situations. Thus, further testing of the method should be performed before conclusion about its clinical usefulness can be made.

Still, LSTM-RNN is a powerful tool, that is able to capture temporal associations that can be hard to find with other methods. As with all powerful tools such as deep learning, the possibility and limitation of overfitting is present. To reduce the probability of overfitting we made sure to utilize a number of independent parameters that was much lower than the number of data points, and we implemented repeated double cross-validation, which has been reported as a relevant method to avoid overfitting (Filzmoser *et al.*, 2009).

6 Conclusions

This thesis describes the onset and progression of a work focused on using bioimpedance for intestinal viability assessment following ischemia/reperfusion injury. So far, the work has shown that bioimpedance is a promising method for intraoperative assessment of intestinal tissue. At the same time, the work is still far from finished with respect to providing a product as a medically certified tool for the surgeon. The next steps are described in chapter 7. To summarize the conclusions (compare with the objectives described in chapter 2):

1. We can capture the trans-intestinal electrical properties of the porcine small intestine using a 2-electrode setup for bioimpedance measurements.
2. The time development of the passive electrical properties of the small intestine differs when comparing perfused versus ischemic intestine, using a segmental mesenteric occlusion model in a pig.
3. There are significant differences between the time development of electrical parameters in an in-vivo segmental mesenteric occlusion model in a pig versus an ex-vivo model. One cause for the difference is related to the gradual formation of edema in the in-vivo segments.
4. After reperfusion, the time development of *tanδm* amplitude and frequency overlap and periodically increase above the *tanδm* in the ischemic intestine, showing non-linear patterns dependent on pre-reperfusion ischemic duration.
5. Using a segmental mesenteric occlusion model with warm intestinal ischemia in pig, the jejunum can be expected to be irreversibly damaged when exposed to ≥ 4 hours of ischemia before reperfusion.
6. With machine learning[40] we were able to classify histological tissue injury and viability based on bioimpedance data, with accuracies similar to or better than what is reported by using the present clinical method.
    a. LSTM-RNN's appears to be a promising tool for classification of multivariate time series of bioimpedance data.

[40] FNN and RNN-LSTM

7 Future work and perspectives

1. The trans-intestinal electrical properties of the human small intestine.
    - We are in process of starting a project where jejunal resections from patients undergoing Whipple's procedure will be investigated using bioimpedance, in order to assess the electrical properties of the human intestine, using trans-intestinal measurements. The Regional Committees for Medical and Health Research Ethics (REC) recently approved our application. The aim is to compare the electrical properties of pig versus human intestine, in order to assess the translational value of the results from the SMO pig model.
2. Investigation of the trans-intestinal electric properties during non-occlusive ischemia, SMA/SMV occlusion, arterial and venous thrombosis/emboli.
    - To assess the usefulness of using bioimpedance with respect to assessment of intestinal viability, all of the more common bowel ischemia pathologies must be investigated. In order to assess the total usefulness of this method with patients, we need to have bioimpedance data from all the relevant pathological scenarios.
3. Investigate if it is possible to improve the in-vitro model to a level where it can be used to model selected in-vivo problems with respect to ischemia/reperfusion studies in the small intestine.
    - We have recently started a work where we are continuing to investigate the use of an in-vitro model.
    - Using sutures, clamps and stapling to keep all the blood and liquid in the resected intestinal segments.
    - Using protein solutions like albumin to store the resected segments in an environment closer to the in-vivo setting.
4. Synergies from other experimental approaches.
    - Several other experimental approaches to assessment of intestinal viability have been reported as promising. When performing bioimpedance measurements, there is the possibility of performing other measurements in parallel with the same equipment, that can provide further relevant information to the surgeon. For example, while measurement of electrical bioimpedance is a measure of the passive electrical properties of the intestine, measurement of basal electrical rhythm (the active electrical signals produced by peristalsis) can be implemented using the same equipment.

8 References

AHREN, C. & HAGLUND, U. 1973. Mucosal lesions in the small intestine of the cat during low flow. *Acta Physiol Scand,* 88**,** 541-50.

AMANO, H., BULKLEY, G. B., GOREY, T., HAMILTON, S. R., HORN, S. D. & ZUIDEMA, G. D. 1980. Role of Micro-Vascular Patency in the Recovery of Small-Intestine from Ischemic-Injury. *Surgical Forum,* 31**,** 157-159.

ANDERSON, C., ANDERSSON, T. & WARDELL, K. 1994. Changes in skin circulation after insertion of a microdialysis probe visualized by laser Doppler perfusion imaging. *J Invest Dermatol,* 102**,** 807-11.

ANDO, M., ITO, M., NIHEI, Z. & SUGIHARA, K. 2000. Assessment of intestinal viability using a non-contact laser tissue blood flowmeter. *Am J Surg,* 180**,** 176-80.

ANDREUCCETTI, D., FOSSI, R. & PETRUCCI, C. 1997. *An Internet resource for the calculation of the dielectric properties of body tissues in the frequency range 10 Hz - 100 GHz* [Online]. Florence (Italy): IFAC-CNR. Available: http://niremf.ifac.cnr.it/tissprop/ [Accessed].

ANDREUCCETTI, D., FOSSI, R. & PETRUCCI, C. 2000. *Dielectric properties of body tissues* [Online]. IFAC-CNR. Available: http://niremf.ifac.cnr.it/tissprop/#inizio [Accessed 04.02 2015].

ASAMI, K. 2007. Dielectric properties of biological tissues in which cells are connected by communicating junctions. *Journal of Physics D-Applied Physics,* 40**,** 3718–3727.

ASCHOFF, A. J., STUBER, G., BECKER, B. W., HOFFMANN, M. H., SCHMITZ, B. L., SCHELZIG, H. & JAECKLE, T. 2009. Evaluation of acute mesenteric ischemia: accuracy of biphasic mesenteric multi-detector CT angiography. *Abdom Imaging,* 34**,** 345-57.

BALA, M., KASHUK, J., MOORE, E. E., KLUGER, Y., BIFFL, W., GOMES, C. A., BEN-ISHAY, O., RUBINSTEIN, C., BALOGH, Z. J., CIVIL, I., COCCOLINI, F., LEPPANIEMI, A., PEITZMAN, A., ANSALONI, L., SUGRUE, M., SARTELLI, M., DI SAVERIO, S., FRAGA, G. P. & CATENA, F. 2017. Acute mesenteric ischemia: guidelines of the World Society of Emergency Surgery. *World J Emerg Surg,* 12**,** 38.

BEAULIEU, R. J., ARNAOUTAKIS, K. D., ABULARRAGE, C. J., EFRON, D. T., SCHNEIDER, E. & BLACK, J. H., 3RD 2014. Comparison of open and endovascular treatment of acute mesenteric ischemia. *J Vasc Surg,* 59**,** 159-64.

BELTRAN, N., SANCHEZ-MIRANDA, G., GODINEZ, M., DIAZ, U. & SACRISTAN, E. 2005. Gastric Impedance Spectroscopy in Cardiovascular Surgery Patients vs. Healthy Volunteers. *Conf Proc IEEE Eng Med Biol Soc,* 3**,** 2516-9.

BELTRAN, N. E., CERON, U., SANCHEZ-MIRANDA, G., REMOLINA, M., GODINEZ, M. M., PERALTA, I. Y. & SACRISTAN, E. 2013a. Incidence of gastric mucosal injury as measured by reactance in critically ill patients. *J Intensive Care Med,* 28**,** 230-6.

BELTRAN, N. E., DE FOLTER, J. J., GODINEZ, M. M., DIAZ, U. & SACRISTAN, E. 2007. Algorithm for characteristic parameter estimation of gastric impedance spectra in humans. *Conf Proc IEEE Eng Med Biol Soc,* 2007**,** 4131-4.

BELTRAN, N. E., GARCIA, L. E. & GARCIA-LORENZANA, M. 2013b. Gastric tissue damage analysis generated by ischemia: bioimpedance, confocal endomicroscopy, and light microscopy. *Biomed Res Int,* 2013**,** 824682.

BELTRAN, N. E. & SACRISTAN, E. 2015. Gastrointestinal ischemia monitoring through impedance spectroscopy as a tool for the management of the critically ill. *Exp Biol Med (Maywood),* 240**,** 835-45.

BENARON, D. A., PARACHIKOV, I. H., CHEONG, W. F., FRIEDLAND, S., RUBINSKY, B. E., OTTEN, D. M., LIU, F. W., LEVINSON, C. J., MURPHY, A. L., PRICE, J. W., TALMI, Y., WEERSING, J. P., DUCKWORTH, J. L., HORCHNER, U. B. & KERMIT, E.

L. 2005. Design of a visible-light spectroscopy clinical tissue oximeter. *J Biomed Opt,* 10**,** 44005.
BENGIO, Y., SIMARD, P. & FRASCONI, P. 1994. Learning Long-Term Dependencies with Gradient Descent Is Difficult. *Ieee Transactions on Neural Networks,* 5**,** 157-166.
BHATIA, R., HASHEMI, P., RAZZAQ, A., PARKIN, M. C., HOPWOOD, S. E., BOUTELLE, M. G. & STRONG, A. J. 2006. Application of rapid-sampling, online microdialysis to the monitoring of brain metabolism during aneurysm surgery. *Neurosurgery,* 58**,** ONS-313-20; discussion ONS-321.
BISCHOF, J. C., PADANILAM, J., HOLMES, W. H., EZZELL, R. M., LEE, R. C., TOMPKINS, R. G., YARMUSH, M. L. & TONER, M. 1995. Dynamics of cell membrane permeability changes at supraphysiological temperatures. *Biophys J,* 68**,** 2608-14.
BLIKSLAGER, A. T., ROBERTS, M. C., RHOADS, J. M. & ARGENZIO, R. A. 1997. Is reperfusion injury an important cause of mucosal damage after porcine intestinal ischemia? *Surgery,* 121**,** 526-34.
BLOCH, A., KOHLER, A., POSTHAUS, H., BERGER, D., SANTOS, L., JAKOB, S., TAKALA, J. & HAENGGI, M. 2017. Gastrointestinal Impedance Spectroscopy to Detect Hypoperfusion During Hemorrhage. *Shock,* 48**,** 185-195.
BONI, L., DAVID, G., DIONIGI, G., RAUSEI, S., CASSINOTTI, E. & FINGERHUT, A. 2016. Indocyanine green-enhanced fluorescence to assess bowel perfusion during laparoscopic colorectal resection. *Surg Endosc,* 30**,** 2736-42.
BRANDT, L. J. & BOLEY, S. J. 2000. AGA technical review on intestinal ischemia. American Gastrointestinal Association. *Gastroenterology,* 118**,** 954-68.
BULKLEY, G. B., ZUIDEMA, G. D., HAMILTON, S. R., O'MARA, C. S., KLACSMANN, P. G. & HORN, S. D. 1981. Intraoperative determination of small intestinal viability following ischemic injury: a prospective, controlled trial of two adjuvant methods (Doppler and fluorescein) compared with standard clinical judgment. *Ann Surg,* 193**,** 628-37.
CARDEN, D. L. & GRANGER, D. N. 2000. Pathophysiology of ischaemia-reperfusion injury. *J Pathol,* 190**,** 255-66.
CAREY, L. C., KAYSER, K., ELLISON, E. H. & LEPLEY, D., JR. 1964. Relative Electrical Impedance as Index to Intestinal Viability. *Arch Surg,* 89**,** 226-8.
CASAS, O., BRAGOS, R., RIU, P. J., ROSELL, J., TRESANCHEZ, M., WARREN, M., RODRIGUEZ-SINOVAS, A., CARRENO, A. & CINCA, J. 1999. In vivo and in situ ischemic tissue characterization using electrical impedance spectroscopy. *Ann N Y Acad Sci,* 873**,** 51-8.
CASSUTO, J., CEDGARD, S., HAGLUND, U., REDFORS, S. & LUNDGREN, O. 1979. Intramural blood flows and flow distribution in the feline small intestine during arterial hypotension. *Acta Physiol Scand,* 106**,** 335-42.
CAVAILLON, J. M., ADRIE, C., FITTING, C. & ADIB-CONQUY, M. 2003. Endotoxin tolerance: is there a clinical relevance? *J Endotoxin Res,* 9**,** 101-7.
CHAN, K. L., CHAN, K. W. & TAM, P. K. H. 1998. Segmental small bowel allograft—Ischemic injury and regeneration. *Journal of Pediatric Surgery,* 33**,** 1703-1706.
CHESTER, C. J., GAYNOR, P. T., JONES, R. D. & HUCKABEE, M.-L. 2014. Electrical bioimpedance measurement as a tool for dysphagia visualisation. *Healthcare Technology Letters,* 1**,** 115-118.
CHIU, C. J., MCARDLE, A. H., BROWN, R., SCOTT, H. J. & GURD, F. N. 1970. Intestinal mucosal lesion in low-flow states. I. A morphological, hemodynamic, and metabolic reappraisal. *Arch Surg,* 101**,** 478-83.
CHOU, C. K., WU, R. H., MAK, C. & LIN, M. 2006. Clinical Significance of Poor CT Enhancement of the Thickened Small-Bowel Wall in Patients with Acute Abdominal Pain. *Am J Ro,* 186**,** 491–498.

CLAIR, D. G. & BEACH, J. M. 2016. Mesenteric Ischemia. *N Engl J Med,* 374**,** 959-68.
CLARK, E. T. & GEWERTZ, B. L. 1991. Intermittent ischemia potentiates intestinal reperfusion injury. *J Vasc Surg,* 13**,** 601-6.
COLE, K. & COLE, R. 1941. Dispersion and absorption in dielectrics I. Alternating current characteristics. *Journal of Chemical Physics,* 9**,** 341-351.
COLE, K. S. 1940. Permeability and impermeability of cell membranes for ions. *Cold Spring Harbor Sympos Quant Biol,* 8**,** 110-122.
COLLANGE, O., CHARLES, A. L., LAVAUX, T., NOLL, E., BOUITBIR, J., ZOLL, J., CHAKFE, N., MERTES, M. & GENY, B. 2015. Compartmentalization of Inflammatory Response Following Gut Ischemia Reperfusion. *Eur J Vasc Endovasc Surg,* 49**,** 60-5.
COLLARD, C. D. & GELMAN, S. 2001. Pathophysiology, clinical manifestations, and prevention of ischemia-reperfusion injury. *Anesthesiology,* 94**,** 1133-8.
COOK, V. L., JONES SHULTS, J., MCDOWELL, M., CAMPBELL, N. B., DAVIS, J. L. & BLIKSLAGER, A. T. 2008. Attenuation of ischaemic injury in the equine jejunum by administration of systemic lidocaine. *Equine Vet J,* 40**,** 353-7.
COTE, K. R. & GILL, R. C. 1987. Development of a platinized platinum/iridium electrode for use in vitro. *Ann Biomed Eng,* 15**,** 419-26.
DABAREINER, R. M., SULLINS, K. E., WHITE, N. A. & SNYDER, J. R. 2001. Serosal injury in the equine jejunum and ascending colon after ischemia-reperfusion or intraluminal distention and decompression. *Vet Surg,* 30**,** 114-25.
DEAN, D. A., RAMANATHAN, T., MACHADO, D. & SUNDARARAJAN, R. 2008. Electrical Impedance Spectroscopy Study of Biological Tissues. *J Electrostat,* 66**,** 165-177.
DEEBA, S., CORCOLES, E. P., HANNA, G. B., PARESKEVAS, P., AZIZ, O., BOUTELLE, M. G. & DARZI, A. 2008. Use of rapid sampling microdialysis for intraoperative monitoring of bowel ischemia. *Dis Colon Rectum,* 51**,** 1408-13.
DODDE, R. E., BULL, J. L. & SHIH, A. J. 2012. Bioimpedance of soft tissue under compression. *Physiol Meas,* 33**,** 1095-109.
DODDE, R. E., KRUGER, G. H. & SHIH, A. J. 2015. Design of Bioimpedance Spectroscopy Instrument With Compensation Techniques for Soft Tissue Characterization. *J Med Device,* 9**,** 0210011-210018.
DOUGLAS, W. R. 1972. Of pigs and men and research: a review of applications and analogies of the pig, sus scrofa, in human medical research. *Space Life Sci,* 3**,** 226-34.
DUTKIEWICZ, W., THOR, P., PAWLICKI, R., BOBRZYNSKI, A. & BUDZYNSKI, A. 1997. [Electromyographic and histologic evaluation of intestinal viability]. *Wiad Lek,* 50 Suppl 1 Pt 1**,** 50-3.
EDSANDER-NORD, A., ROJDMARK, J. & WICKMAN, M. 2002. Metabolism in pedicled and free TRAM flaps: a comparison using the microdialysis technique. *Plast Reconstr Surg,* 109**,** 664-73.
ELMORE, S. 2007. Apoptosis: a review of programmed cell death. *Toxicol Pathol,* 35**,** 495-516.
ELTZSCHIG, H. K. & COLLARD, C. D. 2004. Vascular ischaemia and reperfusion injury. *Br Med Bull,* 70**,** 71-86.
EMMERTSEN, K. J., WARA, P., SOERENSEN, F. B. & STOLLE, L. B. 2005. Intestinal microdialysis--applicability, reproducibility and local tissue response in a pig model. *Scand J Surg,* 94**,** 246-51.
ERIKOGLU, M., KAYNAK, A., BEYATLI, E. A. & TOY, H. 2005. Intraoperative determination of intestinal viability: a comparison with transserosal pulse oximetry and histopathological examination. *J Surg Res,* 128**,** 66-9.
FILZMOSER, P., LIEBMANN, B. & VARMUZA, K. 2009. Repeated double cross validation. *Journal of Chemometrics,* 23**,** 160-171.
FOSTER, K. R. & SCHWAN, H. P. 1989. Dielectric properties of tissues and biological materials: a critical review. *Crit Rev Biomed Eng,* 17**,** 25-104.

GABRIEL, C. 1996. Compilation of the dielectric properties of body tissues at RF and microwave frequencies. Brooks Air Force Base, Texas, USA: US Air Force Laboratories/Armstrong Laboratory/Occupational and Environmental Health Directorate.

GABRIEL, C. & GABRIEL, S. 1996. *APPENDIX C - Modelling the frequency dependence of the dielectric properties to a 4 dispersions spectrum* [Online]. Available: http://niremf.ifac.cnr.it/docs/DIELECTRIC/AppendixC.html#C35 [Accessed 04.02 2015].

GABRIEL, S., LAU, R. W. & GABRIEL, C. 1996. The dielectric properties of biological tissues: II. Measurements in the frequency range 10 Hz to 20 GHz. *Phys Med Biol,* 41**,** 2251-69.

GERSING, E. 1998. Impedance spectroscopy on living tissue for determination of the state of organs. *Bioelectrochemistry and bioenergetics,* 45**,** 145-149.

GHEORGHIU, M. & GERSING, E. 2002. Revealing alteration of membrane structures during ischema using impedance spectroscopy. *Songklanakarin J. Sci. Technol,* 24 (Suppl.)**,** 777-784.

GLOTZER, D. J., VILLEGAS, A. H., ANEKAMAYA, S. & SHAW, R. S. 1962. Healing of the intestine in experimental bowel infarction. *Ann Surg,* 155**,** 183-90.

GONZALEZ, C. A., VILLANUEVA, C., KANEKO-WADA, F. T. & SACRISTAN, E. 2007. Gastric tonometry and impedance spectroscopy as a guide to resuscitation therapy during experimental septic shock in pigs. *In Vivo,* 21**,** 989-1001.

GONZALEZ, C. A., VILLANUEVA, C., OTHMAN, S., NARVAEZ, R. & SACRISTAN, E. 2003. Impedance spectroscopy for monitoring ischemic injury in the intestinal mucosa. *Physiol Meas,* 24**,** 277-89.

GONZALEZ, L. M., MOESER, A. J. & BLIKSLAGER, A. T. 2015. Animal models of ischemia-reperfusion-induced intestinal injury: progress and promise for translational research. *Am J Physiol Gastrointest Liver Physiol,* 308**,** G63-75.

GOREY, T. F. 1980. The recovery of intestine after ischaemic injury. *Br J Surg,* 67**,** 699-702.

GRANGER, D. N. 1988. Role of xanthine oxidase and granulocytes in ischemia-reperfusion injury. *Am J Physiol,* 255**,** H1269-75.

GRIMNES, S. & MARTINSEN, O. G. 2007. Sources of error in tetrapolar impedance measurements on biomaterials and other ionic conductors. *Journal of Physics D-Applied Physics,* 40**,** 9-14.

GRIMNES, S. & MARTINSEN, Ø. G. 2015. *Bioimpedance and Bioelectricity Basics*, Academic press, Elsevier.

GROOTJANS, J., LENAERTS, K., DERIKX, J. P., MATTHIJSEN, R. A., DE BRUINE, A. P., VAN BIJNEN, A. A., VAN DAM, R. M., DEJONG, C. H. & BUURMAN, W. A. 2010. Human intestinal ischemia-reperfusion-induced inflammation characterized: experiences from a new translational model. *Am J Pathol,* 176**,** 2283-91.

GUPTA, D., LAMMERSFELD, C. A., VASHI, P. G., KING, J., DAHLK, S. L., GRUTSCH, J. F. & LIS, C. G. 2009. Bioelectrical impedance phase angle in clinical practice: implications for prognosis in stage IIIB and IV non-small cell lung cancer. *BMC Cancer,* 9**,** 37.

GUTIERREZ, G. 1991. Cellular energy metabolism during hypoxia. *Crit Care Med,* 19**,** 619-26.

HAEMMERICH, D., OZKAN, R., TUNGJITKUSOLMUN, S., TSAI, J. Z., MAHVI, D. M., STAELIN, S. T. & WEBSTER, J. G. 2002. Changes in electrical resistivity of swine liver after occlusion and postmortem. *Med Biol Eng Comput,* 40**,** 29-33.

HAGLUND, U. 1994. Gut ischaemia. *Gut,* 35**,** S73-6.

HAGLUND, U. 2001. Mesenteric Ischemia. *In:* HOLZHEIMER, R. G. M., J. A. (ed.) *Surgical Treatment: Evidence-Based and Problem-Oriented.* Munich, Zuckschwerdt: W. Zuckschwerdt Verlag GmbH.

HAGLUND, U., BULKLEY, G. B. & GRANGER, D. N. 1987. On the pathophysiology of intestinal ischemic injury. Clinical review. *Acta Chir Scand,* 153**,** 321-4.
HALTER, R. J., ZHOU, T., MEANEY, P. M., HARTOV, A., BARTH, R. J., JR., ROSENKRANZ, K. M., WELLS, W. A., KOGEL, C. A., BORSIC, A., RIZZO, E. J. & PAULSEN, K. D. 2009. The correlation of in vivo and ex vivo tissue dielectric properties to validate electromagnetic breast imaging: initial clinical experience. *Physiol Meas,* 30**,** S121-36.
HAUGAA, H., ALMAAS, R., THORGERSEN, E. B., FOSS, A., LINE, P. D., SANENGEN, T., BERGMANN, G. B., OHLIN, P., WAELGAARD, L., GRINDHEIM, G., PISCHKE, S. E., MOLLNES, T. E. & TONNESSEN, T. I. 2013. Clinical experience with microdialysis catheters in pediatric liver transplants. *Liver Transpl,* 19**,** 305-14.
HAUGAA, H., THORGERSEN, E. B., PHARO, A., BOBERG, K. M., FOSS, A., LINE, P. D., SANENGEN, T., ALMAAS, R., GRINDHEIM, G., PISCHKE, S. E., MOLLNES, T. E. & TONNESSEN, T. I. 2012a. Early bedside detection of ischemia and rejection in liver transplants by microdialysis. *Liver Transpl,* 18**,** 839-49.
HAUGAA, H., THORGERSEN, E. B., PHARO, A., BOBERG, K. M., FOSS, A., LINE, P. D., SANENGEN, T., ALMAAS, R., GRINDHEIM, G., WAELGAARD, L., PISCHKE, S. E., MOLLNES, T. E. & INGE TONNESSEN, T. 2012b. Inflammatory markers sampled by microdialysis catheters distinguish rejection from ischemia in liver grafts. *Liver Transpl,* 18**,** 1421-9.
HEGDE, S. S., SEIDEL, S. A., LADIPO, J. K., BRADSHAW, L. A., HALTER, S. & RICHARDS, W. O. 1998. Effects of mesenteric ischemia and reperfusion on small bowel electrical activity. *J Surg Res,* 74**,** 86-95.
HEO, J. & JUNG, D. K. 2011. Bioimpedance Changes in Rats with CCl4-Induced Liver Fibrosis. *Journal of Sensor Science and Technology,* 20**,** 71-76.
HERBERT, G. S. & STEELE, S. R. 2007. Acute and chronic mesenteric ischemia. *Surg Clin North Am,* 87**,** 1115-34, ix.
HILLMAN, H. 2000. Limitations of clinical and biological histology. *Med Hypotheses,* 54**,** 553-64.
HOBALLAH, J. J. & LUMSDEN, A. B. 2012. *Vascular Surgery,* London, Springer Science & Business Media.
HOBSON, R. W., 2ND, WRIGHT, C. B., O'DONNELL, J. A., JAMIL, Z., LAMBERTH, W. C. & NAJEM, Z. 1979. Determination of intestinal viability by Doppler ultrasound. *Arch Surg,* 114**,** 165-8.
HOCHREITER, S. & SCHMIDHUBER, J. 1997. Long short-term memory. *Neural Comput,* 9**,** 1735-80.
HOGBERG, N., CARLSSON, P. O., HILLERED, L., MEURLING, S. & STENBACK, A. 2012. Intestinal ischemia measured by intraluminal microdialysis. *Scand J Clin Lab Invest,* 72**,** 59-66.
HOLMES, N. J., CAZI, G., REDDELL, M. T., GORMAN, J. H., FEDORCIW, B., SEMMLOW, J. L. & BROLIN, R. E. 1993. Intraoperative assessment of bowel viability. *J Invest Surg,* 6**,** 211-21.
HORGAN, P. G. & GOREY, T. F. 1992. Operative assessment of intestinal viability. *Surg Clin North Am,* 72**,** 143-55.
HOUNNOU, G., DESTRIEUX, C., DESME, J., BERTRAND, P. & VELUT, S. 2002. Anatomical study of the length of the human intestine. *Surg Radiol Anat,* 24**,** 290-4.
HUMEAU, A., STEENBERGEN, W., NILSSON, H. & STROMBERG, T. 2007. Laser Doppler perfusion monitoring and imaging: novel approaches. *Med Biol Eng Comput,* 45**,** 421-35.

ISHAI, P. B., TALARY, M. S., CADUFF, A., LEVY, E. & FELDMAN, Y. 2013. Electrode polarization in dielectric measurements: a review. *Measurement Science and Technology,* 24.

IVORRA, A. C. 2005. *Contributions to the measurement of electrical impedance for living tissue ischemia injury monitoring.* PhD, Universitat Politecnica De Catalunya.

JACKSON, W. F. & DULING, B. R. 1983. Toxic effects of silver-silver chloride electrodes on vascular smooth muscle. *Circ Res,* 53**,** 105-8.

JOHNSON, E. K., HARDIN, M. O., WALKER, A. S., HATCH, Q. & STEELE, S. R. 2016. Fluorescence Angiography in Colorectal Resection. *Dis Colon Rectum,* 59**,** e1-e4.

JOSSINET, J., FERRERA R, LARESE A, MARCSEK P & DITTMAR A 1993. Analysis of fluids and membrane activity in heart during hypothermic preservations as detected by electrical bio-impedance. *In:* ELSEVIER (ed.) *Technology and Health Care.* Stuttgart: Elsevier.

KALOGERIS, T., BAINES, C. P., KRENZ, M. & KORTHUIS, R. J. 2012. Cell biology of ischemia/reperfusion injury. *Int Rev Cell Mol Biol,* 298**,** 229-317.

KALVOY, H., JOHNSEN, G. K., MARTINSEN, O. G. & GRIMNES, S. 2011. New method for separation of electrode polarization impedance from measured tissue impedance. *Open Biomed Eng J,* 5**,** 8-13.

KAMINSKI, K. A., BONDA, T. A., KORECKI, J. & MUSIAL, W. J. 2002. Oxidative stress and neutrophil activation--the two keystones of ischemia/reperfusion injury. *Int J Cardiol,* 86**,** 41-59.

KARAKAS, B. R., SIRCAN-KUCUKSAYAN, A., ELPEK, O. E. & CANPOLAT, M. 2014. Investigating viability of intestine using spectroscopy: a pilot study. *J Surg Res,* 191**,** 91-8.

KARLICZEK, A., BENARON, D. A., BAAS, P. C., ZEEBREGTS, C. J., WIGGERS, T. & VAN DAM, G. M. 2010. Intraoperative assessment of microperfusion with visible light spectroscopy for prediction of anastomotic leakage in colorectal anastomoses. *Colorectal Dis,* 12**,** 1018-25.

KASHIWAGI, H. 1993. The lower limit of tissue blood flow for safe colonic anastomosis: an experimental study using laser Doppler velocimetry. *Surg Today,* 23**,** 430-8.

KESHTKAR, A. & KESHTKAR, A. 2008. The effect of applied pressure on the electrical impedance of the bladder tissue using small and large probes. *Journal of Medical Engineering & Technology,* 32**,** 505-511.

KLEIN, D. A. 1978. *Environmental impacts of artificial ice nucleating agents,* Stroudsburg, Pa. New York, Dowden, distributed world wide by Academic Press.

KLINGENSMITH, N. J. & COOPERSMITH, C. M. 2016. The Gut as the Motor of Multiple Organ Dysfunction in Critical Illness. *Critical Care Clinics,* 32**,** 203-+.

KOHLENBERG, E., PAYETTE, J. R., SOWA, M. G., LEVASSEUR, M. A., RILEY, C. B. & LEONARDI, L. 2005. Determining intestinal viability by near infrared spectroscopy: A veterinary application. *Vibrational Spectroscopy,* 38**,** 223-228.

KONG, S. E., BLENNERHASSETT, L. R., HEEL, K. A., MCCAULEY, R. D. & HALL, J. C. 1998. Ischaemia-reperfusion injury to the intestine. *Aust N Z J Surg,* 68**,** 554-61.

KUMAR, S. 2011. *Studies on Microwave Propagation Properties of some Biological Tissues.* PhD, Jawaharlal Nehru Technological University.

KUN, S. & PEURA, R. A. 1994. Tissue ischemia detection using impedance spectroscopy. *IEEE Eng Med Biol Mag,* 1994 IEEE**,** 868 - 869.

LI, J., GEISBUSH, T. R., ROSEN, G. D., LACHEY, J., MULIVOR, A. & RUTKOVE, S. B. 2014. Electrical impedance myography for the in vivo and ex vivo assessment of muscular dystrophy (mdx) mouse muscle. *Muscle Nerve,* 49**,** 829-35.

LINFERT, D., CHOWDHRY, T. & RABB, H. 2009. Lymphocytes and ischemia-reperfusion injury. *Transplant Rev (Orlando),* 23**,** 1-10.

LUKANOV, J. & ATMADJOV, P. 1979. Investigating the effect of silver ions on the contractile function of smooth-muscle preparations from guinea pig stomach, in vitro. *Folia Med (Plovdiv),* 21**,** 11-9.
MA, Y., MAZUMDAR, M. & MEMTSOUDIS, S. G. 2012. Beyond repeated-measures analysis of variance: advanced statistical methods for the analysis of longitudinal data in anesthesia research. *Reg Anesth Pain Med,* 37**,** 99-105.
MARTINSEN, Ø. G., GRIMNES, S. & MIRTAHERI, P. 2000. Non-invasive measurements of postmortem changes in dielectric properties of haddock muscle - a pilot study. *J Food Eng,* 43**,** 189-192.
MATHERS, C. D., STEVENS, G. A., BOERMA, T., WHITE, R. A. & TOBIAS, M. I. 2015. Causes of international increases in older age life expectancy. *Lancet,* 385**,** 540-8.
MATSUO, H., HIROSE, H., MORI, Y., TAKAGI, H., IWATA, H., YAMADA, T., SAKAMOTO, K. & YASUMURA, M. 2004. Experimental studies to estimate the intestinal viability in a rat strangulated ileus model using a dielectric parameter. *Dig Dis Sci,* 49**,** 633-8.
MCCANCE, R. A. 1974. The effect of age on the weights and lengths of pigs' intestines. *J Anat,* 117**,** 475-9.
MEGISON, S. M., HORTON, J. W., CHAO, H. & WALKER, P. B. 1990. A new model for intestinal ischemia in the rat. *J Surg Res,* 49**,** 168-73.
MENKE, J. 2010. Diagnostic accuracy of multidetector CT in acute mesenteric ischemia: systematic review and meta-analysis. *Radiology,* 256**,** 93-101.
MILLAN, M., GARCIA-GRANERO, E., FLOR, B., GARCIA-BOTELLO, S. & LLEDO, S. 2006. Early prediction of anastomotic leak in colorectal cancer surgery by intramucosal pH. *Dis Colon Rectum,* 49**,** 595-601.
MISHIMA, Y., SHIGEMATSU, H., HORIE, Y. & SATOH, M. 1979. Measurement of local blood flow of the intestine by hydrogen clearance method; experimental study. *Jpn J Surg,* 9**,** 63-70.
MITSUDO, S. & BRANDT, L. J. 1992. Pathology of intestinal ischemia. *Surg Clin North Am,* 72**,** 43-63.
MOESER, A. J., NIGHOT, P. K., ENGELKE, K. J., UENO, R. & BLIKSLAGER, A. T. 2007. Recovery of mucosal barrier function in ischemic porcine ileum and colon is stimulated by a novel agonist of the ClC-2 chloride channel, lubiprostone. *Am J Physiol Gastrointest Liver Physiol,* 292**,** G647-56.
MOORE-OLUFEMI, S. D., XUE, H., ATTUWAYBI, B. O., FISCHER, U., HARARI, Y., OLIVER, D. H., WEISBRODT, N., ALLEN, S. J., MOORE, F. A., STEWART, R., LAINE, G. A. & COX, C. S., JR. 2005. Resuscitation-induced gut edema and intestinal dysfunction. *J Trauma,* 58**,** 264-70.
MOQADAM, S. M., GREWAL, P., SHOKOUFI, M. & GOLNARAGHI, F. 2015. Compression-dependency of soft tissue bioimpedance for in-vivo and in-vitro tissue testing. *J Electr Bioimp,* 6**,** 22–32.
MOSS, A. A., KRESSEL, H. Y. & BRITO, A. C. 1978. Thermographic assessment of intestinal viability following ischemic damage. *Invest Radiol,* 13**,** 16-20.
MYERS, C., MUTAFYAN, G., PETERSEN, R., PRYOR, A., REYNOLDS, J. & DEMARIA, E. 2009. Real-time probe measurement of tissue oxygenation during gastrointestinal stapling: mucosal ischemia occurs and is not influenced by staple height. *Surg Endosc,* 23**,** 2345-50.
NEGRONI, A., CUCCHIARA, S. & STRONATI, L. 2015. Apoptosis, Necrosis, and Necroptosis in the Gut and Intestinal Homeostasis. *Mediators Inflamm,* 2015**,** 250762.
NOER, R. J. & DERR, J. W. 1949. Revascularization following experimental mesenteric vascular occlusion. *Arch Surg,* 58**,** 576-89.

OTTE, S., OTTE, C., SCHLAEFER, A., WITTIG, L., HUTTMANN, G., DROMANN, D. & ZELL, A. 2013. Oct a-Scan Based Lung Tumor Tissue Classification with Bidirectional Long Short Term Memory Networks. *2013 Ieee International Workshop on Machine Learning for Signal Processing (Mlsp)*.

PARK, P. O., HAGLUND, U., BULKLEY, G. B. & FALT, K. 1990. The sequence of development of intestinal tissue injury after strangulation ischemia and reperfusion. *Surgery,* 107**,** 574-80.

PARKS, D. A. & GRANGER, D. N. 1986. Contributions of ischemia and reperfusion to mucosal lesion formation. *Am J Physiol,* 250**,** G749-53.

PAULY, H. & SCHWAN, H. P. 1964. The Dielectric Properties of the Bovine Eye Lens. *IEEE Trans Biomed Eng,* 11**,** 103-9.

PETERING, H. G. 1976. Pharmacology and Toxicology of Heavy-Metals - Silver. *Pharmacology & Therapeutics Part a-Chemotherapy Toxicology and Metabolic Inhibitors,* 1**,** 127-130.

PETHIG, R. 1987. Dielectric properties of body tissues. *Clin Phys Physiol Meas,* 8 Suppl A**,** 5-12.

PEYMAN, A. & GABRIEL, C. 2005. Dielectric properties of tissues.

PIERRO, A. & EATON, S. 2004. Intestinal ischemia reperfusion injury and multisystem organ failure. *Semin Pediatr Surg,* 13**,** 11-7.

PISCHKE, S. E., TRONSTAD, C., HOLHJEM, L., LINE, P. D., HAUGAA, H. & TONNESSEN, T. I. 2012. Hepatic and abdominal carbon dioxide measurements detect and distinguish hepatic artery occlusion and portal vein occlusion in pigs. *Liver Transpl,* 18**,** 1485-94.

PLONKA, A. J., SCHENTAG, J. J., MESSINGER, S., ADELMAN, M. H., FRANCIS, K. L. & WILLIAMS, J. S. 1989. Effects of enteral and intravenous antimicrobial treatment on survival following intestinal ischemia in rats. *J Surg Res,* 46**,** 216-20.

POLK, C. & POSTOW, E. 1996. *Handbook of biological effects of electromagnetic fields,* Boca Raton, CRC Press.

PRINZEN, F. W. & BASSINGTHWAIGHTE, J. B. 2000. Blood flow distributions by microsphere deposition methods. *Cardiovasc Res,* 45**,** 13-21.

QUAEDACKERS, J. S., BEUK, R. J., BENNET, L., CHARLTON, A., OUDE EGBRINK, M. G., GUNN, A. J. & HEINEMAN, E. 2000. An evaluation of methods for grading histologic injury following ischemia/reperfusion of the small bowel. *Transplant Proc,* 32**,** 1307-10.

RADHAKRISHNAN, R. S., SHAH, K., XUE, H., MOORE-OLUFEMI, S. D., MOORE, F. A., WEISBRODT, N. W., ALLEN, S. J., GILL, B. & COX, C. S., JR. 2007. Measurement of intestinal edema using an impedance analyzer circuit. *J Surg Res,* 138**,** 106-10.

REDAELLI, C. A., SCHILLING, M. K. & BUCHLER, M. W. 1998a. Intraoperative laser Doppler flowmetry: a predictor of ischemic injury in acute mesenteric infarction. *Dig Surg,* 15**,** 55-9.

REDAELLI, C. A., SCHILLING, M. K. & CARREL, T. P. 1998b. Intraoperative assessment of intestinal viability by laser Doppler flowmetry for surgery of ruptured abdominal aortic aneurysms. *World J Surg,* 22**,** 283-9.

RIGAUD, B., HAMZAOUI, L., FRIKHA, M. R., CHAUVEAU, N. & MORUCCI, J. P. 1995. In vitro tissue characterization and modelling using electrical impedance measurements in the 100 Hz-10 MHz frequency range. *Physiol Meas,* 16**,** A15-28.

ROGERS, M. L., BRENNAN, P. A., LEONG, C. L., GOWERS, S. A., ALDRIDGE, T., MELLOR, T. K. & BOUTELLE, M. G. 2013. Online rapid sampling microdialysis (rsMD) using enzyme-based electroanalysis for dynamic detection of ischaemia during free flap reconstructive surgery. *Anal Bioanal Chem,* 405**,** 3881-8.

RUUD, T. E., GUNDERSEN, Y., WANG, J. E., FOSTER, S. J., THIEMERMANN, C. & AASEN, A. O. 2007. Activation of cytokine synthesis by systemic infusions of lipopolysaccharide and peptidoglycan in a porcine model in vivo and in vitro. *Surg Infect (Larchmt),* 8**,** 495-503.

SALAZAR, Y., CINCA, J. & ROSELL-FERRER, J. 2004. Effect of electrode locations and respiration in the characterization of myocardial tissue using a transcatheter impedance method. *Physiol Meas,* 25**,** 1095-103.

SCHAEFER, M., SCHLEGEL, C., KIRLUM, H.-J., GERSING, E. & GEBHARD, M. M. 1998. Monitoring of damage to skeletal muscle tissue caused by ischemia. *Bioelectrochemistry and bioenergetics,* 45**,** 151-155.

SCHAFER, M., KIRLUM, H. J., SCHLEGEL, C. & GEBHARD, M. M. 1999. Dielectric properties of skeletal muscle during ischemia in the frequency range from 50 Hz to 200 MHz. *Ann N Y Acad Sci,* 873**,** 59-64.

SCHAFER, M., SCHLEGEL, C., KIRLUM, H. J., GERSING, E. & GEBHARD, M. M. 1998. Monitoring of damage to skeletal muscle tissues caused by ischemia. *Bioelectrochemistry and Bioenergetics,* 45**,** 151–155.

SCHWAN, H. P. 1957. Electrical properties of tissue and cell suspensions. *Adv Biol Med Phys,* 5**,** 147-209.

SCHWAN, H. P. 1968. Electrode polarization impedance and measurements in biological materials. *Ann N Y Acad Sci,* 148**,** 191-209.

SCHWAN HP & FOSTER KR 1980. RF-field interactions with biological systems: electrical properties and biophysical mechanisms. *Proc. IEEE,* 68**,** 104–113.

SEETHARAM, P. & RODRIGUES, G. 2011. Short bowel syndrome: a review of management options. *Saudi J Gastroenterol,* 17**,** 229-35.

SEIKE, K., KODA, K., SAITO, N., ODA, K., KOSUGI, C., SHIMIZU, K. & MIYAZAKI, M. 2007. Laser Doppler assessment of the influence of division at the root of the inferior mesenteric artery on anastomotic blood flow in rectosigmoid cancer surgery. *Int J Colorectal Dis,* 22**,** 689-97.

SINGH, D. B., STANSBY, G., BAIN, I. & HARRISON, D. K. 2009. Intraoperative measurement of colonic oxygenation during bowel resection. *Adv Exp Med Biol,* 645**,** 261-6.

SINGH, D. B., STANSBY, G. & HARRISON, D. K. 2008. Assessment of oxygenation and perfusion in the tongue and oral mucosa by visible spectrophotometry and laser Doppler flowmetry in healthy subjects. *Adv Exp Med Biol,* 614**,** 227-33.

SOLLIGARD, E., JUEL, I. S., BAKKELUND, K., JOHNSEN, H., SAETHER, O. D., GRONBECH, J. E. & AADAHL, P. 2004. Gut barrier dysfunction as detected by intestinal luminal microdialysis. *Intensive Care Med,* 30**,** 1188-94.

SOLLIGARD, E., JUEL, I. S., BAKKELUND, K., JYNGE, P., TVEDT, K. E., JOHNSEN, H., AADAHL, P. & GRONBECH, J. E. 2005. Gut luminal microdialysis of glycerol as a marker of intestinal ischemic injury and recovery. *Crit Care Med,* 33**,** 2278-85.

SOLLIGARD, E., JUEL, I. S., SPIGSET, O., ROMUNDSTAD, P., GRONBECH, J. E. & AADAHL, P. 2008. Gut luminal lactate measured by microdialysis mirrors permeability of the intestinal mucosa after ischemia. *Shock,* 29**,** 245-51.

SOMMER, T. 2005. Microdialysis of the bowel: the possibility of monitoring intestinal ischemia. *Expert Rev Med Devices,* 2**,** 277-86.

SOMMER, T. & LARSEN, J. F. 2004. Intraperitoneal and intraluminal microdialysis in the detection of experimental regional intestinal ischaemia. *Br J Surg,* 91**,** 855-61.

SPOTTORNO, J., MULTIGNER, M., RIVERO, G., ALVAREZ, L., DE LA VENTA, J. & SANTOS, M. 2008. Time dependence of electrical bioimpedance on porcine liver and kidney under a 50 Hz ac current. *Phys Med Biol,* 53**,** 1701-13.

STRAND-AMUNDSEN, R. J., REIMS, H. M., REINHOLT, F. P., RUUD, T. E., YANG, R., HOGETVEIT, J. O. & TONNESSEN, T. I. 2018a. Ischemia/reperfusion injury in porcine intestine - Viability assessment. *World J Gastroenterol,* 24**,** 2009-2023.

STRAND-AMUNDSEN, R. J., REIMS, H. M., TRONSTAD, C., KALVOY, H., MARTINSEN, O. G., HOGETVEIT, J. O., RUUD, T. E. & TONNESSEN, T. I. 2017. Ischemic small intestine-in vivo versus ex vivo bioimpedance measurements. *Physiol Meas,* 38**,** 715-728.

STRAND-AMUNDSEN, R. J., TRONSTAD, C., KALVOY, H., GUNDERSEN, Y., KROHN, C. D., AASEN, A. O., HOLHJEM, L., REIMS, H. M., MARTINSEN, O. G., HOGETVEIT, J. O., RUUD, T. E. & TONNESSEN, T. I. 2016. In vivo characterization of ischemic small intestine using bioimpedance measurements. *Physiol Meas,* 37**,** 257-75.

STRAND-AMUNDSEN, R. J., TRONSTAD, C., KALVOY, H., RUUD, T. E., HOGETVEIT, J. O., MARTINSEN, O. G. & TONNESSEN, T. I. 2018b. Small intestinal ischemia and reperfusion - bioimpedance measurements. *Physiol Meas*.

STRAND-AMUNDSEN, R. J., TRONSTAD, C., REIMS, H. M., REINHOLT, F. P., HOGETVEIT, J. O. & TONNESSEN, T. I. 2018c. Machine learning for intraoperative prediction of viability in ischemic small intestine. *Physiol Meas*.

SWERDLOW, S. H., ANTONIOLI, D. A. & GOLDMAN, H. 1981. Intestinal infarction: a new classification. *Arch Pathol Lab Med,* 105**,** 218.

TAKEYOSHI, I., ZHANG, S., NAKAMURA, K., IKOMA, A., ZHU, Y., STARZL, T. E. & TODO, S. 1996. Effect of ischemia on the canine large bowel: a comparison with the small intestine. *J Surg Res,* 62**,** 41-8.

TENHUNEN, J. J., JAKOB, S. M. & TAKALA, J. A. 2001. Gut luminal lactate release during gradual intestinal ischemia. *Intensive Care Med,* 27**,** 1916-22.

TENHUNEN, J. J., KOSUNEN, H., ALHAVA, E., TUOMISTO, L. & TAKALA, J. A. 1999. Intestinal luminal microdialysis: a new approach to assess gut mucosal ischemia. *Anesthesiology,* 91**,** 1807-15.

TILSED, J. V., CASAMASSIMA, A., KURIHARA, H., MARIANI, D., MARTINEZ, I., PEREIRA, J., PONCHIETTI, L., SHAMIYEH, A., AL-AYOUBI, F., BARCO, L. A., CEOLIN, M., D'ALMEIDA, A. J., HILARIO, S., OLAVARRIA, A. L., OZMEN, M. M., PINHEIRO, L. F., POEZE, M., TRIANTOS, G., FUENTES, F. T., SIERRA, S. U., SOREIDE, K. & YANAR, H. 2016. ESTES guidelines: acute mesenteric ischaemia. *Eur J Trauma Emerg Surg,* 42**,** 253-70.

TORRE, M., FAVRE, A., PINI PRATO, A., BRIZZOLARA, A. & MARTUCCIELLO, G. 2002. Histologic study of peritoneal adhesions in children and in a rat model. *Pediatr Surg Int,* 18**,** 673-6.

URBANAVICIUS, L., PATTYN, P., DE PUTTE, D. V. & VENSKUTONIS, D. 2011. How to assess intestinal viability during surgery: A review of techniques. *World J Gastrointest Surg,* 3**,** 59-69.

VALLET, B., LUND, N., CURTIS, S. E., KELLY, D. & CAIN, S. M. 1994. Gut and muscle tissue PO2 in endotoxemic dogs during shock and resuscitation. *J Appl Physiol (1985),* 76**,** 793-800.

VAN DEN HEIJKANT, T. C., AERTS, B. A., TEIJINK, J. A., BUURMAN, W. A. & LUYER, M. D. 2013. Challenges in diagnosing mesenteric ischemia. *World J Gastroenterol,* 19**,** 1338-41.

VIGNALI, A., GIANOTTI, L., BRAGA, M., RADAELLI, G., MALVEZZI, L. & DI CARLO, V. 2000. Altered microperfusion at the rectal stump is predictive for rectal anastomotic leak. *Dis Colon Rectum,* 43**,** 76-82.

WAELGAARD, L., DAHL, B. M., KVARSTEIN, G. & TONNESSEN, T. I. 2012. Tissue gas tensions and tissue metabolites for detection of organ hypoperfusion and ischemia. *Acta Anaesthesiol Scand,* 56**,** 200-9.

WEIXIONG, H., ANEMAN, A., NILSSON, U. & LUNDGREN, O. 1994. Quantification of tissue damage in the feline small intestine during ischaemia-reperfusion: the importance of free radicals. *Acta Physiol Scand,* 150**,** 241-50.

WILLERSON, J. T. 1997. Pharmacologic approaches to reperfusion injury. *Adv Pharmacol,* 39**,** 291-312.

WYERS, M. C. 2010. Acute mesenteric ischemia: diagnostic approach and surgical treatment. *Semin Vasc Surg,* 23**,** 9-20.

YANAR, H., TAVILOGLU, K., ERTEKIN, C., OZCINAR, B., YANAR, F., GULOGLU, R. & KURTOGLU, M. 2007. Planned second-look laparoscopy in the management of acute mesenteric ischemia. *World J Gastroenterol,* 13**,** 3350-3.

YANDZA, T., TAUC, M., SAINT-PAUL, M. C., OUAISSI, M., GUGENHEIM, J. & HEBUTERNE, X. 2012. The pig as a preclinical model for intestinal ischemia-reperfusion and transplantation studies. *J Surg Res,* 178**,** 807-19.

YASUHARA, H. 2005. Acute mesenteric ischemia: the challenge of gastroenterology. *Surg Today,* 35**,** 185-95.

YASUMURA, M., MORI, Y., TAKAGI, H., YAMADA, T., SAKAMOTO, K., IWATA, H. & HIROSE, H. 2003. Experimental model to estimate intestinal viability using charge-coupled device microscopy. *Br J Surg,* 90**,** 460-5.

YELLON, D. M. & HAUSENLOY, D. J. 2007. Myocardial reperfusion injury. *N Engl J Med,* 357**,** 1121-35.

ZIEGLER, A., GONZALEZ, L. & BLIKSLAGER, A. 2016. Large Animal Models: The Key to Translational Discovery in Digestive Disease Research. *Cell Mol Gastroenterol Hepatol,* 2**,** 716-724.

IV

World Journal of Gastroenterology

Submit a Manuscript: http://www.f6publishing.com

World J Gastroenterol 2018 May 14; 24(18): 2009-2023

DOI: 10.3748/wjg.v24.i18.2009

ISSN 1007-9327 (print) ISSN 2219-2840 (online)

ORIGINAL ARTICLE

Basic Study

Ischemia/reperfusion injury in porcine intestine - Viability assessment

Runar J Strand-Amundsen, Henrik M Reims, Finn P Reinholt, Tom E Ruud, Runkuan Yang, Jan O Høgetveit, Tor I Tønnessen

Runar J Strand-Amundsen, Jan O Høgetveit, Department of Clinical and Biomedical Engineering, Oslo University Hospital, Oslo 0424, Norway

Runar J Strand-Amundsen, Jan O Høgetveit, Department of Physics, University of Oslo, Oslo 0316, Norway

Henrik M Reims, Finn P Reinholt, Department of Pathology, Oslo University Hospital, Oslo 0424, Norway

Tom E Ruud, Institute for Surgical Research, Oslo University Hospital, Oslo 0424, Norway

Tom E Ruud, Department of Surgery, Baerum Hospital, Vestre Viken Hospital Trust, Drammen 3004, Norway

Runkuan Yang, Tor I Tønnessen, Department of Emergencies and Critical Care, Oslo University Hospital, Oslo 0424, Norway

Tor I Tønnessen, Institute of Clinical Medicine, University of Oslo, Oslo 0424, Norway

ORCID number: Runar J Strand-Amundsen (0000-0002-2224-9355); Henrik M Reims (0000-0002-2018-7787); Finn P Reinholt (0000-0002-9906-3540); Tom E Ruud (0000-0002-5753-0550); Runkuan Yang (0000-0001-7401-7057); Jan O Høgetveit (0000-0001-6246-0254); Tor I Tønnessen (0000-0002-3511-5815).

Author contributions: Strand-Amundsen RJ, Yang R and Tønnessen TI performed the experiments, collected the histological samples and analyzed the microdialysis data; Reims HM and Reinholt FP analyzed, described and graded the histological samples; Strand-Amundsen RJ, Tønnessen TI, Ruud TE and Høgetveit JO designed and coordinated the research; Strand-Amundsen RJ wrote the paper with assistance and input from all the co-authors.

Supported by the Norwegian Research Council through the Integrisc project number 219819, and by Sensocure AS, Langmyra 11, 3185 Skoppum, Norway.

Institutional review board statement: The study was reviewed and approved by the Research and Development section at the Department of Clinical and Biomedical Engineering at the Oslo University Hospital.

Institutional animal care and use committee statement: All procedures involving animals were reviewed and approved by the Animal Ethics and Welfare Committee of Oslo University Hospital, and the Norwegian Food Authority (FOTS ID 8304 and 12695). The experiment was conducted in accordance with Norwegian animal welfare guidelines (FOR-2015-06-18-761) and EU directive (2010/63/EU).

Conflict-of-interest statement: The authors declare that they have no competing interests.

Data sharing statement: Readers can request the data of this paper by contacting us via runar.strand-amundsen@fys.uio.no.

ARRIVE guidelines statement: The authors have read the ARRIVE guidelines, and the manuscript was prepared and revised according to the ARRIVE guidelines.

Manuscript source: Unsolicited manuscript

Correspondence to: Runar J Strand-Amundsen, MSc, Research Scientist, Department of Physics, University of Oslo, Postboks 1048 Blindern, Oslo 0316, Norway. runar.strand-amundsen@fys.uio.no
Telephone: +47-40029762

Received: March 9, 2018
Peer-review started: March 10, 2018
First decision: April 11, 2018

Revised: April 20, 2018
Accepted: April 23, 2018
Article in press: April 23, 2018
Published online: May 14, 2018

Abstract

AIM

To investigate viability assessment of segmental small bowel ischemia/reperfusion in a porcine model.

METHODS

In 15 pigs, five or six 30-cm segments of jejunum were simultaneously made ischemic by clamping the mesenteric arteries and veins for 1 to 16 h. Reperfusion was initiated after different intervals of ischemia (1-8 h) and subsequently monitored for 5-15 h. The intestinal segments were regularly photographed and assessed visually and by palpation. Intraluminal lactate and glycerol concentrations were measured by microdialysis, and samples were collected for light microscopy and transmission electron microscopy. The histological changes were described and graded.

RESULTS

Using light microscopy, the jejunum was considered as viable until 6 h of ischemia, while with transmission electron microscopy the ischemic muscularis propria was considered viable until 5 h of ischemia. However, following $\geqslant$ 1 h of reperfusion, only segments that had been ischemic for $\leqslant$ 3 h appeared viable, suggesting a possible upper limit for viability in the porcine mesenteric occlusion model. Although intraluminal microdialysis allowed us to closely monitor the onset and duration of ischemia and the onset of reperfusion, we were unable to find sufficient level of association between tissue viability and metabolic markers to conclude that microdialysis is clinically relevant for viability assessment. Evaluation of color and motility appears to be poor indicators of intestinal viability.

CONCLUSION

Three hours of total ischemia of the small bowel followed by reperfusion appears to be the upper limit for viability in this porcine mesenteric ischemia model.

Key words: Viability; Histology; Reperfusion; Ischemia; Microdialysis; Jejunum; Porcine model

Core tip: Research on experimental methods to improve the surgeon's assessment of viability of ischemic bowel with higher accuracy than currently possible, requires an accurate reference model. We investigated viability assessment in a porcine model of warm ischemia on jejunum with mesenteric occlusion, followed by reperfusion. Our aim was to determine the time point of irreversible damage, to provide a reference model. We created parallel segmental models on the jejunum in 15 pigs and compared the results from visual inspection with histology and microdialysis. Three hours of ischemia followed by reperfusion appeared to be the upper limit for viability in this model.

Strand-Amundsen RJ, Reims HM, Reinholt FP, Ruud TE, Yang R, Høgetveit JO, Tønnessen TI. Ischemia/reperfusion injury in porcine intestine - Viability assessment. *World J Gastroenterol* 2018; 24(18): 2009-2023 Available from: URL: http://www.wjgnet.com/1007-9327/full/v24/i18/2009.htm DOI: http://dx.doi.org/10.3748/wjg.v24.i18.2009

INTRODUCTION

Evaluation of intestinal viability is essential in surgical decision-making in patients with acute intestinal ischemia[1-3], but can be challenging as the appearance of the ischemic or reperfused intestine can be deceptive[4]. The standard clinical method for intraoperative assessment of intestinal viability is evaluation of color, motility and bleeding of cut ends[3]. This method is not very specific and requires a high level of clinical experience[4,5].

There is a risk of short bowel syndrome if resection is performed too extensively, and on the other hand, a risk of peritonitis, sepsis and death if non-viable intestine is not removed[6]. The gold standard for determination of bowel viability is a second-look laparotomy (within 48 h) to reinspect areas of questionable viability[7]. Up to 57% of patients need further bowel resection at a later time, and this number includes patients undergoing second look surgery (40% of the patients)[8].

The intestinal wall consists of several tissue layers that have varying ability to tolerate ischemic insults. While the mucosa has a lower tolerance for ischemic damage than the muscularis propria, the mucosa has a very potent ability for rapid regeneration and repair[9]. When the muscularis propria and the muscularis mucosae are damaged, peristalsis and the movement of the villi will be lost. Regenerated scar tissue might not uphold sufficient peristalsis, and may lead to later stricture[2].

While intestinal ischemia may have a number of underlying causes, an early and essential element of the clinical treatment in nearly all cases is the restoration of perfusion[10]. However, it may cause both local and systemic responses, potentially creating damage far beyond the direct ischemic injury[11-13]. The extent of ischemia/reperfusion injury is variable and dependent on the underlying mechanisms, the duration of ischemia, the length of the affected segment and hypoxic tolerance of the tissue[10,14].

Experimental studies on intestinal viability have reported that the time before irreversible damage occurs varies between species, between anatomical locations (*e.g.* jejunum, ileum, or colon), and between the ischemia models used[15-17]. Rat intestine is reported

to be irreversibly damaged after 45 min of ischemia[18], whereas in juvenile pig jejunum irreversible damage to mucosal regeneration has been reported after 6.5 h of ischemia[19]. To judge the accuracy of clinical and experimental methods in the assessment of intestinal viability, histological analysis and/or patient outcome approaches have been used as the standard for comparison[4].

There is presently no standard classification method for the histological assessment of ischemia/reperfusion damage in the gut[20] and several approaches have been proposed, focusing on different aspects of the damage process[21]. Many previous studies of intestinal viability have concentrated on mucosal injury[13,22-25]. A commonly used histological classification system for ischemic mucosal lesions is based on the grading system proposed by Chiu *et al*[22], including modifications proposed by Park *et al*[26] to include evaluation of damage in the deeper layers of the intestine. Swerdlow *et al*[21] proposed a classification system, suggesting that mixing etiologic and morphologic terms should be avoided. This classification system has later been modified[27,28].

Microdialysis has been suggested as a way to monitor bowel ischemia[29], and can be used to measure changes in local metabolic substrate concentrations related to ischemia/reperfusion injury[30-32]. The principle is to place a tubular microdialysis membrane in the tissue of interest, to pump a slow and steady flow of isotonic fluid through the inside of the membrane and on to a sampling vial. The tubular semi-permeable membrane will allow low molecular weight substances in the area surrounding the probe to diffuse through the porous membrane due to differences in concentration gradient[33]. When using intraluminal microdialysis in the small intestine, the substrates of interest are primarily lactate and glycerol. The anaerobic metabolism in the ischemic cells leads to an increase in lactate, and glycerol is released as cell membranes deteriorate. Ischemia/reperfusion experiments have shown, however, that intraluminal microdialysis measurements of glucose and pyruvate can be unreliable[34,35].

In this study, we compared the results from visual inspection, intraluminal microdialysis and histology (light and transmission electron microscopy) with the aim of assessing the viability of porcine jejunum following segmental mesenteric occlusion with warm ischemia and further reperfusion. We evaluated the injury occurring in all layers of the intestinal wall. The overall aim was to determine when irreversible damage occurs, and to establish a reference for use with experimental approaches of viability assessment on the porcine jejunum.

MATERIALS AND METHODS

Animals and experimental design

The animal protocol was designed to minimize pain or discomfort to the animals and reduce the overall number of animals used. The experiment was approved by the Norwegian Food Safety Authority (FOTS ID 8304 and 12695) and conducted in accordance with Norwegian animal welfare guidelines (FOR-2015-06-18-761) and EU directive (2010/63/EU). We conducted the study on 15 Norwegian Landrace pigs, with a weight range 44.3-58.6 kg, 11 were females. Food was withheld 12 h prior to surgery. We used a segmental mesenteric occlusion (SMO) model utilizing several small bowel segments in the same pig[12,19,36,37], selecting 30 cm segments of the jejunum, starting 30 cm distal from the duodenum. More than 30 cm free intervals were maintained between the segments. Local ischemia was induced by atraumatic clamping of the arteries and veins of the jejunal mesentery on the selected segments[17,19], resulting in a 20-cm central zone of warm ischemia and two surrounding approximately 5 cm edge zones of marginal tissue hypoxia[38]. Reperfusion was initiated by releasing the clamps and verified by observing the return of color in the previously ischemic segments. We conducted a series of ischemia/reperfusion intervals (ischemia 1-16 h, reperfusion for 5-15 h post 1-8 h of ischemia, control 1-16 h) in order determine the occurrence of irreversible injury. At the end of the experiment, the animals were sacrificed by a lethal dose of potassium chloride (100 mmol).

Anesthesia and monitoring

Anesthesia was induced with intramuscular ketamine (Warner Lambert, Morris Plains, NJ, United States) 15 mg/kg, azaperone (Janssen-Cilag Pharma, Austria) 1 mg/kg, and atropine (Nycomed Pharma, Asker, Norway) 0.02 mg/kg. Tracheotomy was performed, and anesthesia was maintained with isoflurane (Abbott Scandinavia AB, Kista, Sweden) (1%-1.5%) and a mixture of air and O_2 to obtain an FIO_2 of 30%. Morphine (Alpharma, Oslo, Norway) 0.4-0.7 mg/kg/h was administered as a continuous intravenous infusion. Ventilation was adjusted to a pCO_2 of 5-6 kPa (37.5-45.0 mmHg). A continuous infusion of Ringer acetate 10-30 mL/kg/h was administered as fluid replacement.

Surgery

Surgery was performed under sterile conditions. Tracheostomy was performed initially for mechanical ventilation. The left internal jugular vein was cannulated with a triple lumen catheter for blood sampling, measuring of central venous pressure and infusion of fluids. Arterial pressure was measured through a catheter placed in a carotid artery, the urinary bladder temperature was measured with a thermistor probe. Arterial and venous blood gases were regularly measured throughout the experimental period. Pulse oximetry, heart rate, respiratory rate and expiratory pCO_2 were continuously monitored. The jejunum was made accessible through midline laparotomy. The mesentery of the selected jejunal segments were marked and clamped using Satinsky clamps[39].

Table 1 Comparison of modified Swerdlow *et al*[21,27,28] and Park/Chiu *et al*[22,26] systems for grading of histological damage on the intestine

Grade	Modified Swerdlow	Park/Chiu
0	No pathological change	Normal mucosa
1	Focal loss of surface epithelium	Subepithelial space at villus tips
2	Mucosal infarction (extensive loss of surface epithelium, loss of variable amounts of lamina propria, sparing of basal glands, intact muscularis mucosae)	Extension of subepithelial space with moderate lifting
3	Submucosal infarction (variable necrosis of submucosa, complete mucosal necrosis, intact muscularis mucosae)	Massive lifting down the sides of the villi, some denuded tips
4	Mural infarction (loss of muscularis mucosae, complete necrosis of mucosa and submucosa)	Denuded villi, dilated capillaries
5	Mural infarction (involvement of inner layer of muscularis propria, complete necrosis of mucosa and submucosa)	Disintegration of lamina propria
6	Transmural infarction (complete necrosis of the bowel wall)	Crypt layer injury
7		Transmucosal infarction
8		Transmural infarction

Peristalsis and color

The presence of peristalsis in the bowel segments was monitored by visual observation and palpation, and registered hourly for the duration of the experiments. We photographed the intestinal segments hourly to monitor alterations in color.

Microdialysis

CMA65 Custom made Microdialysis Catheter (65CMC) with 30 mm membrane length, 100 kDa cut-off (M Dialysis AB, Stockholm, Sweden) was perfused with 60 mg/mL Voluven (Fresenius Kabi Norge AS, Halden, Norway) for 30 min, before being inserted into the lumen of the selected jejunal segments, with a split-needle technique. The flow rate was adjusted to 1 μL/min using CMA 107 microdialysis pumps (CMA Microdialysis, Stockholm, Sweden). A baseline measurement was obtained (30 min) before the initiation of ischemia, and then for every hour during the experiment duration. An ISCUSflex Microdialysis Analyzer (M Dialysis AB, Stockholm, Sweden) was used to analyze the samples continuously after sampling, using Reagent set A (M Dialysis AB, Stockholm, Sweden). The reagent set was used to analyze glucose, lactate, pyruvate and glycerol. The ISCUSflex was set to normal linear range, 0.1-12 mmol/L (lactate) and 10-1500 μmol/L (glycerol). After a period of ischemia our results reached values above the linear range. Seven of the microdialysis catheters failed to operate normally and were excluded from the study.

Histology

We collected a total of 128 intestinal tissue samples from 5 pigs for light microscopy (LM) at selected time intervals from control jejunum, ischemic jejunum and reperfused jejunum. The biopsies were fixed overnight in buffered 10% formalin. The samples were then processed according to a routine protocol and embedded in paraffin wax, and 2-3 histological sections from each sample were stained with hematoxylin and eosin. The sections were reviewed with LM by two pathologists (HMR & FPR) and pathological changes in each layer of the intestine were assessed. The intestinal tissue damage was also classified using a system devised by Antonioli and Swerdlow, as modified by Hegde *et al*[27,28] and a modification of the grading system devised by Chiu[22], proposed by Park *et al*[26] (Table 1).

In addition, 58 samples at selected time intervals from 3 pigs were collected and fixed in a phosphate-buffered mixture of 2% glutaraldehyde and 0.5% paraformaldehyde overnight. From each sample, four specimens were subsequently embedded in an epoxy resin according to a standard protocol. Toluidine blue-stained semi-thin sections were used to select areas of interest and ultra-thin sectioning of one block. The ultra-thin sections were examined by transmission electron (TEM) microscopy by one pathologist (FPR). The focus was on cellular and subcellular changes as a basis of estimating tissue viability in the muscularis propria.

Statistical analysis

The microdialysis data was analyzed for distribution, skewness, kurtosis and homogeneity of variance to assess distribution. Continuous data were described with mean and SD and categorical data with counts and proportions. Comparisons of the intraluminal lactate and glycerol levels between the control and ischemia/reperfusion segments of jejunum were made using two-way repeated measures analysis of variance (RM ANOVA). For the ANOVA's the responses of interest were lactate and glycerol level, and the factors used were "case" (control, ischemic, reperfusion) and time duration [h]. *P*-values were adjusted for multiple comparisons using Holm-Sidak's correction. The ANOVA's were run using GraphPad Prism version 7.00 (GraphPad Software, United States).

RESULTS

All the animals (n = 15) were hemodynamically stable during the experiments. 10-20 min after reperfusion was initiated in a segment of the jejunum after a period of ischemia, there was an increase in heart rate (+20 to 60 beats per minute) that lasted for 5 to 30 min (increasing with the late reperfusion intervals), and there was also an initial decrease in mean arterial

Table 2 Clinical parameters during ischemia/reperfusion in porcine jejunum

Ischemia (h)	Observations on the ischemic jejunum	Minutes after reperfusion before color has returned (mean ± SD)	Observable peristalsis in No. of pigs	Reperfusion (h)	Observations on the reperfused jejunum	No. of pigs
0	Normal color					15
1	Purple	0.9 ± 0.1	15 of 15	8	Edema	15
2	Darker purple	2 ± 0.1	2 of 2	8	Edema, slight fibrinous coating	2
3	Darker purple	4 ± 0.3	13 of 13	8	Edema, fluid droplets, slight fibrinous coating	13
4	Darker purple	6 ± 0.7	4 of 4	8	Edema, fluid droplets, fibrinous coating, darker internal hue	4
5	Darker purple	15 ± 1.6	11 of 11	8	Edema, fluid droplets, fibrinous coating, darker internal hue	11
6	Darker purple	26 ± 3.3	3 of 4	8	Edema, fluid droplets, fibrinous coating, deeper red color, darker internal hue	4
8	Black	49 ± 9[1]	0 of 4	8	Edema, fluid droplets, fibrinous coating, deeper red color, darker internal hue	4
12	Patches of paler color					4
16	Necrotic					4

[1]There was a lot of internal bleeding in the jejunum, so determination of the time before return of color was difficult. Images in Figure 1.

blood pressure (5-25 Torr) lasting for 5-15 min, before returning to normal after increased fluid administration. SpO_2 (measured at the pig tail) was above 98% in all animals during the entire experiment. Mean body temperature increased from 38.5 ℃ at the start of the experiments to 40.5 ℃ by the end of the experiment.

Peristalsis and color

After initiating ischemia of a bowel segment, we observed a period of hyperperistalsis that lasted for approximately 30-40 min. Ischemia leads to a change in color of the involved tissue (Figure 1 and Table 2), and edema is the hallmark of reperfusion. Upon reperfusion, peristalsis was visible in all jejunal segments that had been ischemic for ⩽ 5 h and most of the segments that had been ischemic for 6 h. We observed an initial hyperemia, and a return of color even in the jejunum that had been ischemic for 8 h. In the samples that had been ischemic for ⩾ 2 h there was a gradual formation of a fibrinous exudate on the serosa after reperfusion. Following reperfusion, we observed the formation of small fluid droplets on the surface of the samples that had been ischemic for ⩾ 3 h, which was associated with a gradual increase in peritoneal fluid. We observed a darker "internal hue" in the samples that were reperfused after ⩾ 4 h of ischemia.

Microdialysis

Levels of the intraluminal lactate increased significantly during the first hour of ischemia ($P < 0.001$) from mean (SD) 0.65 (0.28) to 8.54 (3.43) mmol/L, peaking around 4-5 h of ischemia compared to the control (Figure 2). Following reperfusion after 1 h of ischemia, the intraluminal lactate level showed little change during the first hour of reperfusion with 10.42 (1.97) mmol/L compared to 13.69 (2.33) mmol/L in the ischemic tissue. In the second hour of reperfusion the lactate levels decreased significantly to 4.64 (1.36) mmol/L compared to 15.43 (2.47) mmol/L in the ischemic tissue ($P < 0.001$). In the series with ischemia duration > 1 h, the lactate levels decreased over the first hour following reperfusion. In the tissue that was ischemic for the whole duration of the experiment there was a gradual decrease in lactate level from mean (SD) 17.22 (3.48) mmol/L at 6 h of ischemic duration to 12.96 (2.01) mmol/L by the end of the experiment. Only in the jejunum that was reperfused after 1 hour of ischemia, did the lactate values approach pre-ischemic levels during the experiment. There was no significant change in arterial lactate throughout the experiment (data not shown).

The intraluminal glycerol level increased significantly from mean (SD) 5.7 (2.0) to 554.1 (215) μmmol/L during the first hour after the initiation of ischemia ($P < 0.001$), peaking around 6-8 h of ischemia compared to the control (Figure 2). In the segments that were reperfused after 1-3 h of ischemia, the glycerol levels continued to increase during the first hour of reperfusion, while decreasing during the first hour of reperfusion following longer ischemia intervals. The glycerol levels in the lumen of the reperfused intestinal segments approached the control level after 6 to 7 h of reperfusion, regardless of previous ischemic exposure. In the tissue that was ischemic for the duration of the experiment, there was a gradual decrease in glycerol level from mean (SD) 3180.4 (382.8) μmmol/L at 7 h of ischemia to 2780.2 (471.0) μmmol/L by the end of the experiment.

Histopathology

Light microscopy: LM of cross-sections of jejunum showed gradually increasing signs of injury in the ischemic tissue with time, and more pronounced injury following reperfusion. There was some variation in the pattern and extent of pathological changes between different samples from the same time point, and between different areas within the same samples, but the lesions were reproducible and the predominant

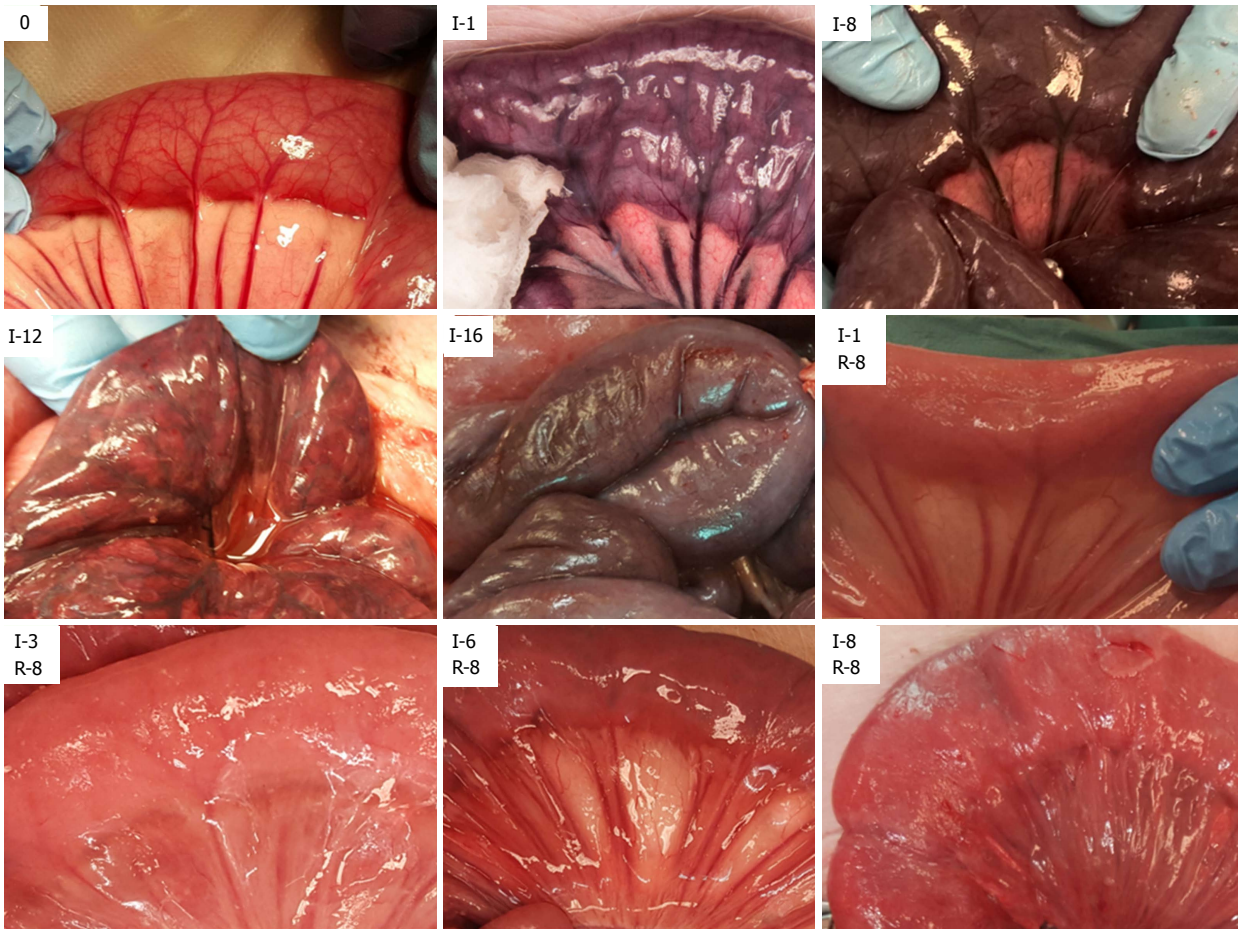

Figure 1 Jejunum at selected intervals of ischemia and reperfusion. 0: Perfused jejunum at the start of the experiment. I-1: 1 h of ischemia. I-8: 8 h of ischemia. I-12: 12 h of ischemia. I-16: 16 h of ischemia. I-1 R-8: 1 h of ischemia and 8 h of reperfusion. I-3 R-8: 3 h of ischemia and 8 h of reperfusion. I-6 R-8: 6 h of ischemia and 8 h of reperfusion. I-8 R-8: 8 h ischemia and 8 h of reperfusion. See Table 1 for description.

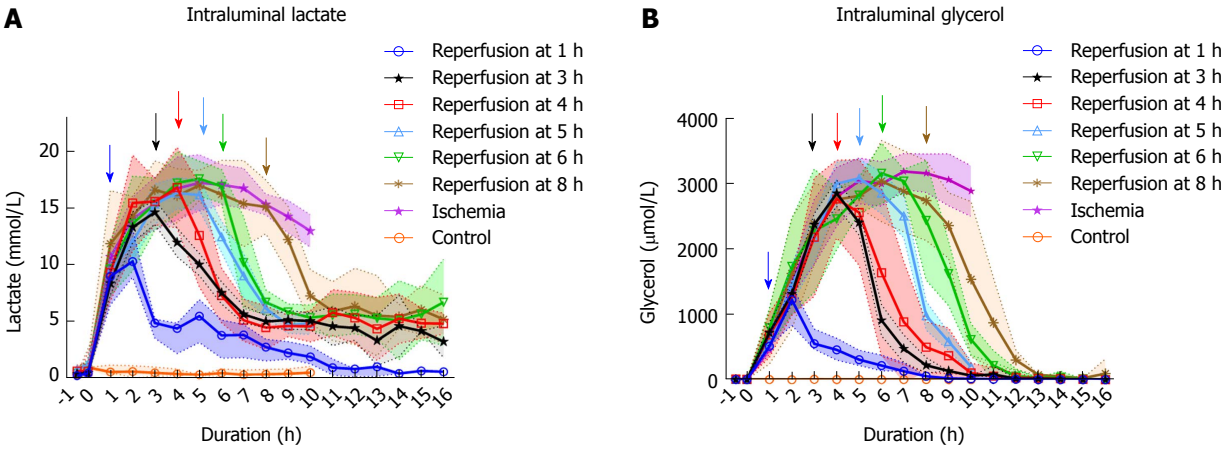

Figure 2 Intraluminal microdialysis in pig jejunum. A: Plots show intraluminal lactate median with 95%CI bands of the median. B: Plots show intraluminal glycerol median with 95%CI bands of the median. Both: Measurements starts with a baseline 30 min before the initiation of ischemia at t = 0. Colored arrows show time points for start of reperfusion. Ischemia and reperfusion at 1, 3 and 5 h n = 14. Reperfusion at 4, 6 and 8 h n = 4. Control n = 5.

findings at each time point are shown in Table 3. Based on the observations of total loss of crypt epithelium and pronounced smooth muscle cell shrinkage in the muscle layers, the samples from tissue exposed only to ischemia were considered irreversibly damaged by ischemia at 6 h exposure.

After one hour of ischemia and 8 h of reperfusion, there was increased apoptosis in the crypt epithelium, mild inflammation with neutrophils mainly in capillaries in all layers of the intestine, edema in the subserosa and submucosa and signs of focal injury to the outer layer of the muscularis propria. After 3 h of ischemia

Table 3 Summary of main findings from light microscopy of 128 biopsies from 5 pigs at selected intervals of ischemia/reperfusion time

Ischemia	1 h isc, 8 h rep	2 h isc, 8 h rep	3 h isc, 8 h rep	4 h isc, 8 h rep	6 h isc, 8 h rep	8 h isc, 8 h rep	Control
I-1: Early loss of SE[1]	I-1: Early loss of SE[1]	I-2: Total loss of SE[2]	I-3: Early loss of CE, congestion and bleeding LP[2]	I-4: Total loss of SE, focal damage to outer layer of MP[2]	I-6: Total loss of CE, damage to LP, MM. Bacteria in LP[2]	I-8: Damage to all components[3]	N-0: Normal[1]
I-2: Total loss of SE[2]	I-1/R-1: Total loss of SE, apoptosis in CE, light N[2]	I-2/R-1: Apoptosis in CE, light N, congestion and focal bleeding in LP[2]	I-3/R-1: Apoptosis in CE, N, wavy myocytes in MP[2]	I-4/R-1: Focal damage to both layers of MP (most to outer layer)[2]	I-6/R-1: Damage to all components[3]	I-8/R-1: Damage to all components[3]	N-6: Few instances of apoptosis in CE, light N and light edema in MP[1]
I-3: Early loss of CE[2]	I-1/R-3: Focal damage to outer layer of MP[2]	I-2/R-3: Early regeneration of SE, congestion, bleeding and necrosis in LP, apoptosis in CE, interstitial inflammation in MP[2]	I-3/R-3: Edema, inflammation, and focal necrosis in outer layer of MP[2]	I-4/R-3: Total loss of CE, NGR, cell disintegration in MM and MP[3]	I-6/R-3: Damage to all components[3]	I-8/R-3: Damage to all components[3]	N-12: Few instances of apoptosis in CE, light N and light edema in MP[1]
I-4: Focal damage to outer layer of MP[2]	I-1/R-6: SE regenerated. Focal damage to outer layer of MP[1]	I-2/R-6: Regeneration of SE, wavy myocytes and focal necrosis in MP[2]	I-3/R-6: Most of CE is lost, wavy myocytes and focal necrosis in MP[2]	I-4/R-6: Total loss of CE, NGR, loss of myocytes, disintegration[3]	I-6/R-6: Damage to all components[3]	I-8/R-6: Damage to all components[3]	
I-5: Damage to inner layer of MP[2]	I-1/R-8: SE regenerated. Focal damage to outer layer of MP[1]	I-2/R-8: Regeneration of SE with focal loss and erosion, focal damage to the MP with wavy myocytes and necrosis[2]	I-3/R-8: Most of CE is lost, wavy myocytes and focal necrosis in both layers of MP[2]	I-4/R-8: Damaged SE, CE, MM, submucosa, MP, PM[3]	I-6/R-8: Damage to all components[3]	I-8/R-8: Damage to all components[3]	
I-6: Total loss of CE, damage to LP, MM and bacteria in LP[3]							
I-7: Hemorrhage in subserosa, peritonitis, and damage to all components[3]							
I ⩾ 8: Damage to all components[3]							

Each column shows the results from a series of tissue samples, with time progression from the top to the bottom. The table is indexed using "I" for ischemia, "R" for reperfusion and "N" for normal perfusion, followed by a number showing the hour duration. The results are indexed by a superscript number by the end of each sentence. [1]Normal/light changes, [2]Visible cell damage, but still probably viable, [3]Probably irreversible cell damage. CE: Crypt epithelium; LP: Lamina propria; MM: Muscularis mucosae; MP: Muscularis propria; N: Neutrophils; SE: Surface epithelium.

and 8 h of reperfusion there was focal damage to all layers. After 4 h of ischemia and 8 h of reperfusion there was a total loss of crypt epithelium, extensive shrinkage and loss of myocytes in the outer layer of the muscularis propria, suggesting likely irreversible damage (Figure 3). In intestine subjected to 6-8 h of ischemia followed by 1 h of reperfusion, there were signs of damage to all components of the intestinal wall.

Histological damage according to grading systems: The predominant findings at each time point are shown in Figure 4. The highest score in both grading systems was reached after 8 h of ischemia. The reperfused tissue received a full score for intervals ⩾ 4 h of ischemia followed by 2 h of reperfusion. The observed sequence of ischemia/reperfusion injury did not necessarily follow the outwards direction from the mucosa to the outer muscular layer, as the grading systems suggest (compare Tables 3 and 4 with Table 1 and Figure 4).

Table 4 Summary of main findings from transmission electron microscopy of porcine jejunum at selected intervals of mesenteric occlusive ischemia and reperfusion

Ischemia (h)	Observations	Ischemia/reperfusion (h/h)	Observations
0	Intact musculature. Some variation in the electron density in the muscle cells, focal swollen mitochondria's with vacuolized matrixes[1]		
1	Intact musculature. Discrete intercellular edema. Lymphocytes in the interstitial space. Increased variation in the electron density in the muscle cells. Some cells have increased electron density (darker). Some of the mitochondria are more prominent. Some minimal fat vacuoles are visible[2]	1-3	Inflammation, cell death, sparse fine-vacuolization of the sarcoplasm, slightly swollen mitochondria[2]
2	More prominent variation in electron density between muscle cells. Increased number of vacuoles, some of them are fat vacuoles. Focal edema, thickening of the mitochondrial cristae. Some lysosomes with membrane fragments[2]	2-3	Inflammation, cell death, more comprehensive fine-vacuolization of the sarcoplasm, slightly swollen mitochondria[2]
3	Same results as at 2 h, but a few more interstitial immune response cells are visible. Monocytes, macrophages, and a few granulocytes. Vacuoles in the sarcoplasm. Slightly swollen mitochondria[2]	3-3	Inflammation, cell death, more comprehensive fine-vacuolization of the sarcoplasm, slightly swollen mitochondria, focal single cell necrosis, swollen cell nuclei[2]
4	Same changes as at 3 h, but the changes are more prominent as the cells with higher electron density are more condensed, and there are more vacuoles around the mitochondria[2]	4-3	Pronounced cell shrinking/cell death, swollen cell nuclei, loss of cohesion, interstitial edema[3]
5	Focal edema, variations in electron density, thickening of the mitochondrial cristae, vacuoles in the sarcoplasm, swollen mitochondria, interstitial lymphocytes/monocytes/granulocytes, loss of plasma-membrane and coherence, focal single cell necrosis[3]	5-3	Increased cell shrinking/cell death, swollen cell nuclei, loss of cohesion, interstitial edema[3]
6	Necrosis, focal large vacuoles in some mitochondria[3]	6-3	Increased cell shrinking/cell death, swollen cell nuclei, loss of cohesion, interstitial edema[3]
7	Necrosis with macrophages. Non-necrotic cells appear like the cells at time intervals 3-6 h[3]		
8	Like the results at 7 h[3]		

Changes in the muscularis propria and serosa are described (3 pigs, a total of 58 samples). The results are indexed by a superscript number by the end of each sentence. [1]Normal/light changes, [2]Visible cell damage, but still probably viable, [3]Probably irreversible cell damage.

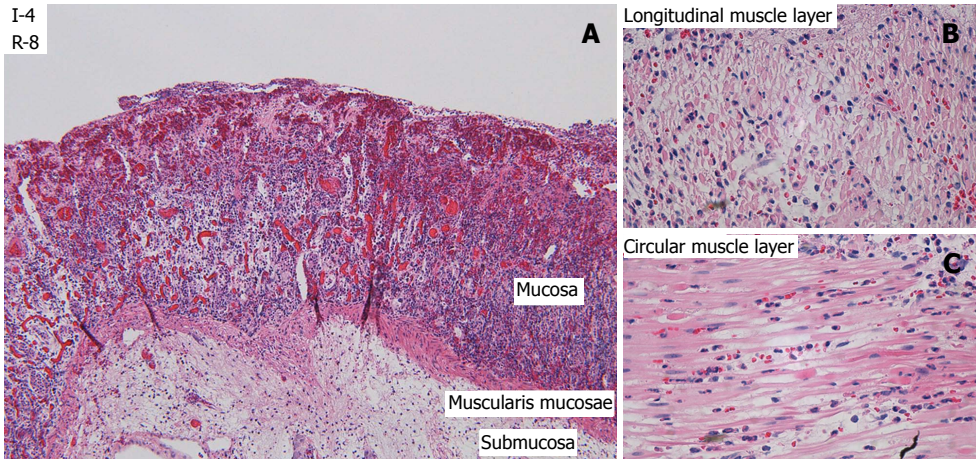

Figure 3 Light microscopy of selected structures of the jejunum after 4 h of ischemia and 8 h of reperfusion. A: Mucosa and submucosa (HE, × 10), showing necrotic villi, total loss of crypt epithelium, shrinkage of myocytes in the muscularis mucosae, and edema in the submucosa. B: Longitudinal (outer) layer of the muscularis propria, showing edema and extensive shrinkage and loss of myocytes (HE, × 60). C: Circular (inner) layer of the muscularis propria, showing edema and extensive myocyte damage (HE, × 60).

Transmission electron microscopy: Using TEM on the muscularis propria and serosa we observed a gradual increase in damage to the cell structures during ischemia (Table 4, left columns), with probably irreversible damage in the muscularis propria after 5 h of ischemia. Interestingly, even at 7 to 8 h of ischemia, focal areas of muscle cells still appeared viable, illustrating heterogeneity in the development of ischemic damage to the muscularis propria.

There was reperfusion induced inflammation and cell death of varying degrees in all the tissue that had been subjected to ischemia. After 3 h of ischemia and 3

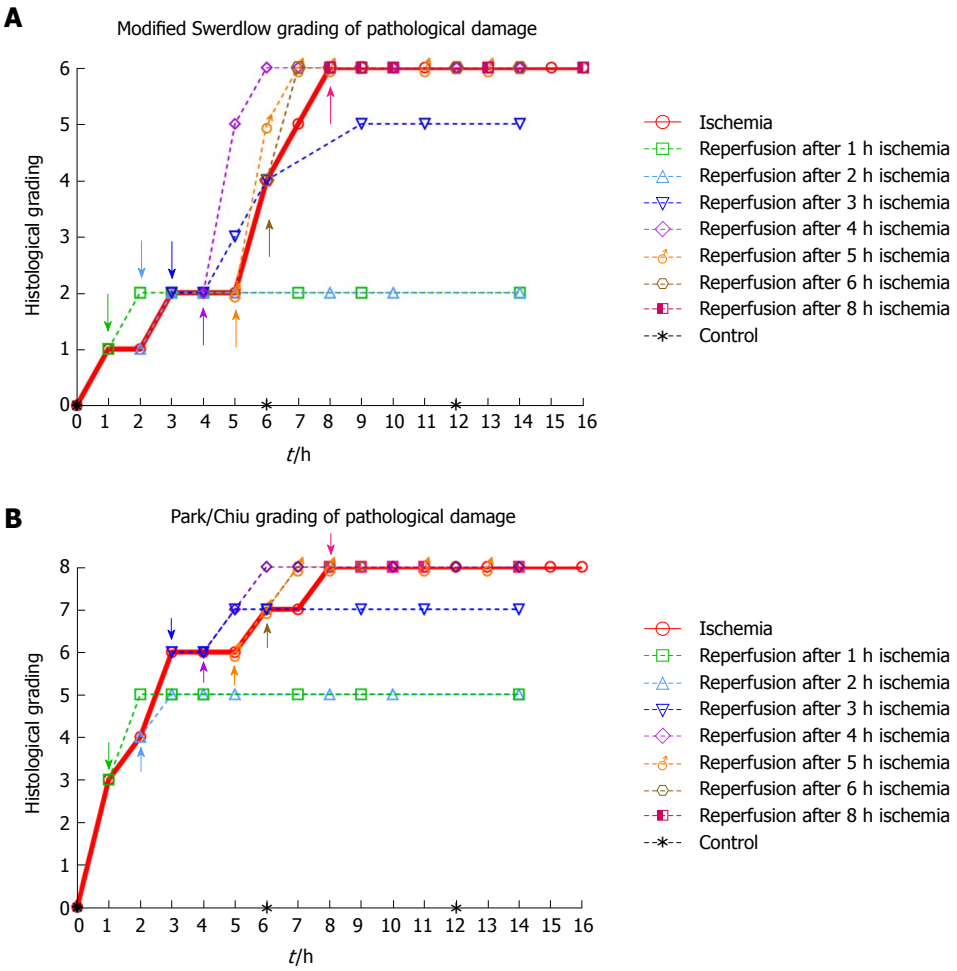

Figure 4 Histological grading of pathological damage (5 pigs, *n* = 128 biopsies total) at selected ischemia/reperfusion intervals. Colored arrows show time points for start of reperfusion. Stippled lines show progression of injury following reperfusion. A: Modified Swerdlow *et al*[21,27,28]. B: Park/Chiu *et al*[22,26].

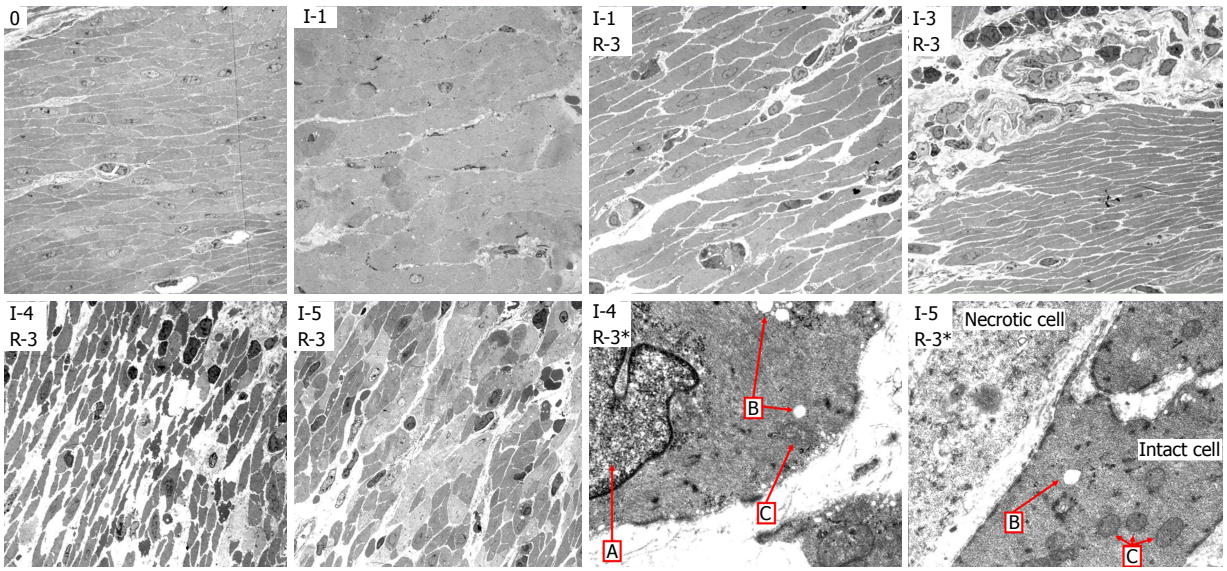

Figure 5 Transmission electron microscopy of jejunum (muscularis propria) sampled at selected time intervals of ischemia and reperfusion. Images are indexed with I = ischemia hours and R = reperfusion hours. 0: Intact muscle. I-1: Mild intercellular edema, with increased variation in the electron density in the muscle cells. Some minimal fat vacuoles are visible. I-1 R-3: Focal/single cell necrosis with inflammatory response, low grade fine-vacuolization of the sarcoplasm. I-3 R-3: Active interstitial inflammation, swollen muscle cell nuclei. I-4 R-3: Severe interstitial edema and loss of coherence among muscle cells. Swollen nuclei and focal, mostly single cell necrosis. I-5 R-3: Focal multi cell necrosis, interstitial inflammation, vacuolization of sarcoplasm. I-4 R-3*: Swollen nucleus (A), vacuolated sarcoplasm (B) and swollen mitochondria (C). I-5 R-3*: Necrotic muscle cell adjacent to a more intact cell with some vacuoles (B) and slightly swollen mitochondria (C).

h of reperfusion (Table 4, left), there was inflammation, cell death, slightly swollen mitochondria, and swollen cell nuclei, and the muscle tissue appeared to be approaching irreversible damage. After 4 h of ischemia and 3 h of reperfusion (Table 4, right), there was pronounced cell shrinking/death, swollen cell nuclei, loss of cohesion, substantial interstitial edema and the muscle tissue no longer appeared viable. Figure 5 shows TEM images with typical observations described in Table 4.

DISCUSSION

The viability of ischemic small bowel is determined in a clinical setting by observation of color, peristalsis and bleeding from cut ends. As this method is not very specific and requires a high level of clinical experience[5], there is a need for increased accuracy of the viability assessment[4]. Intraoperatively, decision on the resection margin is the most important factor contributing to postoperative mortality and morbidity[40,41]. We approached the question of viability assessment in ischemic and reperfused porcine jejunum by using microdialysis and by histological assessment of pathological changes. Microdialysis allowed monitoring of metabolic changes related to ischemia and reperfusion. Presumed irreversible tissue damage was detected after shorter duration of ischemia using TEM than with LM. Subsequent reperfusion aggravated ischemic damage to the jejunum. Likely irreversible damage (when including the effects of reperfusion) occurs between 3 and 4 h of full mesenteric warm ischemia in the porcine jejunum, indicating a time limit for viability in the model.

Visual inspection

While return of color and peristalsis does not correlate uniformly with intestinal viability[2,42], these are the most common criteria in the clinical assessment of intestinal viability[3]. A small variation in the nuance of darkness was the only change in color from 2-9 h of full occlusion ischemia, showing that intestinal color alone is a poor indicator of viability. The later change in appearance from dark (8 h), to patchy colored (11-12 h), to necrotic (15-16 h), indicates the time window between the initiation of full occlusion warm ischemia and the presence of pronounced necrotic bowel in the SMO model.

We observed return of color and peristalsis (Table 2) in intestine that histologically contained areas of probably irreversible damage (Table 3). Following reperfusion, the increase in time before return of color associated with an increase in ischemic exposure, indicating that the time before return of color is affected by the level of tissue injury. However, confounding effects such as internal bleeding and edema in the intestinal wall may have reduced the accuracy of the return of color assessment after the long reperfusion intervals.

Macroscopically, fibrin exudate was seen on the serosal surface (Table 2) on the segments that had been ischemic for more than 1 hour. In addition to being triggered by ischemia/reperfusion[43], the formation of fibrinous exudate on the serosa was probably exacerbated by handling and exposure of the intestine to foreign material during the course of the experiment[44].

Microdialysis

Using microdialysis to measure intraluminal lactate and glycerol, we were able to closely monitor the onset and duration of ischemia, and the onset of reperfusion (Figure 2). In the segments that were reperfused after $\geqslant$ 6 h of ischemia, we observed increasing leakage of fluid from the intestines into the abdominal cavity and increasing amounts of fluid accumulating inside the lumen. Granger *et al*[45] reported a doubling of vascular permeability during ischemia and a fourfold increase in vascular permeability after reperfusion. This probably dilutes the luminal lactate and glycerol concentrations, limiting the accuracy of intraluminal microdialysis during prolonged ischemia/reperfusion experiments[46]. The phenomenon is expressed by a gradual decrease in lactate and glycerol levels in the ischemic intestine past the 6-h duration.

Intraluminal lactate and glycerol levels have been reported to mirror the permeability (polyethylene glycol 4000) of the intestinal mucosa after ischemia, and lactate more precisely so than glycerol[47]. The lactate and glycerol levels started to decrease before reperfusion and dropped after reperfusion even in severely ischemic intestine (8 h), where we observed histological damage to all layers (Table 3). This suggests that the relationship between permeability and lactate/glycerol levels may be valid only after shorter periods of ischemia, and that our late results may be confounded by the dilution effect of leakage into the lumen.

In comparison to previous experiments using intraluminal microdialysis in ischemia/reperfusion of the small intestine in pigs[30,34,35,48,49], we have monitored the intestine over a longer period of ischemic time and over more ischemia/reperfusion intervals than previously reported. Interestingly, Solligard *et al*[47] monitored a single clamp for 9 h of reperfusion after 1 h of ischemia with similar results as ours.

After start of reperfusion, there appears to be no clear difference in the time course of metabolic marker concentration between reversibly and irreversibly damaged tissue, indicating that prediction of viability based on intraluminal microdialysis alone is unreliable. Ideally, placement of microdialysis catheters into the intestinal wall would be preferable, as this would circumvent the late ischemia/reperfusion effects related to intraluminal leakage and dilution. Still, intraluminal microdialysis has been recommended over microdialysis catheters inserted into the intestinal wall, because of the reported poor reliability of the latter method[30,35,47,49-53]. The present results confirm

that intraluminal microdialysis has high specificity and sensitivity for detecting and monitoring ischemia in the small intestine.

Histology and grading

LM (Figure 3, Table 3) and TEM (Figure 5, Table 4) showed a gradual increase in injury in the ischemic tissue with probable irreversible damage appearing around 6 h and 5 h, respectively, indicating that the pathological changes related to viability are visible somewhat earlier on the ultrastructural level than with LM. Tissue that still appeared viable after 4 h of ischemia was considered irreversibly injured after subsequent 3 h of reperfusion, indicating the limit of viability in the model.

When investigating what others have reported with respect to a viability limit in the porcine jejunum, we did not find much information. In most papers discussing viability in the small intestine, observations are reported as histological grading scores or as morphological observations[20], but few contain explicit statements about viability. The most common time duration reported for porcine intestine related to viability is that it takes approximately 8 h of full ischemia to induce transmural necrosis[22,54]. We observed the same result in the present study (Table 3, Figure 4).

Chan *et al*[18], reporting that irreversible damage in porcine jejunum, defined as lack of mucosal regeneration in samples taken 24 h after reperfusion, occurred after 6.5 h of ischemia followed by reperfusion[19]. We acknowledge that mucosal necrosis will heal completely in most cases, except in cases with necrosis of long mucosal segments with substantial damage to the crypt layer, where there is a risk of complications due to hemorrhage and fluid loss[15,21]. The mucosa can regenerate on injured segments of intestine that do not develop into transmural infarction. However, such segments may develop persistent injury with large degree of fibrosis and stricture formation[21]. The exacerbation of injury following reperfusion indicates that reperfusion is a major contributor to injury in the porcine SMO model.

As the Park/Chiu grading system was created to be sensitive to early mucosal changes, the initial grading after one hour of ischemia is 3, indicating that a finer resolution than 1 h of ischemia should be used to utilize its potential. The grading system may have been designed for assessment of inflammatory diseases and the status of cold preserved tissue for transplantation, rather than with respect to overall viability. The Swerdlow grading system has a more evenly distributed resolution with respect to injury in the whole intestinal wall, including two levels of injury with respect to mural infarction. Nevertheless, both systems arrive at similar results, as the structures are similar. We agree with Quaedackers *et al*[20] that a better description of the last grades of the Park/Chiu system would further strengthen its suitability.

We found that more than 3 h of ischemia gave a full score in both grading systems within two hours following reperfusion (Figure 4). This indicates that to assess jejunal viability using histology after an ischemic event of unknown duration, at least two hours of reperfusion is needed before the histological sampling will accurately illustrate the outcome. We generally observed slightly higher levels of injury than Blikslager *et al*[55] in a similar model used on the ileum in pigs, and Chan *et al*[19] in a similar model on the jejunum in two juvenile pigs. As the ileum is more resistant to ischemic damage than the jejunum we expected a slightly higher injury grade in the jejunum.

In the samples from the reperfused tissue that had been exposed to only one hour of ischemia, there was visible regeneration of the epithelial cells after 3 h of reperfusion, with a large degree of regeneration after 6 h. This is similar to what has been reported previously both in humans[56] and pigs[9,57].

An important observation from the present study is that the sequence of ischemia/reperfusion injury using the SMO model does not necessarily follow the outwards direction from the mucosa to the outer muscular layer, as most grading and classification systems suggest[16,20]. Rather, the ischemic damage may be patchy and somewhat unpredictable, as we observed tissue damage in the outer layer of the muscularis propria while the inner muscular layer still appeared viable. This is illustrated when comparing Figure 4 (histological grading) with Table 3 (morphologic observations).

Evaluation of tissue viability based on histological assessment is difficult[58], as the samples are small and lesions are heterogeneous in composition and distribution[59] with areas of viable and necrotic tissue in the same tissue sample. Predicting the healing potential of the various intestinal layers after ischemia/reperfusion is also challenging. Although we observed injury to the jejunal wall that we considered irreversible, the ability to regenerate is likely to vary with the total volume of damaged tissue, making exact assessments from tissue samples difficult. With respect to the observation of heterogeneous injury, Guan *et al*[60] speculated that this may be related to difference in the flow in the mesenteric versus antimesenteric side of the small intestine.

The model

We selected the pig model for viability assessment of the small intestine, as it has important anatomical and physiological similarities to humans[61], the pathophysiology of ischemia/reperfusion in the porcine model is similar to humans[12], and because the pig model has been suggested as a reference standard in intestinal transplantation research. The SMO model[17] was selected as it provides a well-defined area of ischemic injury affecting the whole intestinal wall in the occluded segment[12], as opposed to the commonly used intestinal ischemia model of occlusion of the superior

mesenteric artery[17,62]. The SMO model simulates ischemic injury as caused by strangulation-ileus.

A 50 kg pig has approximately 15 meters of small intestine[63], allowing for the creation of several parallel SMO models[19,36,37], reducing the total number of animals needed for the experiment. However, there are some disadvantages with parallel ischemia/reperfusion models in the same pig. Previous studies have shown that the cytokine levels are reduced when reperfusion of segments is continued in the same pig, due to increasing tolerance levels[64,65]. In addition, we observed periods of increasing heart rate, decreasing blood pressure, fever, and increasing permeability of the intestines, following the late reperfusion intervals. Increased heart rate, decreased blood pressure and fever may be systemic responses related to the release of increasing quantities of harmful substances following the late reperfusion intervals[66,67]. The increasing permeability[45] was visible as fluid droplets on the surface of the reperfused segments and increasing amounts of peritoneal fluid.

Inspection of the control tissue after 12 h gave an indication of the systematic effects on the surrounding perfused jejunum. LM showed mild reactive and inflammatory changes (Table 3), while TEM of the muscularis propria and serosa showed cells with some swollen mitochondria with vacuolated matrices. The microdialysis results and the histological grading systems did not indicate any changes in the control specimens. So, although some minor changes could be observed in the control intestine, we find it unlikely that this had any confounding effects on the outcome of the experiments. Thus, the observed ischemic changes in each occluded segment in the same pig are likely independent of systemic effects until the onset of reperfusion.

In conclusion, in the present porcine model with segmental occlusion of the jejunal mesentery, the intestinal tissue was judged to be probably irreversibly damaged when exposed to $\geqslant$ 4 h of ischemia and then reperfused. Using microdialysis to monitor intraluminal lactate and glycerol allowed us to closely monitor the onset and duration of ischemia, and the onset of reperfusion, but we were unable to find sufficient level of association between tissue viability and metabolic markers to be clinically relevant. The sequence of ischemia/reperfusion injury using the SMO model does not follow the outwards direction from the mucosa to the outer muscular layer, as most current histological grading and classification system suggest. Evaluation of intestinal viability based on return of color and the presence of peristalsis did not match well with histologic assessment of tissue viability.

ARTICLE HIGHLIGHTS

Research background

The clinical gold standard used on humans for assessment of intestinal viability is still based on palpation, visual inspection, bleeding from cut ends and the use of second look operations. The high mortality rates related to acute mesenteric ischemia have not been reduced drastically since the 1980's.

Research motivation

We are investigating methods to improve the accuracy of intraoperative surgical decision making with respect to assessment of the viability of ischemic/reperfused intestine. To assess the accuracy of these methods we need a reference for the limits of intestinal tissue viability. As the pathophysiology of ischemia/reperfusion in the porcine model is similar to humans, and because the pig model has been suggested as a reference standard in intestinal transplantation research, we decided to investigate the jejunal viability limit in a pig model. Our hypothesis is that the results with a pig model can have translational relevance for humans.

Research objectives

We investigated viability assessment in a porcine model of warm ischemia on jejunum with mesenteric occlusion, followed by reperfusion. Our aim was to determine the time point of irreversible damage, to provide a reference for experimental approaches to intestinal viability assessment.

Research methods

We created parallel segmental models on the jejunum in 15 pigs, by clamping the mesenteric arteries and veins for 1 to 16 h. Reperfusion was initiated after different intervals of ischemia (1-8 h) and subsequently monitored for 5-15 h. We compared the results from visual inspection with histology (light microscopy and transmission electron microscopy) and intraluminal microdialysis. The intestinal injury was graded using Park/Chiu and modified Swerdlow grading.

Research results

Only jejunal segments that had been ischemic for $\leqslant$ 3 h appeared viable (following $\geqslant$ 1 h of reperfusion). The jejunal segments that had been ischemic for 4 h showed (following $\geqslant$ 1 h of reperfusion) a total loss of crypt epithelium, extensive shrinkage and loss of myocytes in the outer layer of the muscularis propria. Intraluminal microdialysis allowed us to closely monitor the onset and duration of ischemia and the onset of reperfusion. We observed return of color and peristalsis in intestine that histologically contained areas of probably irreversible damage. The sequence of ischemia/reperfusion injury using the SMO model does not follow the outwards direction from the mucosa to the outer muscular layer, as most current histological grading and classification system suggest.

Research conclusions

In the present porcine model with segmental occlusion of the jejunal mesentery, the intestinal tissue was judged to be probably irreversibly damaged when exposed to $\geqslant$ 4 h of ischemia and then reperfused. Three hours of ischemia followed by reperfusion appeared to be the upper limit for viability in this model. We were unable to find sufficient level of association between tissue viability and metabolic markers to conclude that microdialysis is clinically relevant for viability assessment. Evaluation of color and motility appears to be poor indicators of intestinal viability.

Research perspectives

Segmental mesenteric occlusion provides reproducible injury in porcine jejunum and appears to be a relevant model for studies on viability assessment. Future studies should consider viability assessment in settings where the various etiologic factors related to acute mesenteric ischemia (emboli, arterial and venous thrombus and nonocclusive ischemia) can be evaluated, as good reference models are needed for each etiology.

ACKNOWLEDGMENTS

We want to thank Rune Veddegjerde at Sensocure, and the medical staff at the Department of Emergencies and Critical Care at Oslo University Hospital, for invaluable assistance during the animal experiments. We want

to thank Sheraz Yacub at the Department of HPB Surgery at Oslo University Hospital for suggestions and guidance. We want to thank Ellen Hellesylt and her staff at the Department of Pathology at Oslo University Hospital for preparation of the histological samples for light microscopy. We also want to thank Sverre-Henning Brorson at The Core Facility for Electron Microscopy, Oslo University Hospital, for his work with preparation of samples for transmission electron microscopy.

REFERENCES

1 **Bala M**, Kashuk J, Moore EE, Kluger Y, Biffl W, Gomes CA, Ben-Ishay O, Rubinstein C, Balogh ZJ, Civil I, Coccolini F, Leppaniemi A, Peitzman A, Ansaloni L, Sugrue M, Sartelli M, Di Saverio S, Fraga GP, Catena F. Acute mesenteric ischemia: guidelines of the World Society of Emergency Surgery. *World J Emerg Surg* 2017; **12**: 38 [PMID: 28794797 DOI: 10.1186/s13017-017-0150-5]

2 **Horgan PG**, Gorey TF. Operative assessment of intestinal viability. *Surg Clin North Am* 1992; **72**: 143-155 [PMID: 1731381 DOI: 10.1016/S0039-6109(16)45632-X]

3 **Tilsed JV**, Casamassima A, Kurihara H, Mariani D, Martinez I, Pereira J, Ponchietti L, Shamiyeh A, Al-Ayoubi F, Barco LA, Ceolin M, D'Almeida AJ, Hilario S, Olavarria AL, Ozmen MM, Pinheiro LF, Poeze M, Triantos G, Fuentes FT, Sierra SU, Soreide K, Yanar H. ESTES guidelines: acute mesenteric ischaemia. *Eur J Trauma Emerg Surg* 2016; **42**: 253-270 [PMID: 26820988 DOI: 10.1007/s00068-016-0634-0]

4 **Urbanavičius L**, Pattyn P, de Putte DV, Venskutonis D. How to assess intestinal viability during surgery: A review of techniques. *World J Gastrointest Surg* 2011; **3**: 59-69 [PMID: 21666808 DOI: 10.4240/wjgs.v3.i5.59]

5 **Bulkley GB**, Zuidema GD, Hamilton SR, O'Mara CS, Klacsmann PG, Horn SD. Intraoperative determination of small intestinal viability following ischemic injury: a prospective, controlled trial of two adjuvant methods (Doppler and fluorescein) compared with standard clinical judgment. *Ann Surg* 1981; **193**: 628-637 [PMID: 7016053 DOI: 10.1097/00000658-198105000-00014]

6 **Herbert GS**, Steele SR. Acute and chronic mesenteric ischemia. *Surg Clin North Am* 2007; **87**: 1115-1134, ix [PMID: 17936478 DOI: 10.1016/j.suc.2007.07.016]

7 **Yanar H**, Taviloglu K, Ertekin C, Ozcinar B, Yanar F, Guloglu R, Kurtoglu M. Planned second-look laparoscopy in the management of acute mesenteric ischemia. *World J Gastroenterol* 2007; **13**: 3350-3353 [PMID: 17659674 DOI: 10.3748/wjg.v13.i24.3350]

8 **Clair DG**, Beach JM. Mesenteric Ischemia. *N Engl J Med* 2016; **374**: 959-968 [PMID: 26962730 DOI: 10.1056/NEJMra1503884]

9 **Blikslager AT**, Moeser AJ, Gookin JL, Jones SL, Odle J. Restoration of barrier function in injured intestinal mucosa. *Physiol Rev* 2007; **87**: 545-564 [PMID: 17429041 DOI: 10.1152/physrev.00012.2006]

10 **Kalogeris T**, Baines CP, Krenz M, Korthuis RJ. Cell biology of ischemia/reperfusion injury. *Int Rev Cell Mol Biol* 2012; **298**: 229-317 [PMID: 22878108 DOI: 10.1016/B978-0-12-394309-5.00006-7]

11 **Eltzschig HK**, Collard CD. Vascular ischaemia and reperfusion injury. *Br Med Bull* 2004; **70**: 71-86 [PMID: 15494470 DOI: 10.1093/bmb/ldh025]

12 **Yandza T**, Tauc M, Saint-Paul MC, Ouaissi M, Gugenheim J, Hébuterne X. The pig as a preclinical model for intestinal ischemia-reperfusion and transplantation studies. *J Surg Res* 2012; **178**: 807-819 [PMID: 22884450 DOI: 10.1016/j.jss.2012.07.025]

13 **Parks DA**, Granger DN. Contributions of ischemia and reperfusion to mucosal lesion formation. *Am J Physiol* 1986; **250**: G749-G753 [PMID: 3717337 DOI: 10.1152/ajpgi.1986.250.6.G749]

14 **Liao YF**, Zhu W, Li DP, Zhu X. Heme oxygenase-1 and gut ischemia/reperfusion injury: A short review. *World J Gastroenterol* 2013; **19**: 3555-3561 [PMID: 23801856 DOI: 10.3748/wjg.v19.i23.3555]

15 **Brolin RE**, Bibbo C, Petschenik A, Reddell MT, Semmlow JL. Comparison of ischemic and reperfusion injury in canine bowel viability assessment. *J Gastrointest Surg* 1997; **1**: 511-516 [PMID: 9834386 DOI: 10.1016/S1091-255X(97)80066-2]

16 **Haglund U**, Bulkley GB, Granger DN. On the pathophysiology of intestinal ischemic injury. Clinical review. *Acta Chir Scand* 1987; **153**: 321-324 [PMID: 3310486]

17 **Gonzalez LM**, Moeser AJ, Blikslager AT. Animal models of ischemia-reperfusion-induced intestinal injury: progress and promise for translational research. *Am J Physiol Gastrointest Liver Physiol* 2015; **308**: G63-G75 [PMID: 25414098 DOI: 10.1152/ajpgi.00112.2013]

18 **Illyés G**, Hamar J. Sequence of morphological alterations in a small intestinal ischaemia/reperfusion model of the anesthetized rat. A light microscopy study. *Int J Exp Pathol* 1992; **73**: 161-172 [PMID: 1571276]

19 **Chan KL,** Chan KW, Tam PKH. Segmental small bowel allograft—Ischemic injury and regeneration. *J Pediatr Surg* 1998; **33**: 1703-1706 [DOI: 10.1016/S0022-3468(98)90614-5]

20 **Quaedackers JS**, Beuk RJ, Bennet L, Charlton A, oude Egbrink MG, Gunn AJ, Heineman E. An evaluation of methods for grading histologic injury following ischemia/reperfusion of the small bowel. *Transplant Proc* 2000; **32**: 1307-1310 [PMID: 10995960 DOI: 10.1016/S0041-1345(00)01238-0]

21 **Swerdlow SH**, Antonioli DA, Goldman H. Intestinal infarction: a new classification. *Arch Pathol Lab Med* 1981; **105**: 218 [PMID: 6894232]

22 **Chiu CJ**, McArdle AH, Brown R, Scott HJ, Gurd FN. Intestinal mucosal lesion in low-flow states. I. A morphological, hemodynamic, and metabolic reappraisal. *Arch Surg* 1970; **101**: 478-483 [PMID: 5457245 DOI: 10.1001/archsurg.1970.01340280030009]

23 **Ahrén C**, Haglund U. Mucosal lesions in the small intestine of the cat during low flow. *Acta Physiol Scand* 1973; **88**: 541-550 [PMID: 4765601 DOI: 10.1111/j.1748-1716.1973.tb05483.x]

24 **Clark ET**, Gewertz BL. Intermittent ischemia potentiates intestinal reperfusion injury. *J Vasc Surg* 1991; **13**: 601-606 [PMID: 2027198 DOI: 10.1016/0741-5214(91)90342-R]

25 **Weixiong H**, Aneman A, Nilsson U, Lundgren O. Quantification of tissue damage in the feline small intestine during ischaemia-reperfusion: the importance of free radicals. *Acta Physiol Scand* 1994; **150**: 241-250 [PMID: 8010131 DOI: 10.1111/j.1748-1716.1994.tb09683.x]

26 **Park PO**, Haglund U, Bulkley GB, Fält K. The sequence of development of intestinal tissue injury after strangulation ischemia and reperfusion. *Surgery* 1990; **107**: 574-580 [PMID: 2159192]

27 **Plonka AJ**, Schentag JJ, Messinger S, Adelman MH, Francis KL, Williams JS. Effects of enteral and intravenous antimicrobial treatment on survival following intestinal ischemia in rats. *J Surg Res* 1989; **46**: 216-220 [PMID: 2921861 DOI: 10.1016/0022-4804(89)90059-0]

28 **Hegde SS**, Seidel SA, Ladipo JK, Bradshaw LA, Halter S, Richards WO. Effects of mesenteric ischemia and reperfusion on small bowel electrical activity. *J Surg Res* 1998; **74**: 86-95 [PMID: 9536980 DOI: 10.1006/jsre.1997.5232]

29 **Deeba S**, Corcoles EP, Hanna GB, Pareskevas P, Aziz O, Boutelle MG, Darzi A. Use of rapid sampling microdialysis for intraoperative monitoring of bowel ischemia. *Dis Colon Rectum* 2008; **51**: 1408-1413 [PMID: 18500500 DOI: 10.1007/s10350-008-9375-4]

30 **Tenhunen JJ**, Kosunen H, Alhava E, Tuomisto L, Takala JA. Intestinal luminal microdialysis: a new approach to assess gut mucosal ischemia. *Anesthesiology* 1999; **91**: 1807-1815 [PMID: 10598625 DOI: 10.1097/00000542-199912000-00035]

31 **Waelgaard L**, Dahl BM, Kvarstein G, Tønnessen TI. Tissue gas tensions and tissue metabolites for detection of organ hypoperfusion and ischemia. *Acta Anaesthesiol Scand* 2012; **56**: 200-209 [PMID: 22103593 DOI: 10.1111/j.1399-6576.2011.02572.x]

32 **Pischke SE**, Tronstad C, Holhjem L, Line PD, Haugaa

H, Tønnessen TI. Hepatic and abdominal carbon dioxide measurements detect and distinguish hepatic artery occlusion and portal vein occlusion in pigs. *Liver Transpl* 2012; **18**: 1485-1494 [PMID: 22961940 DOI: 10.1002/lt.23544]
33 **Sommer T**. Microdialysis of the bowel: the possibility of monitoring intestinal ischemia. *Expert Rev Med Devices* 2005; **2**: 277-286 [PMID: 16288591 DOI: 10.1586/17434440.2.3.277]
34 **Högberg N**, Carlsson PO, Hillered L, Meurling S, Stenbäck A. Intestinal ischemia measured by intraluminal microdialysis. *Scand J Clin Lab Invest* 2012; **72**: 59-66 [PMID: 22103734 DOI: 10.3109/00365513.2011.629307]
35 **Sommer T**, Larsen JF. Intraperitoneal and intraluminal microdialysis in the detection of experimental regional intestinal ischaemia. *Br J Surg* 2004; **91**: 855-861 [PMID: 15227691 DOI: 10.1002/bjs.4586]
36 **Cook VL**, Jones Shults J, McDowell M, Campbell NB, Davis JL, Blikslager AT. Attenuation of ischaemic injury in the equine jejunum by administration of systemic lidocaine. *Equine Vet J* 2008; **40**: 353-357 [PMID: 18321812 DOI: 10.2746/042516408X293574]
37 **Moeser AJ**, Nighot PK, Engelke KJ, Ueno R, Blikslager AT. Recovery of mucosal barrier function in ischemic porcine ileum and colon is stimulated by a novel agonist of the ClC-2 chloride channel, lubiprostone. *Am J Physiol Gastrointest Liver Physiol* 2007; **292**: G647-G656 [PMID: 17053162 DOI: 10.1152/ajpgi.00183.2006]
38 **Noer RJ**, Derr JW. Revascularization following experimental mesenteric vascular occlusion. *Arch Surg* 1949; **58**: 576-589 [PMID: 18127337 DOI: 10.1001/archsurg.1949.01240030586002]
39 **Strand-Amundsen RJ**, Tronstad C, Kalvøy H, Gundersen Y, Krohn CD, Aasen AO, Holhjem L, Reims HM, Martinsen ØG, Høgetveit JO, Ruud TE, Tønnessen TI. In vivo characterization of ischemic small intestine using bioimpedance measurements. *Physiol Meas* 2016; **37**: 257-275 [PMID: 26805916 DOI: 10.1088/0967-3334/37/2/257]
40 **Karakaş BR**, Sırcan-Küçüksayan A, Elpek OE, Canpolat M. Investigating viability of intestine using spectroscopy: a pilot study. *J Surg Res* 2014; **191**: 91-98 [PMID: 24746953 DOI: 10.1016/j.jss.2014.03.052]
41 **Oldenburg WA**, Lau LL, Rodenberg TJ, Edmonds HJ, Burger CD. Acute mesenteric ischemia: a clinical review. *Arch Intern Med* 2004; **164**: 1054-1062 [PMID: 15159262 DOI: 10.1001/archinte.164.10.1054]
42 **Glotzer DJ**, Villegas AH, Anekamaya S, Shaw RS. Healing of the intestine in experimental bowel infarction. *Ann Surg* 1962; **155**: 183-190 [PMID: 13899281 DOI: 10.1097/00000658-196200000-00003]
43 **Schoots IG**, Levi M, Roossink EH, Bijlsma PB, van Gulik TM. Local intravascular coagulation and fibrin deposition on intestinal ischemia-reperfusion in rats. *Surgery* 2003; **133**: 411-419 [PMID: 12717359 DOI: 10.1067/msy.2003.104]
44 **Torre M**, Favre A, Pini Prato A, Brizzolara A, Martucciello G. Histologic study of peritoneal adhesions in children and in a rat model. *Pediatr Surg Int* 2002; **18**: 673-676 [PMID: 12598961 DOI: 10.1007/s00383-002-0872-6]
45 **Granger DN**. Role of xanthine oxidase and granulocytes in ischemia-reperfusion injury. *Am J Physiol* 1988; **255**: H1269-H1275 [PMID: 3059826 DOI: 10.1152/ajpheart.1988.255.6.H1269]
46 **Haglund U**. Gut ischaemia. *Gut* 1994; **35**: S73-S76 [PMID: 8125397 DOI: 10.1136/gut.35.1_Suppl.S73]
47 **Solligård E**, Juel IS, Spigset O, Romundstad P, Grønbech JE, Aadahl P. Gut luminal lactate measured by microdialysis mirrors permeability of the intestinal mucosa after ischemia. *Shock* 2008; **29**: 245-251 [PMID: 17693938 DOI: 10.1097/SHK.0b013e3180cab3ce]
48 **Tenhunen JJ**, Jakob SM, Takala JA. Gut luminal lactate release during gradual intestinal ischemia. *Intensive Care Med* 2001; **27**: 1916-1922 [PMID: 11797028 DOI: 10.1007/s00134-001-1145-x]
49 **Solligård E**, Juel IS, Bakkelund K, Johnsen H, Saether OD, Grønbech JE, Aadahl P. Gut barrier dysfunction as detected by intestinal luminal microdialysis. *Intensive Care Med* 2004; **30**: 1188-1194 [PMID: 14991095 DOI: 10.1007/s00134-004-2173-0]
50 **Pynnönen L**, Minkkinen M, Perner A, Räty S, Nordback I, Sand J, Tenhunen J. Validation of intraluminal and intraperitoneal microdialysis in ischemic small intestine. *BMC Gastroenterol* 2013; **13**: 170 [PMID: 24325174 DOI: 10.1186/1471-230X-13-170]
51 **Emmertsen KJ**, Wara P, Soerensen FB, Stolle LB. Intestinal microdialysis--applicability, reproducibility and local tissue response in a pig model. *Scand J Surg* 2005; **94**: 246-251 [PMID: 16259177 DOI: 10.1177/145749690509400314]
52 **Davies MI**, Lunte CE. Microdialysis sampling for hepatic metabolism studies. Impact of microdialysis probe design and implantation technique on liver tissue. *Drug Metab Dispos* 1995; **23**: 1072-1079 [PMID: 8654194]
53 **Anderson C**, Andersson T, Wårdell K. Changes in skin circulation after insertion of a microdialysis probe visualized by laser Doppler perfusion imaging. *J Invest Dermatol* 1994; **102**: 807-811 [PMID: 8176267 DOI: 10.1111/1523-1747.ep12378630]
54 **Amano H,** Bulkley GB, Gorey T, Hamilton SR, Horn SD, Zuidema GD. Role of Micro-Vascular Patency in the Recovery of Small-Intestine from Ischemic-Injury. *Surg Forum* 1980; **31**: 157-159
55 **Blikslager AT**, Roberts MC, Rhoads JM, Argenzio RA. Is reperfusion injury an important cause of mucosal damage after porcine intestinal ischemia? *Surgery* 1997; **121**: 526-534 [PMID: 9142151 DOI: 10.1016/S0039-6060(97)90107-0]
56 **Derikx JP**, Matthijsen RA, de Bruïne AP, van Bijnen AA, Heineman E, van Dam RM, Dejong CH, Buurman WA. Rapid reversal of human intestinal ischemia-reperfusion induced damage by shedding of injured enterocytes and reepithelialisation. *PLoS One* 2008; **3**: e3428 [PMID: 18927609 DOI: 10.1371/journal.pone.0003428]
57 **Gayle J**, Jones SL, Argenzio RA, Blikslager AT. Neutrophils increase paracellular permeability of restituted ischemic-injured porcine ileum. *Surgery* 2002; **132**: 461-470 [PMID: 12324760 DOI: 10.1067/msy.2002.125320]
58 **Hillman H**. Limitations of clinical and biological histology. *Med Hypotheses* 2000; **54**: 553-564 [PMID: 10859638 DOI: 10.1054/mehy.1999.0894]
59 **Dabareiner RM**, Sullins KE, White NA, Snyder JR. Serosal injury in the equine jejunum and ascending colon after ischemia-reperfusion or intraluminal distention and decompression. *Vet Surg* 2001; **30**: 114-125 [PMID: 11230765 DOI: 10.1053/jvet.2001.21393]
60 **Guan Y**, Worrell RT, Pritts TA, Montrose MH. Intestinal ischemia-reperfusion injury: reversible and irreversible damage imaged in vivo. *Am J Physiol Gastrointest Liver Physiol* 2009; **297**: G187-G196 [PMID: 19407214 DOI: 10.1152/ajpgi.90595.2008]
61 **Douglas WR**. Of pigs and men and research: a review of applications and analogies of the pig, sus scrofa, in human medical research. *Space Life Sci* 1972; **3**: 226-234 [PMID: 4556756 DOI: 10.1007/BF00928167]
62 **Megison SM**, Horton JW, Chao H, Walker PB. A new model for intestinal ischemia in the rat. *J Surg Res* 1990; **49**: 168-173 [PMID: 2381206 DOI: 10.1016/0022-4804(90)90257-3]
63 **McCance RA**. The effect of age on the weights and lengths of pigs' intestines. *J Anat* 1974; **117**: 475-479 [PMID: 4419517]
64 **Cavaillon JM**, Adrie C, Fitting C, Adib-Conquy M. Endotoxin tolerance: is there a clinical relevance? *J Endotoxin Res* 2003; **9**: 101-107 [PMID: 12803883 DOI: 10.1179/096805103125001487]
65 **Ruud TE**, Gundersen Y, Wang JE, Foster SJ, Thiemermann C, Aasen AO. Activation of cytokine synthesis by systemic infusions of lipopolysaccharide and peptidoglycan in a porcine model in vivo and in vitro. *Surg Infect* (Larchmt) 2007; **8**: 495-503 [PMID: 17999582 DOI: 10.1089/sur.2006.083]
66 **Willerson JT**. Pharmacologic approaches to reperfusion injury.

Adv Pharmacol 1997; **39**: 291-312 [PMID: 9160118 DOI: 10.1016/S1054-3589(08)60074-5]
67 **Carden DL**, Granger DN. Pathophysiology of ischaemia-reperfusion injury. *J Pathol* 2000; **190**: 255-266 [PMID: 10685060 DOI: 10.1002/(SICI)1096-9896(200002)190:3<255::AID-PATH526>3.0.CO;2-6]

P- Reviewer: Salvadori M, Zhu X **S- Editor**: Gong ZM
L- Editor: A **E- Editor**: Huang Y